

Report No. BMI-1403

UC-25 Metallurgy and Ceramics  
(TID-4500, 15th Ed.)

Contract No. W-7405-eng-92

PROGRESS RELATING TO CIVILIAN APPLICATIONS  
DURING DECEMBER, 1959

by

Russell W. Dayton  
Clyde R. Tipton, Jr.

January 1, 1960

BATTELLE MEMORIAL INSTITUTE  
505 King Avenue  
Columbus 1, Ohio

## **DISCLAIMER**

**This report was prepared as an account of work sponsored by an agency of the United States Government. Neither the United States Government nor any agency Thereof, nor any of their employees, makes any warranty, express or implied, or assumes any legal liability or responsibility for the accuracy, completeness, or usefulness of any information, apparatus, product, or process disclosed, or represents that its use would not infringe privately owned rights. Reference herein to any specific commercial product, process, or service by trade name, trademark, manufacturer, or otherwise does not necessarily constitute or imply its endorsement, recommendation, or favoring by the United States Government or any agency thereof. The views and opinions of authors expressed herein do not necessarily state or reflect those of the United States Government or any agency thereof.**

## **DISCLAIMER**

**Portions of this document may be illegible in electronic image products. Images are produced from the best available original document.**

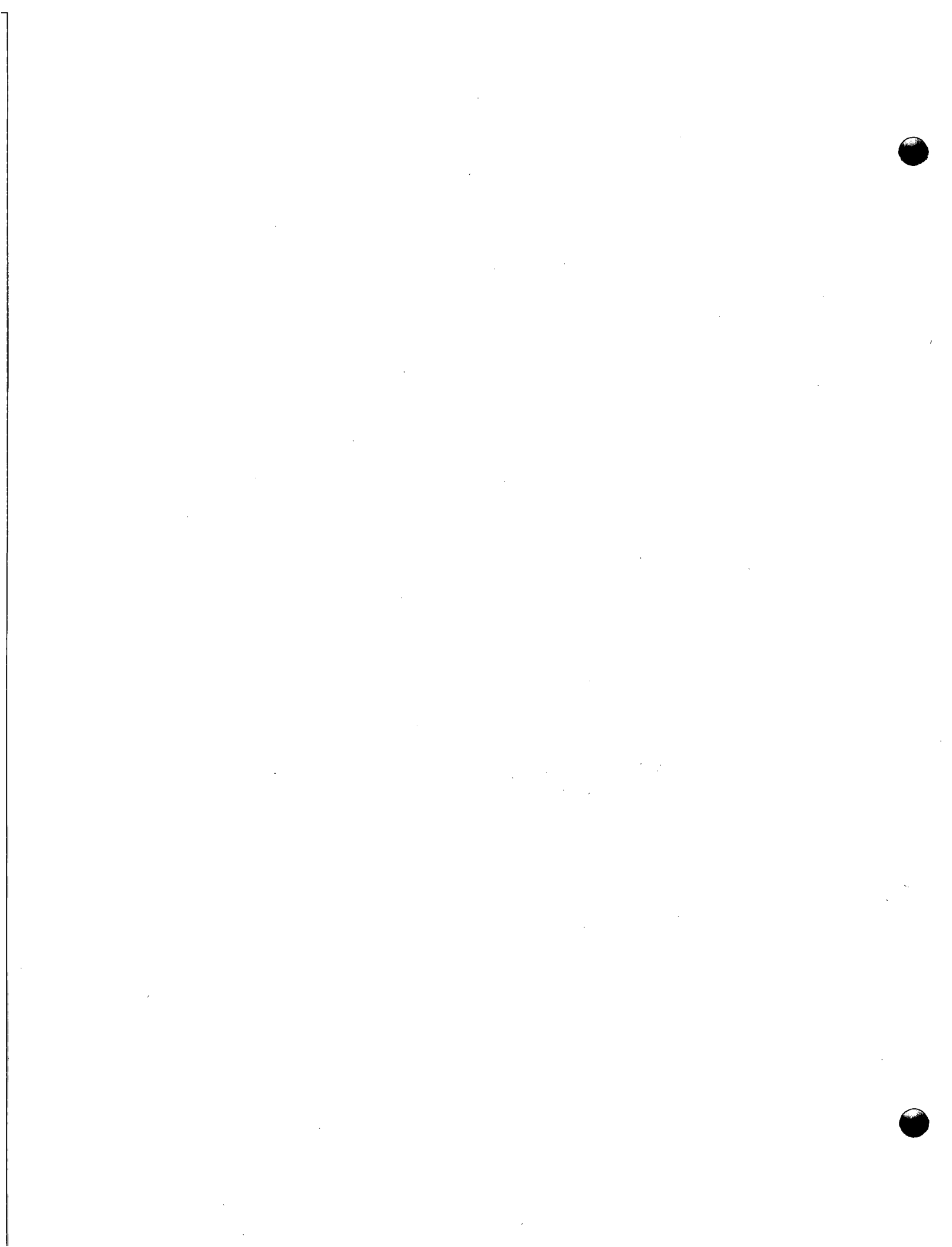


TABLE OF CONTENTS

	<u>Page</u>
REPORTS RELATING TO CIVILIAN APPLICATIONS ISSUED DURING DECEMBER, 1959 . . . . .	5
A. ASSISTANCE TO HAPO . . . . .	7
Mechanical Properties of Zirconium Alloys . . . . .	7
Development of a Fuel-Element Leak Detector . . . . .	7
Thermal-Neutron-Flux Monitoring System . . . . .	10
Development of Corrosion-Resistant Welding Alloys for Use With Hastelloy F to Contain Decladding Solutions . . . . .	11
B. DEVELOPMENTS FOR ALUMINUM-CLAD FUEL ELEMENTS . . . . .	13
Preparation of Aluminum-Uranium Alloys . . . . .	13
C. RADIOISOTOPE AND RADIATION APPLICATIONS . . . . .	17
Development of Radioactive-Tracer Quality-Control Systems . . . . .	18
Use of Intrinsic Radioactive Tracers for Process Control . . . . .	19
Graft-Polymerization Studies . . . . .	20
Nitration of Hydrocarbons . . . . .	21
D. VARIABLE-MODERATOR REACTOR CRITICAL-ASSEMBLY STUDIES . . . . .	25
F. RESEARCH FOR AEC REACTOR DEVELOPMENT DIVISION PROGRAM . . . . .	27
REACTOR MATERIALS AND COMPONENTS . . . . .	27
Valence Effects of Oxide Additions to Uranium Dioxide . . . . .	28
High-Pressure High-Temperature Solid-State Studies . . . . .	28
Irradiation-Surveillance Program on Type 347 Stainless Steel . . . . .	29
Development of Niobium-Base Alloys . . . . .	30
Development of Corrosion-Resistant Niobium Alloys . . . . .	33
Investigation of the Creep Properties of Zircaloy-2 During Irradiation at Elevated Temperatures . . . . .	38
Determination of Oxygen in Sodium at Concentrations Below 10 PPM . . . . .	39
STUDIES OF ALLOY FUELS . . . . .	41
Development of Niobium-Uranium Alloys . . . . .	41
Development of Thorium-Uranium Alloys . . . . .	43
FISSION-GAS RELEASE FROM REFRactory FUELS . . . . .	44
Characterization of Sintered UO <sub>2</sub> and Model of Gas Release . . . . .	44
Diffusion in UO <sub>2</sub> . . . . .	45
Preparation for In-Pile Study . . . . .	46
GENERAL FUEL-ELEMENT DEVELOPMENT . . . . .	47
Fabrication of Cermet Fuel Elements . . . . .	47
Gas-Pressure Bonding of Molybdenum- and Niobium-Clad Fuel Elements . . . . .	49
Factors Affecting Pressure Bonding . . . . .	50
FF. FUEL-CYCLE PROGRAM STUDIES . . . . .	51
GAS-PRESSURE BONDING OF CERAMIC, CERMET, AND DISPERSION FUEL ELEMENTS . . . . .	51
DEVELOPMENT OF URANIUM CARBIDE-TYPE FUEL MATERIALS . . . . .	56
Alternate Fabrication Methods for UC . . . . .	58
Melting and Casting Techniques for Uranium-Carbon Alloys . . . . .	60
Metallurgical and Engineering Properties of Uranium Monocarbide . . . . .	60
Uranium Monocarbide Diffusion Studies . . . . .	61
Irradiation Effects in UC . . . . .	62
GG. VOID-DISTRIBUTION AND HEAT-TRANSFER STUDIES . . . . .	63

TABLE OF CONTENTS  
(Continued)

	Page
H. PHYSICAL RESEARCH . . . . .	65
Niobium-Gas Reactions . . . . .	65
Growth of UO <sub>2</sub> Crystals From the Vapor Phase . . . . .	66
Fusion Methods to Prepare Single Crystals of UO <sub>2</sub> . . . . .	67
I. SOLID HOMOGENEOUS FUELED REACTORS . . . . .	69
LABORATORY EVALUATIONS OF FUELED-GRAPHITE SPHERES . . . . .	69
FABRICATION DEVELOPMENT OF Al <sub>2</sub> O <sub>3</sub> -CLAD UO <sub>2</sub> FUEL PARTICLES . . . . .	69
FISSION-PRODUCT RELEASE FROM FUELED-GRAPHITE SPHERES. . . . .	70
Neutron-Activation Studies . . . . .	70
In-Pile Capsule Experiments . . . . .	71
J. PROBLEMS ASSOCIATED WITH THE RECOVERY OF SPENT REACTOR FUEL ELEMENTS . . . . .	73
CORROSION STUDIES OF THE FLUORIDE-VOLATILITY PROCESS . . . . .	73
STUDY OF THE EFFECTS OF IRRADIATION ON CLADDING- AND CORE-DISSOLUTION PROCESSES . . . . .	73
Sulfex Process . . . . .	73
Darex Process . . . . .	74
K. DEVELOPMENTS FOR SRE . . . . .	75
EVALUATION OF URANIUM MONOCARBIDE AS A REACTOR FUEL . . . . .	75
Irradiation of Uranium Monocarbide . . . . .	75
Postirradiation Examination of Irradiated Uranium Monocarbide . . . . .	75
L. TANTALUM AND TANTALUM ALLOYS . . . . .	79
Development of Container Materials for Lampre Applications . . . . .	79
Effect of Irradiation Damage of Tantalum . . . . .	79
Precipitate Phase Identification and Interstitial-Type Solid Solubility in Tantalum . . . . .	80
M. DEVELOPMENTAL STUDIES FOR THE PWR . . . . .	81
Fabrication of Large-Scale PWR-Type Fuel Plates . . . . .	81
N. DEVELOPMENTS FOR THE MGGR. . . . .	83
FABRICATION AND CHARACTERIZATION OF FUEL MATERIALS . . . . .	83
HIGH-BURNUP IRRADIATION EFFECTS IN FUEL MATERIALS . . . . .	83
DIFFUSION OF FISSION PRODUCTS IN CLADDING MATERIALS . . . . .	84
CARBON-TRANSPORT CORROSION STUDIES. . . . .	84
P. DEVELOPMENTAL STUDIES FOR THE SM-2 . . . . .	87
Materials Development . . . . .	87
Encapsulation Studies . . . . .	90
Q. GAS-COOLED REACTOR PROGRAM . . . . .	93
MATERIALS DEVELOPMENT PROGRAM . . . . .	93
Fabrication of BeO-UO <sub>2</sub> Fuel Pellets . . . . .	93
Encapsulation Studies . . . . .	94
Effects of Irradiation . . . . .	95
GCRE Critical-Assembly Experiments . . . . .	97
IN-PILE-LOOP PROGRAM . . . . .	98
BRR Loop Program . . . . .	98
ETR Loop Program . . . . .	99

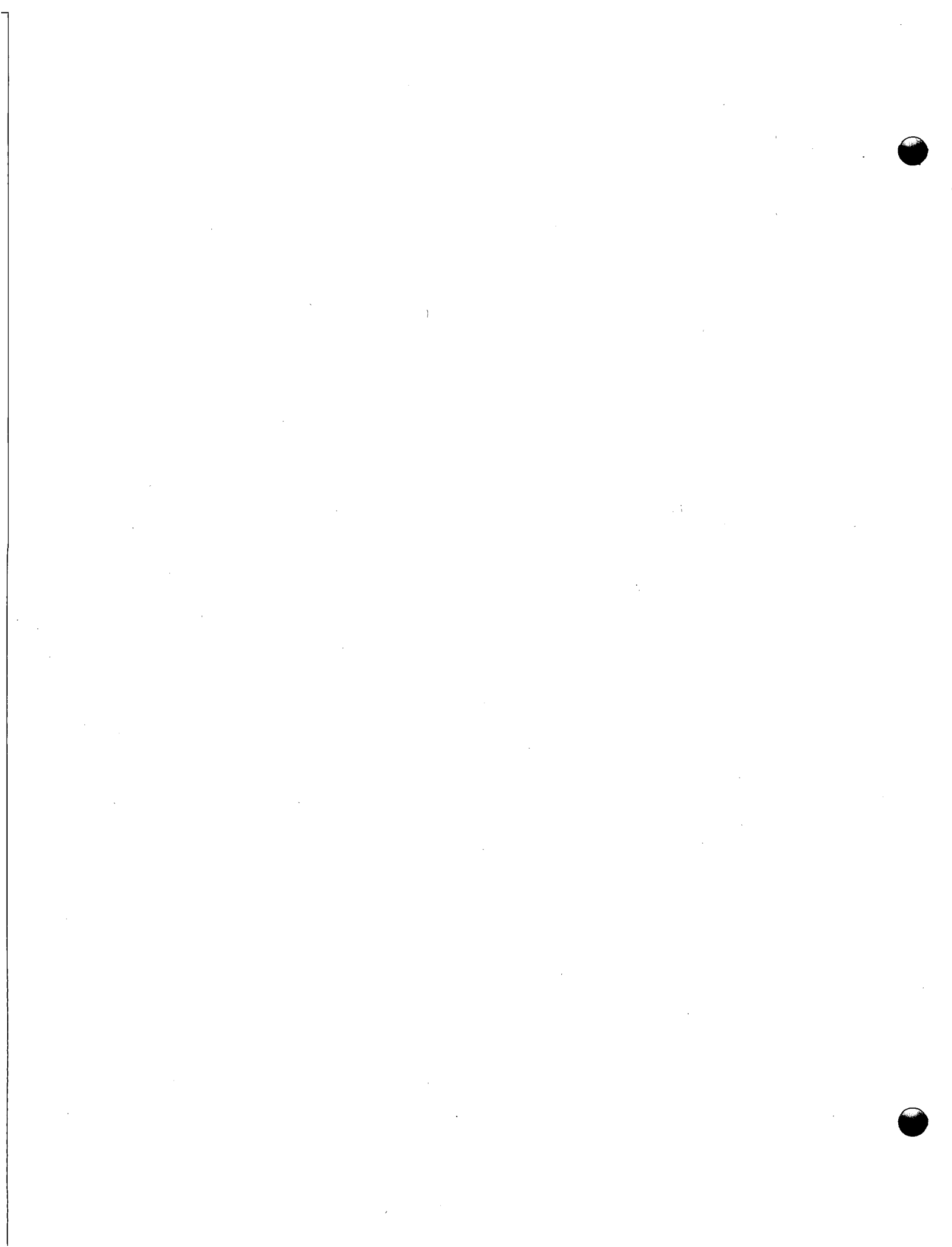
REPORTS RELATING TO CIVILIAN APPLICATIONS  
ISSUED DURING DECEMBER, 1959

BMI-1376 "Solubility Limits of Yttrium and the Lanthanide Rare-Earth Elements in Chromium and Chromium-Iron Alloys", by Seymour G. Epstein, Arthur A. Bauer, and Ronald F. Dickerson.

BMI-1386 "The Solid Solubility and Constitution of Yttrium in Iron-20 to 40 w/o Chromium Alloys", by Martin S. Farkas and Arthur A. Bauer.

BMI-1390 "Experimental and Theoretical Studies of the Solidification of Uranium Castings", by Ellis L. Foster, Jr., Billie L. Fletcher, Charles K. Franklin, Andrew Lechler, and Ronald F. Dickerson.

BMI-1398 "Progress Relating to Civilian Applications During November, 1959", by Russell W. Dayton and Clyde R. Tipton, Jr.



## A-1

## A. ASSISTANCE TO HAPO

F. R. Shober

The creep and stress-rupture properties of annealed and of 15 per cent cold-worked Zircaloy-2 are being determined at 290, 345, and 400 C. Creep tests 12,000 hr in curation are expected. In further studies to develop a AgBr fuel-element leak detector for use in water-cooled reactors, it appears that the gamma-ray background on an AgBr column would be undesirably high after several days of normal operations. The past work period has been spent investigating ways of preventing the buildup of undesirable fission products on the AgBr column. Future work will be concerned with continued attempts to reduce fission-product absorption and with in-pile tests of the leak detector at the ETR.

The development of a thermal-neutron-flux monitoring system has been directed toward extending the sensing-probe life, increasing the effective instrument range, and improving the instrument reliability. Resistivity of  $\text{Al}_2\text{O}_3\text{-MoSi}_2\text{-UO}_2$  ceramic tubes has been determined to investigate the effects of  $\text{MoSi}_2$  proportion and of extrusion pressures. In the development of corrosion-resistant welding alloys for use with Hastelloy F, a number of alloys are being exposed in boiling Sulfex and Niflex solutions to determine corrosion resistance to these liquids.

Mechanical Properties of Zirconium Alloys

L. P. Rice and J. A. VanEcho

The determination of creep and stress-rupture properties of Zircaloy-2 sheet material has been under way for several years. This has included annealed and cold-worked (15 per cent) material at temperatures of 290, 345, and 400 C.

The report (BMI-1398) for November summarized the stress-rupture behavior of the current batch of annealed and cold-worked Zircaloy-2 material.

At the end of December there were 19 tests still in progress. The creep behavior in the current tests on the annealed Zircaloy-2 is summarized in Table A-1.

Development of a Fuel-Element Leak Detector

J. E. Howes, Jr., T. S. Elleman, and D. N. Sunderman

This report summarizes the results obtained during December on the development of a AgBr fuel-element leak detector.

Previous progress reports have indicated that a successful leak detector can be constructed from a AgBr column operated in conjunction with a delayed-neutron monitor.

## A-2

TABLE A-1. SUMMARY OF CREEP AND RUPTURE DATA ON ANNEALED ZIRCALOY-2 ALLOY

Specimen	Stress, psi	Load on Deformation, per cent	Rupture			Present Status		Minimum Creep Rate, per cent per hr <sup>(a)</sup>
			Time, hr	Elongation, per cent	Time, hr	Deformation, per cent		
<u>290 C (550 F)</u>								
Zr-A-7	27,500	1.56	0.9	20.3	--	--	--	8.0
Zr-A-6	25,000	--	0.3	44.3	--	--	--	--
Zr-A-10	22,500	3.18	--	--	6500	4.306	0.00001	
Zr-A-13	20,000	1.51	--	--	4000	2.828	0.00001	
Zr-A-14	17,500	1.25	--	--	3500	1.950	0.000003	
Zr-A-14	15,000	0.64	--	--	3500	0.960	<0.000003	
Zr-A-27	12,500	0.22	--	--	500	0.396	--	
<u>345 C (650 F)</u>								
Zr-A-8	25,000	1.67	858	18.0	--	--	--	0.004
Zr-A-3	22,500	4.27	--	--	5000	6.580	0.0001	
Zr-A-15	20,000	2.24	--	--	3500	4.580	0.000065	
Zr-A-17	17,500	1.78	--	--	3500	1.995	0.000030	
Zr-A-25	15,000	0.97	--	--	2000	1.045	0.000016	
<u>400 C (750 F)</u>								
Zr-A-9	21,860	--	On loading	36.6	--	--	--	--
Zr-A-2	21,800	1.03	49	21.3	--	--	--	0.15
Zr-A-12	17,500	2.20	1036	45.7	--	--	--	0.025
Zr-A-5	15,000	0.90	3664	46.0	--	--	--	0.006
Zr-A-16	12,500	0.45	--	--	3500	2.605	0.00055	
Zr-A-21	10,000	0.11	--	--	3000	0.795	0.00028	
Zr-A-26	9,000	0.08	--	--	1000	0.225	0.00009	

(a) Minimum creep values subject to revision as tests progress.

## A-3

During a fuel-element failure, delayed-neutron-emitting halide fission products in the reactor coolant are selectively absorbed on the AgBr column, and the delayed neutrons trigger the detector attached to the column. The use of a gross gamma-ray detector in place of the neutron detector is hampered by adsorption of gamma-ray-emitting fission products on the AgBr. It appears from the experimental results that the gamma-ray background on the AgBr would be undesirably high after several days of normal operation.

Since the intended operation of the leak detector is best suited to a gross gamma-detection system, the past month has been spent investigating ways of preventing the buildup of undesirable fission products on the AgBr column. A number of experiments were carried out in which fission-product solutions were passed through a column containing ethylenediaminetetraacetic acid pellets before the solution was passed into the AgBr column. The purpose of this experiment was to complex the cationic fission products before they reached the AgBr and thus prevent deposition of the column. This technique reduced the fission-product absorption by a factor of two or so but the reduction was not sufficient. Experiments in which the fission products were equilibrated with an excess of dissolved complexing agent before passage through the AgBr also yielded significant fission-product absorption on the column. Attempts were made to saturate the AgBr with nonradioactive fission-product carriers before the AgBr was contacted with fission products, but this approach did not appear to reduce the fission-product absorption.

In another experiment, lanthanum and zirconium carriers were added to the fission products immediately before they were passed through the AgBr column. Again, appreciable deposition of fission products on the AgBr was observed. Since the concentration of carrier was many times higher than the fission-product concentration, the continued deposition of fission products suggests that the fission products were absorbed on particulate matter and did not rapidly exchange with the carrier cations.

Future work on this program will be concerned with continued attempts to reduce fission-product absorption on the AgBr column and with in-pile tests of the leak detector at the ETR.

The experiments performed on fission-product absorption indicate that the fission products which deposit on the AgBr column are themselves deposited on microscopic particles in the solution. A number of experiments will be carried out to test the effect of various filters in removing this particulate matter before it reaches the AgBr column.

In the ETR loop experiments, fuel elements will be intentionally ruptured to release fission products to the coolant. Silver bromide columns will be set up to sample the coolant, and the time required to detect a leak, the signal-to-noise ratio, the normal coolant background, the rate of fission-product buildup, and other quantities of importance to leak-detector operation will be determined.

Thermal-Neutron-Flux Monitoring System

J. W. Lennon, M. J. Snyder, D. R. Grieser,  
P. M. Steinback, and W. H. Goldthwaite

Ceramic tubes of  $\text{Al}_2\text{O}_3\text{-MoSi}_2\text{-UO}_2$  containing enriched uranium for the fission-power elements and depleted uranium for the matching electric-heating elements are the primary components of the thermal-neutron-flux measuring instrument previously developed by Battelle (BMI-1083). The thermal neutron flux is determined directly from the measured electric power developed in the power matching electric-heating element.

Extending sensing-probe life and increasing the effective instrument range and

Severe attack occurred on all of the weldments exposed to the Niflex solutions. Attack also was severe in the heat-affected zones adjacent to the weldments. None of the alloys seemed much better than Hastelloy F as a filler material. Weldments made with Alloys 1, 2, 7, 8, and 9 were perforated by the end of three periods. These alloys all contain niobium additions which, on first appraisal, seem to be detrimental to the corrosion resistance of the weldment.

All of the exposures have been conducted using Allihn condensers to which free access of air has been hindered. The next series of experiments in boiling Sulfex solutions will be run with air sparged through the solutions. Such a condition has been reported to increase the corrosion rates by a factor of ten, and may help point out differences in weld-metal attack by the Sulfex solution. This next series involves the alloys welded with their own filler materials. Possibly such welds may show improved resistance over similar welds made on Hastelloy F.

Preliminary room-temperature data from the specimens presently in process will be obtained. All of the data obtained thus far will be re-evaluated in the light of the recent work, and sufficient definitive tests will be designed and completed to permit a more clear evaluation of the progress to date and to aid in a reappraisal of the scope of the program. This work will be completed by the end of the next report period.

Development of Corrosion-Resistant Welding Alloys  
for Use With Hastelloy F to Contain Decladding Solutions

C. L. Peterson, J. D. Jackson, A. M. Hall,  
R. E. Monroe, and W. K. Boyd

Machined, coupon-type specimens of unwelded vacuum-melted Hastelloy F and of the 12 unwelded, rolled experimental alloys described in BMI-1391 and BMI-1398 have been exposed to boiling Sulfex and Niflex solutions. Five 24-hr periods of exposure to the vapor and to the liquid of each solution were completed for duplicate specimens of all materials.

In the Sulfex solution all of the experimental alloys behaved similarly to vacuum-melted Hastelloy F with corrosion rates in the liquid ranging from 1 to 4 mils per month (Hastelloy F was 2 mils per month) over the five periods. From period to period, however, the rates for all the experimental alloys and for Hastelloy F varied considerably, being high (3 to 10 mils per month) for some periods and less than 1 mil per month during others. This indicates that all of these materials exhibit borderline passivity in this solution. The over-all corrosion rates were always lower for the vapor-phase specimens.

In the more aggressive Niflex solutions all of the specimens were active during each period. A few of the experimental alloys appeared to have short induction periods, but all corroded at a uniform rate after the first 24-hr period. This was not true of the vacuum-melted Hastelloy F, for which the rate constantly increased during the five exposure periods. During the last period the rate for Hastelloy F specimens exposed to the liquid had reached 110 mils per month and showed signs of further increase. The corrosion rates of Alloys 3, 4, 10, and 11 had leveled off in the 30 to 40 mils-per-month range; Alloys 9 and 12 in the 50 to 60; Alloys 1, 5, and 6 in the 60 to 70; and Alloys 2, 7, and 8 were in the 70 to 100 mils-per-month range. Thus, all of the alloys were superior to vacuum-melted Hastelloy F, some by a substantial amount, but all were considerably attacked by the Niflex solution.

Similar series of exposures have been conducted on specimens of vacuum-melted Hastelloy F which were butt welded with each of the experimental alloys as filler material. Five 24-hr periods in boiling Sulfex solution were not sufficient to bring about any significant differences in the corrosion of any of the weldments. There appeared to be a slight attack on the weldments of the liquid specimens welded with Alloys 3 and 4 and with Hastelloy F as filler materials. Also, some of the liquid-phase specimens were lightly etched while others were not. Other than this, there was little difference in the specimens at the end of the exposure. The corrosion rates again varied from period to period, indicating borderline passivity.

Severe attack occurred on all of the weldments exposed to the Niflex solutions. Attack also was severe in the heat-affected zones adjacent to the weldments. None of the alloys seemed much better than Hastelloy F as a filler material. Weldments made with Alloys 1, 2, 7, 8, and 9 were perforated by the end of three periods. These alloys all contain niobium additions which, on first appraisal, seem to be detrimental to the corrosion resistance of the weldment.

All of the exposures have been conducted using Allihn condensers to which free access of air has been hindered. The next series of experiments in boiling Sulfex solutions will be run with air sparged through the solutions. Such a condition has been reported to increase the corrosion rates by a factor of ten, and may help point out differences in weld-metal attack by the Sulfex solution. This next series involves the alloys welded with their own filler materials. Possibly such welds may show improved resistance over similar welds made on Hastelloy F.

B-1

## B. DEVELOPMENTS FOR ALUMINUM-CLAD FUEL ELEMENTS

N. E. Daniel

Corrosion tests in 200 C water for 30 days have shown that the aluminum-35 w/o uranium alloys containing tin or zirconium additives are equivalent to the binary aluminum-35 w/o uranium and superior to 2S aluminum in their resistance to the corrosion attack of 200 C water. Six full-size aluminum-35 w/o uranium extrusion billets have been made containing 2.5 to 3 w/o tin or zirconium. The uranium concentrations in these billets varied less than 1 w/o from top to bottom. Tensile tests at 100, 250, and 400 C have been conducted on selected alloys.

Preparation of Aluminum-Uranium Alloys

N. E. Daniel, E. L. Foster, and R. F. Dickerson

Aluminum-uranium alloys in the form of hollow cylindrical tubes clad inside and outside with aluminum are desired for use as reactor fuels. The proposed fabrication techniques employ a hollow cylindrical casting containing 35 w/o uranium. This casting is coextruded with the aluminum cladding. Therefore, it is desirable that the casting be dense and sound with good end-to-end homogeneity. It is also desirable that the cast material possess extrusion characteristics as close as possible to those of the aluminum cladding. One possible method of enhancing both the castability and the extrusion characteristics of the alloy is through the use of selected ternary additions. Previous studies have shown that tin and zirconium will inhibit the  $UAl_3$ -to- $UAl_4$  peritectic reaction, thereby increasing the quantity of free aluminum present in the alloys. The studies also indicated that the casting characteristics of the alloy could be improved by the use of ternary additions on the order of 3 w/o.

Corrosion tests have been conducted with aluminum-35 w/o uranium alloys containing additions of 0.5, 1.0, 1.5, 2.0, and 3.0 w/o tin or zirconium in 200 C demineralized water for periods up to 30 days of total exposure. Specimens were examined after 1, 5, 10, 20, and 30 days. Control specimens of 2S aluminum and of the binary aluminum-35 w/o uranium alloy were run in the autoclaves with the alloys containing ternary additions. After 30 days of exposure, all of the alloys exhibited weight gains less than that exhibited by the 2S aluminum. The weight gains exhibited by the as-cast and the extruded material obtained from vacuum-melted alloys were comparable. The weight gains exhibited by the air-melted material were greater in the as-cast condition than in the extruded condition. This may be attributed to the closing of porosity that may have existed in the as-cast material. The weight gains exhibited by the air-melted alloys containing tin in the as-cast condition were 0.79 to 1.15 g per  $cm^2$  and for the same alloys in the extruded condition the weight gains were 0.57 to 0.67 mg per  $cm^2$ . The weight gains exhibited by the air-melted alloys containing zirconium in the as-cast condition were from 0.79 to 3.52 mg per  $cm^2$ , and were from 0.44 to 0.58 mg per  $cm^2$  for the alloys in the extruded condition.

## B-2

Casting studies preparatory to making enriched castings of the alloys in the form of hollow cylindrical extrusion billets have been completed. Three ingots containing ternary additions of tin and three ingots containing ternary additions of zirconium have been shipped to another site for extrusion studies. The alloy contents of the ingots are shown in Table B-1.

TABLE B-1. COMPOSITION OF ALUMINUM-URANIUM ALLOY INGOTS

Casting	Composition, w/o									
	Nominal			Uranium		Zirconium		Tin		
	Uranium	Zirconium	Tin	Top	Bottom	Top	Bottom	Top	Bottom	
1	35.0	--	3.00	34.5	35.3	--	--	2.99	2.91	
2	35.0	2.50	--	34.4	34.8	2.13	2.23	--	--	
3	35.0	3.00	--	33.6	34.6	2.80	3.26	--	--	
4	35.0	--	2.75	36.2	35.8	--	--	2.72	2.64	
5	35.0	--	2.75	34.2	33.9	--	--	2.72	2.68	
6	35.0	2.75	--	33.7	33.4	3.16	2.71	--	--	

These ingots are approximately 6 in. in OD by 4 in. in ID by 7 in. long. Four similar ingots containing enriched uranium will be made at a future date.

Tensile tests of the extruded materials were conducted at 100, 250, and 400 C. At 100 C there is no discernible difference in the tensile strengths of the various alloys. As shown in Table B-2, at 250 C there appears to be a significant and reproducible difference between the tensile strengths of the air-melted aluminum-35 w/o uranium alloy and the air-melted alloys containing tin or zirconium. At 400 C, the binary alloy appears to possess greater tensile strength than the alloys containing ternary additions; however, the results of the tests at 400 C were not as consistent as at the lower temperatures. The vacuum-melted alloys containing zirconium exhibited greater tensile strengths than did the air-melted alloys of similar composition. This apparent superiority in tensile properties exhibited by the vacuum-melted alloys is attributed to the superior soundness of vacuum-cast material.

Future work will be concerned with obtaining creep and stress-rupture data on selected alloy compositions. The alloys of paramount interest will be those containing 2 to 3 w/o of the ternary additions. Studies will also be made concerning the effect on the cast structure of two or more elemental additions to the aluminum-35 w/o uranium alloy. An evaluation of these effects will dictate the desirability of obtaining further information on the physical properties of these alloys.

## B-3 and B-4

TABLE B-2. TENSILE STRENGTH OF ALUMINUM-35 w/o URANIUM ALLOYS

Alloy Composition, w/o	Method of Preparation	Tensile Strength at Temperature Shown, psi		
		100 C	250 C	400 C
Al-35 U	Air melted	18,500	12,340	4,950
		18,700	13,120	5,240
Al-35 U-2 Sn	Air melted	17,700	10,820	4,350
		18,000	10,830	3,990
Al-35 U-3 Sn	Air melted	18,300	10,240	4,630
		18,500	10,630	4,150
Al-35 U-2 Zr	Air melted	18,500	11,930	4,600
		18,400	12,120	4,530
Al-35 U-3 Zr	Air melted	17,000	11,180	4,010
		17,140	10,670	3,730
Al-35 U-2 Zr	Vacuum melted	18,760	12,000	4,850
		18,900	11,950	4,740
Al-35 U-3 Zr	Vacuum melted	18,750	11,940	5,140
		18,900	11,860	4,880



C-1

## C. RADIOISOTOPE AND RADIATION APPLICATIONS

D. N. Sunderman

Research is continuing on a series of programs for the Office of Isotopes Development. These programs involve the application of radioisotopes to industrial quality control, the use of intrinsic tracers in process control, a study of the effect of structure on radiation-induced graft polymerization, and the radiation-induced nitration of hydrocarbons.

Further experimentation on the sequential determination of iron and aluminum in the same solution show that the presence of aluminum increases the solubility of the  $Y_2^{91}(C_2O_4)_3$  indicator prematurely, giving a titration curve which is difficult to interpret quantitatively. The titration of iron alone using a similar procedure appears promising, but further experimentation is necessary to establish its accuracy and precision. A somewhat different technique for the determination of aluminum is being studied. This technique involves the addition of an excess of EDTA followed by the addition of phosphate ion tagged with phosphorus-32 and back-titration of the excess EDTA with barium. A radioassay of the solution provides a measure of the amount of phosphate consumed in the precipitation of  $Ba_3(P^{32}O_4)_2$  and, therefore, a measure of the excess EDTA.

The determination of detector sensitivity by batch studies has been confirmed using a circulating-loop system. The effect of salt concentration on detector sensitivity has been evaluated over the range of interest in the iron-removal process. Results indicate the effect of salt concentration will not be significant. Other applications of the iron-removal process have been found in the electrolytic process for the preparation of nickel and zinc. These applications are very similar to the ammonia-leach nickel system and could be demonstrated in similar equipment.

The effect of radiation dose on active-site formation has been determined for polymethyl-, polyethyl-, and polybutylmethacrylates. The number of active sites was found to increase to a maximum value and then decrease with increased radiation dose. Several explanations are suggested for this phenomenon. These include a change in fluidity of the polymer system, the formation of two separate free-radical species, or the existence of highly radiation sensitive points in the polymer structure. The G-values have been determined for active-site formation, and good agreement was obtained with literature values where available.

The effect of radiation on the nitration of cyclohexane has been studied over the range of 15 to 70 w/o nitric acid with a 10-to-1 ratio of organic to acid. Results confirmed earlier findings that radiation inhibits the nitration of this material under the conditions studied. Further work will be directed toward an evaluation of nitrating agents other than nitric acid.

Development of Radioactive-Tracer Quality-Control Systems

C. W. Townley, C. T. Brown, R. Lieberman, and D. N. Sunderman

During the past month work was continued on the development of a radiometric-titration method of determining aluminum and iron in portland cement. Investigations were carried out involving consecutive titrations of both iron and aluminum in single solutions as well as assay of the elements in separate analyses.

The combined EDTA titration procedure employed  $Y_2^{91}(C_2O_4)_3$  as an indicator in the iron (III) determination and  $Ag^{110}IO_3$  as an endpoint indicator for the aluminum. The initial solution used in the iron titrations contained 11.2 mg of iron (III) and 11.3 mg of aluminum in a volume of 40 to 50 ml. The pH range studied was from 4 to 6.

It was found that the presence of the aluminum interfered with the accurate determination of the iron (III). The initial solubility of the  $Y_2^{91}(C_2O_4)_3$  was markedly increased, causing a premature rise in counting rate of the filtered solution. Attempts to mask the aluminum during the iron (III) titration using excess tartaric acid, fluoride, and oxalate ions were not successful.

The study of the iron (III) titration in the absence of aluminum was continued. The optimum pH was found to be between 5 and 6 with sodium acetate as a buffer. Tartaric acid (50 mg) was used as a weak initial complexing agent to hold the iron in solution at this pH. It was found that excess tartaric acid interfered with the determination.

The separate aluminum titration was also studied during the month. Use of  $Ag^{110}IO_3$  in this procedure necessitated carrying out the titration at a pH greater than 7. This was due to the instability of the silver complex with EDTA at lower pH values. In order to prevent precipitation of  $Al(OH)_3$  from the basic solution, tartaric acid was used as an initial chelating agent. It was found that the presence of the tartrate prevented the accurate determination of aluminum using  $Ag^{110}IO_3$ .

The aluminum procedure was modified by chelating the cation with a known excess of standard EDTA. The pH was adjusted to 10, and an excess of soluble phosphate tagged with phosphorus-32 was added to the mixture. A back-titration for the excess EDTA was carried out using a standard  $BaCl_2$  solution. The formation of insoluble  $Ba_2(P^{32}O_4)_2$  with the subsequent decrease in counting rate of the solution was used to determine the endpoint.

During the coming month the limits of precision and accuracy of the individual iron (III) and aluminum procedures will be determined. Work on a procedure for the radiometric determination of sulfate in portland cement will also be carried out during the next report period.

Use of Intrinsic Radioactive Tracers for Process Control

J. L. McFarling, J. F. Kircher, and D. N. Sunderman

The previously reported experimental work on count rate versus tracer concentration was confirmed this month. The effect of variations in dissolved salt concentration on solution and count rate was also studied. The evaluation of iron-removal operations in various nonferrous metal refineries was continued.

The results of both bench-type and loop experiments on the variation of count rate with iron-59 tracer concentration show a linear relationship over the concentration range studied. Deviations from the expected average count rate were within the statistical accuracy to be expected for the counting rates employed.

A series of experiments has been carried out to determine the effect of varying dissolved salt concentration on the observed solution counting rate. The averages of several experimental results are shown in Table C-1. The experiments show that the observed count rate is independent of salt concentration within the range of interest.

TABLE C-1. THE EFFECT OF SALT CONCENTRATION  
ON DETECTOR EFFICIENCY

Metal Salt Concentration, g per liter	Number of Experimental Runs	Average Count Rate, CPM $\pm \sigma$
10	4	2990 $\pm$ 25
20	4	3020 $\pm$ 25
30	4	3040 $\pm$ 25
40	5	3000 $\pm$ 25
50	5	2990 $\pm$ 25
60	5	3020 $\pm$ 25
70	5	3030 $\pm$ 25
80	4	3020 $\pm$ 25

Construction has begun on pilot-plant-scale equipment for study of iron-removal processes. This equipment, which is planned to operate at a solution throughput of 1/2 liter per min, will be used initially to study iron removal in the ammonia-leach nickel process.

Along with the equipment-construction phase now under way, the study of other cases of iron removal in nonferrous metal refining is being continued. The aluminum, copper, lead, nickel, and zinc industries have been surveyed so far.

In addition to applications discussed in previous reports, there is a possible application of radiotracer control in the electrolytic nickel-refining process. In this process it is necessary to remove iron from the electrolyte so that pure nickel is deposited on the cathodes. Since the iron is precipitated as the hydroxide in this case, it appears that this application would be quite similar to the process now being studied.

Another application which is being investigated is in electrolytic zinc refining where one step of the process removes by precipitation iron and aluminum hydroxide plus other impurities. This potential application will be studied in more detail.

Next month emphasis will be placed on construction of the model process equipment. The literature survey of other potential processes will be continued as time permits.

#### Graft-Polymerization Studies

I. S. Ungar, J. F. Kircher, W. B. Gager, and R. I. Leininger

During December the investigation of the formation and decay of radiation-induced free radicals was continued. Data are being obtained to determine the effect of total dose on site formation. Thus far, the experiments with polymethyl- (PMMA), polyethyl- (PEMA), and polybutylmethacrylates (PEMA) have been completed. A comparison of the curves of dose versus sites for the three polymers reveals that in each case the number of total sites increases to a maximum and then decreases with increased dosage. As a further indication that some change has occurred, an examination of the EPR spectra after the maximum has been reached shows that the spectra have changed from a relatively simple form to a complex nine-line structure usually found in commercial PMMA or PMMA contaminated with monomer.

Several possible reasons for the decrease in active sites at high dosages are possible. Among these are:

- (1) There is a physical or chemical change in the polymer caused by radiation. For example, an increase in fluidity (decrease in rigidity) caused by the formation of monomer could allow an increase in the rate of disappearance of the free radicals, or the amount of polymer present could be decreased by the formation of monomer. Both seem unlikely because very small amounts of monomer are formed and the change in fluidity does not seem important because PBMA, which is much less rigid than PMMA, also shows this effect.
- (2) There seems to be a possibility that two free-radical species are formed during the irradiation. In the initial stages, the free radical results from the irradiation of the pure polymer which gives the diffuse, unresolved spectrum. As the irradiation proceeds, monomer is formed and the resultant nine-peak spectrum results from an interaction between the irradiated polymer and monomer. If the second species formed has a shorter half-life, it would lead to a decrease in free radicals at some large dose.
- (3) If there are highly radiation-sensitive points in the polymer these would be affected first by the radiation, leaving more resistant groups during the latter stages of the irradiation. This could also

## C-5

account for the decrease in number of sites after longer irradiations. Branching in the polymer could lead to sites more vulnerable to radiation.

A study of  $G_{sites}$  for different dosages indicates that the  $G$ -value decreases with increasing dosage. Extrapolation of the curve to zero dose permits the determination of the initial value for  $G_{site}$  formation at a time when the decay reaction is small. The values obtained for site formation were  $G_{site} = 22$  (PMMA),  $G_{site} = 12$  (PEMA), and  $G_{site} = 10$  (PBMA). The values reported for PMMA is in very good agreement with Prevost-Bernas and co-workers who reported  $G_{radical} = 22.5$ . It should be noted that they employed a very low dose in determining the rate of radical formation.

The investigation is continuing along the lines indicated above. The effect of dose on site concentration is being determined for selected polymethacrylates in an attempt to elucidate the mechanism of site formation. Other polymer samples are being irradiated to different dosages to determine if the half-lives of the radicals formed at low dosages are different from those of radicals formed at high dosages. Samples of PMMA of different molecular weights are being irradiated to determine if a molecular-weight effect exists.

#### Nitration of Hydrocarbons

M. J. Oestmann, G. A. Lutz, E. J. Kahler,  
and J. F. Kircher

During December, 12 irradiation and thermal runs were completed with nitric acid-cyclohexane in the liquid phase. Analytical results were obtained chiefly by gas chromatography and are reported in Table C-2.

Glass reaction vessels were used in all runs to contain the 10-to-1 mole ratio of cyclohexane to nitric acid. Samples were heated at 60 or 110 C from 6.5 to 96 hr. In the irradiation runs the gamma doses ranged from  $1 \times 10^6$  to  $1.8 \times 10^7$  rads.

To investigate the effect of nitric acid dilution on the nitration reaction, Runs 32 and 33 were made at 60 C with a 70 w/o nitric acid solution and Runs 34 and 35 with about 35 w/o acid. At 110 C Run 36 was made with a 35 w/o nitric acid solution for comparison with Run 15 reported last month in BMI-1398. In all runs, the mole ratio of C-C<sub>6</sub>H<sub>12</sub>/HNO<sub>3</sub> was kept constant at 10-to-1. At both temperatures, the yield of nitrocyclohexane was smaller in the dilute nitric acid. Runs 34 and 35 yielded no measurable products at all. In Run 15, 4.5 w/o of nitrocyclohexane was produced as against 3.8 w/o in the dilute acid Run 35.

Several explosions occurred during dilute nitric acid runs at 110 C, and runs at 140 C. The literature suggests that formation of a cyclic ketone is responsible for explosions in nitric acid-cyclohexane systems. In all future runs temperatures will be limited to 100 C.

TABLE C-2. PRODUCT ANALYSIS OF NITRIC ACID-CYCLOHEXANE RUNS<sup>(a)</sup>

Run	Temperature, C	Time, hr	Gamma Dose, 10 <sup>6</sup> rads	Product Analysis, w/o of recovered organic solution						(CH <sub>2</sub> ) <sub>4</sub> (COOH) <sub>2</sub> or Other Solids
				C <sub>6</sub> H <sub>11</sub> NO <sub>2</sub>	(C <sub>6</sub> H <sub>11</sub> ) <sub>m</sub> (NO <sub>2</sub> ) <sub>n</sub>	C <sub>6</sub> H <sub>11</sub> ONO <sub>2</sub>	(C <sub>6</sub> H <sub>11</sub> ) <sub>2</sub>	C <sub>6</sub> H <sub>11</sub> OH	C <sub>5</sub> H <sub>10</sub> C=O	
32	60	6.5	1.2	0.03	--	--	--	Trace	--	--
33	60	6.5	--	0.04	--	--	--	--	--	--
34	60	7.5	1.4	--	--	--	--	--	--	--
35	60	7.5	--	--	--	--	--	--	--	--
40	60	15	2.8	0.2	--	--	--	--	--	--
38	60	30	5.7	0.6	--	--	--	--	--	0.21
29	60	45	8.6	0.8	Trace	--	0.04	Trace	Trace	0.21
39	60	45	8.6	0.8	--	--	--	Trace	Trace	0.45
28	60	45	--	2.7	0.2	--	0.1	Trace	Trace	2.13
36	110	24	4.5	3.8	--	--	--	0.3	0.04	0.38
31	110	96	18.2	5.9	Trace	Trace	0.07	0.5	0.6	0.76
30	110	96	--	7.0	Trace	Trace	0.2	0.3	0.2	1.35

(a) All runs were made at a 10/1 mole ratio of cyclohexane/nitric acid in glass vessels.

(b) The weight per cent of adipic acid or other solids is based on the original charge of cyclohexane.

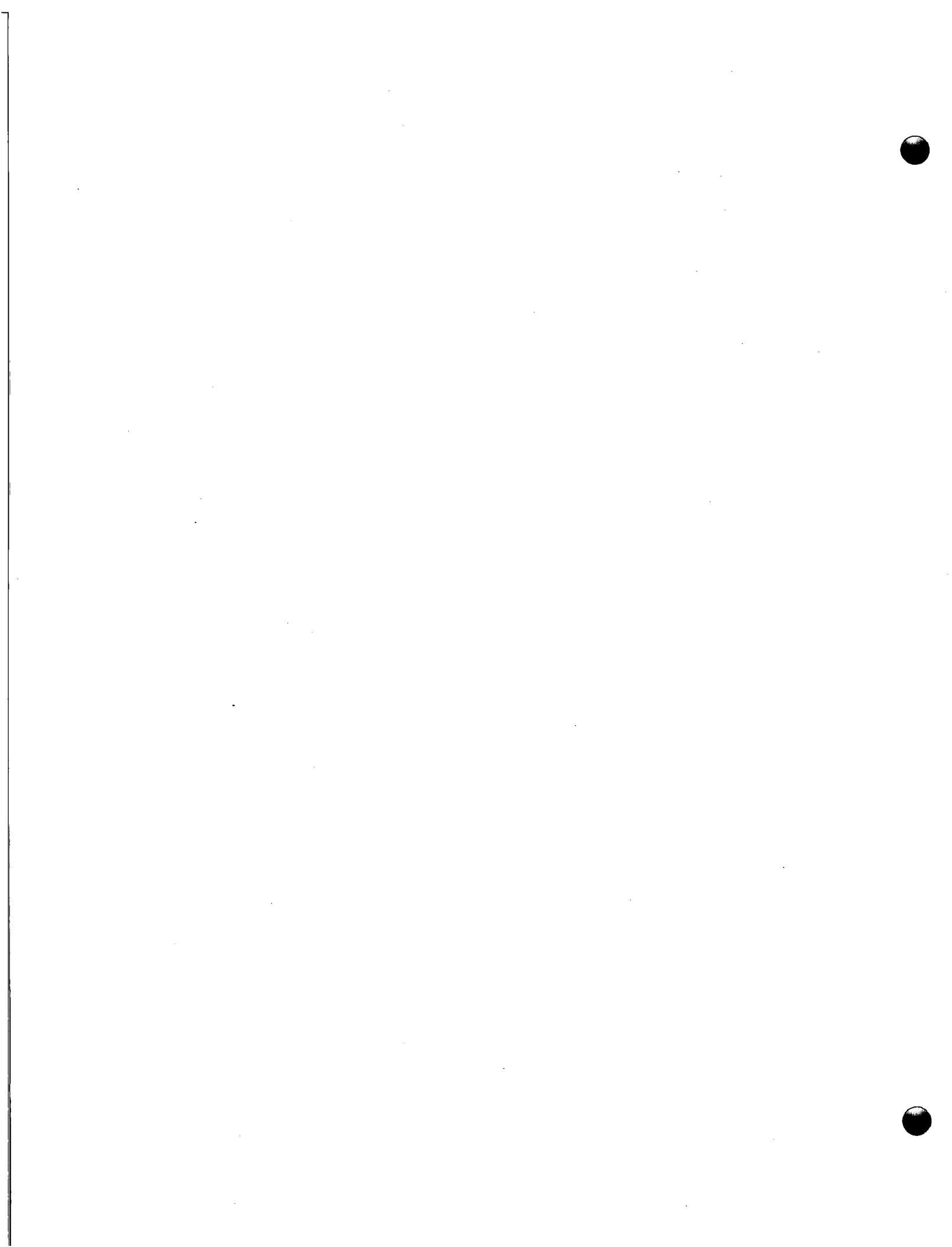
C-6

## C-7 and C-8

A review of runs in Table C-2 and those reported last month in BMI-1398 confirms the general inhibitory effect of radiation at all temperatures investigated. However, at or near 20-hr exposures, radiation produces a slight increase in the amount of nitration (nitrocyclohexane) at all temperatures. This radiation effect is not understood.

A few additional runs with the nitric acid-cyclohexane system will be conducted in January. It is hoped that analyses of gaseous products in these runs will help clarify the retarding effect of radiation on nitration. The apparent increase in nitration at 20-hr exposures will be confirmed, and the stability of nitrocyclohexane in this system will be investigated.

A few exploratory runs with the  $\text{NO}_2$ -cyclohexane system are planned. The purpose of this series of experiments is to determine whether the inhibitory effect of radiation depends on the type of nitrating agent.



D-1 and D-2

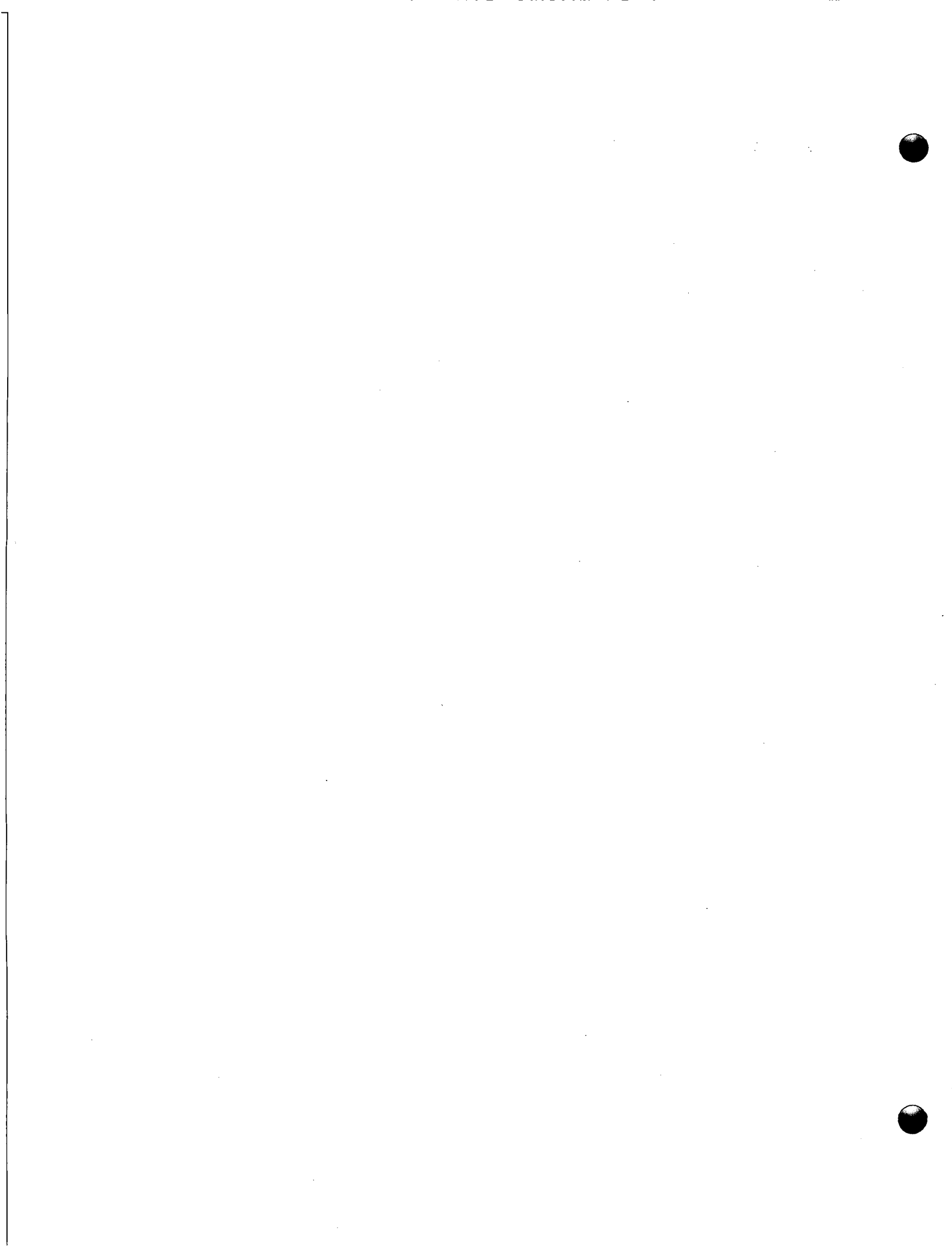
D. VARIABLE-MODERATOR REACTOR CRITICAL-ASSEMBLY STUDIES

R. A. Egen, D. A. Dingee, and J. W. Chastain

Critical-assembly studies will be performed by Battelle for the Advanced Technology Laboratories of the American Standard Corporation to aid in the development of the Variable-Moderator Reactor.

Preparation for the critical-assembly studies have been in progress since November, 1959. During December the Hazards Summary Report was completed. The critical-assembly support stand was constructed, and construction of the core vessel, base plate, and liquid-storage facilities was begun. Most of the remaining components were ordered.

All of the components should be available for assembly before the end of January. These include core components from the Advanced Technology Laboratories which are scheduled to arrive late in the month. The fuel is not expected to arrive until early February.



F-1

## F. RESEARCH FOR AEC REACTOR DEVELOPMENT DIVISION PROGRAM

S. J. Paprocki and R. F. Dickerson

REACTOR MATERIALS AND COMPONENTS

R. F. Dickerson

In an attempt to reduce the amount of  $\text{La}_2\text{O}_3$  or  $\text{Y}_2\text{O}_3$  additive needed to stabilize  $\text{UO}_2$  in high-temperature air, bodies have been prepared with ternary additions of  $\text{CaO}$ . These materials, as sintered in vacuum at 1700 C, initially have a low electrical conductivity. Oxidation, produced by heating in air, causes a rapid increase in this conductivity. Bodies of  $\text{U}_3\text{O}_8$  containing 40, 50, and 60 mole per cent  $\text{La}_2\text{O}_3$  are being produced so that information with respect to electrical characteristics and thermal conductivity of fully oxidized solid solutions can be obtained. Studies of the effects of combined high pressure and high temperature on the uranium oxides and on the reaction of uranium oxides with other oxide systems are still in progress.

The irradiation of tensile, cyclic-strain fatigue, and impact specimens of Type 347 stainless steel continues. Estimated exposures as high as  $4.5 \times 10^{21}$  nvt have been achieved to date, with the ultimate exposure goal at  $1.8 \times 10^{22}$  nvt. At present there is a lack of correlation between the fast-flux data obtained as a result of spot checks at the ETR and dosimetry data obtained by BMI. Attempts are being made to resolve this apparent difference in flux values. Negotiations are in progress to obtain space for the gamma-heat capsules in the WTR.

In order to determine the weldability of niobium-base binary alloys containing 1.84 or 3.21 w/o chromium, or 4.33 w/o zirconium and niobium-base ternary alloys containing chromium, tantalum, and titanium, welding studies on 0.010-in. sheet are in progress. Quality of welds will be evaluated by bend testing and tensile testing. Additional ingots of the alloys have been made in order to obtain more sheet material for tensile testing. Experimental work concerned with the development of water-corrosion-resistant niobium alloys has been completed, and data are being evaluated prior to the preparation of a topical report.

The design of the testing device for use in the study of the in-pile creep of Zircaloy-2 is being completed. Principal features of the design include several thermocouples located between a stressed sheet-type specimen and an identical unstressed specimen parallel with it, electric heaters cast into aluminum blocks designed for uniform heat dissipation, and a stainless steel bellows which, when compressed by helium pressure inside the capsule, will apply stress to the specimen. Four of these test devices will be constructed; two will be used for out-of-pile tests, and two will be inserted in the WTR. Internal-friction studies have been continued in an attempt to detect strain aging in the material at elevated temperatures.

The studies concerned with the development of techniques capable of determining the amount of oxygen in sodium at levels below 10 ppm have been continued.

Valence Effects of Oxide Additions to Uranium Dioxide

W. B. Wilson and C. M. Schwartz

An investigation is being conducted on the effect of oxide additions to uranium oxide. Previous research has been directed toward determination of the mechanism of stabilization of uranium oxide by appropriate additions of  $\text{La}_2\text{O}_3$  and  $\text{Y}_2\text{O}_3$ .

Recent work has been directed toward reduction of the amount of oxide addition required to achieve a stable material with respect to high-temperature-air oxidation. In conjunction with this phase of the work, conductivity and thermoelectric-power studies were conducted on the following solid solutions, for which oxidation behavior was previously reported:

Composition, mole per cent $\text{UO}_2\text{-20 La}_2\text{O}_3\text{-20 CaO}$  $\text{UO}_2\text{-25 La}_2\text{O}_3\text{-25 CaO}$  $\text{UO}_2\text{-20 Y}_2\text{O}_3\text{-20 CaO}$  $\text{UO}_2\text{-25 Y}_2\text{O}_3\text{-20 CaO}$ 

These materials, as sintered in vacuum at 1700 C, initially have a very low conductivity. Oxidation, produced by heating in air, caused a rapid increase in conductivity. Thermoelectric power for these stabilized solid solutions was low with its sign changing reversibly from *p*-type to *n*-type with increasing temperature. Such behavior has previously been observed to be associated with the more stable compositions exhibiting the smallest vapor pressure.

Final preparation of compositions of  $\text{U}_3\text{O}_8$  containing 40, 50, and 60 mole per cent  $\text{La}_2\text{O}_3$  are in process. These will be utilized to obtain additional information with respect to the electrical characteristics and thermal conductivity of the fully oxidized solid solutions. The solid solution of  $\text{UO}_2$  containing 2 mole per cent  $\text{La}_2\text{O}_3$  has been resintered and reprepared for thermal-conductivity studies.

High-Pressure High-Temperature Solid-State Studies

W. B. Wilson and C. M. Schwartz

An investigation is being conducted on the effects of combined high pressure and high temperature on the uranium oxides and on the reaction of uranium oxides with other oxide systems. In previous work emphasis has been placed on the study of the effects of pressure on  $\text{U}_3\text{O}_8$ .

A new modification, designated gamma  $\text{U}_3\text{O}_8$ , was produced at pressures above 16,000 atm at temperatures above 400 C. Structural studies were continued in an

## F-3

attempt to index the X-ray diffraction pattern obtained by powder techniques. A tentative indexing was established based upon an hexagonal (rhombohedral) cell with  $a = 8.78 \text{ \AA}$  and  $c = 9.19 \text{ \AA}$ . Since the volume of this unit cell is similar, although smaller, than that of the other modifications of  $\text{U}_3\text{O}_8$ , it was assumed to contain the same number of  $\text{U}_3\text{O}_8$  molecules. On this basis a theoretical density was obtained for gamma  $\text{U}_3\text{O}_8$  at  $\rho = 9.15 \text{ g per cm}^3$ . Measured density of the gamma modification, obtained by vacuum pycnometric technique, averaged  $\rho = 9.25 \text{ g per cm}^3$ . Deviation from stoichiometry and errors inherent in the lattice-parameter and pycnometric data could well account for the small difference obtained between the theoretical and measured density.

The density of both the alpha and beta modifications of  $\text{U}_3\text{O}_8$ , which occur at normal pressure, is known to be  $8.38 \text{ g per cm}^3$ . Thus, the high-pressure modification with a value of  $9.15 \text{ g per cm}^3$  exhibits an increase in density of about 10 per cent.

In previous work, results were obtained indicating the possible pressure decomposition of  $\text{U}_4\text{O}_9$ , which is believed to be cubic of fluorite structure with a lattice parameter slightly smaller than  $\text{UO}_2$ . Since  $\text{U}_4\text{O}_9$  is assumed to be the most dense oxide of uranium, its pressure decomposition appears anomalous. In order to confirm or disprove the previous results,  $\text{U}_4\text{O}_9$  samples were subjected to pressure and temperature. Results are not as yet available.

In order to extend the ultimate pressure obtainable in the high-pressure equipment, minor design modifications were introduced. Evaluation of these modifications has been initiated.

#### Irradiation-Surveillance Program on Type 347 Stainless Steel

W. E. Murr, F. R. Shober, R. Ritzman, and J. F. Lagedrost

An irradiation surveillance program on AISI Type 347 stainless steel is continuing in support of the KAPL C-33 loop and other loops using this material in their construction. The program consists of irradiation and postirradiation mechanical testing of Type 347 stainless steel. Mechanical-property determinations will include tensile tests, cyclic-strain fatigue tests, and impact tests. A considerable fast-neutron exposure range and three irradiation-temperature parameters will be explored by the program. Included are a group of specimens to be irradiated at process-water temperature (120 F), a group of specimens to be irradiated "hot" (600 F), and a group of specimens to be irradiated at 120 F and annealed after irradiation prior to mechanical testing. It is thought that postirradiation annealing represents an intermediate condition between that produced by irradiation at 120 and 600 F. The KAPL loop will operate for an estimated 3 years at temperatures near 570 F, during this time accumulating a fast-neutron flux (above 1 Mev) exposure of between 1.4 and  $1.8 \times 10^{22} \text{ nvt}$ . The aim of this program is to provide information on mechanical properties of Type 347 stainless steel at exposures between  $3.76 \times 10^{21} \text{ nvt}$  (the maximum exposure level reported in literature) and the ultimate level to be reached by the loop.

Eight capsules have been irradiated in ETR core process water since June, 1958. Three capsules to be annealed prior to postirradiation testing have been in the ETR since August, 1959. The irradiation of these two groups of specimens is proceeding routinely.

The capsules to be irradiated near 600 F have not been inserted in the reactor as yet since suitable space has not been available. The capsules require approximately 20 w per g of gamma heating to maintain the specimen design temperature.

Total neutron exposures obtained by the eleven capsules in the ETR as of the end of Cycle 23 (November 30, 1959) are reported in Table F-1. Cycle 23 was for 1660 megawatt-days at an average power level of 163 megawatts. The accumulated exposures reported in Table F-1 are based on flux maps obtained during Cycle 13. Spot checks made at the ETR of the fast fluxes in K and L positions during Cycle 18 indicate that the fast flux was from 4 to 22 per cent higher than that used for calculating the exposures reported in Table F-1. The BMI dosimetry data obtained from these positions during these and subsequent cycles indicate that the flux was considerably lower. Attempts are being made to determine the reasons for this difference.

Negotiations are in progress to insert the "hot" capsules in core positions of the Westinghouse Test Reactor in late January. The initial capsule will be provided with thermocouples and will monitor temperatures of the test specimens at power levels of from 20 to 60 megawatts in order that the additional seven capsules can be most judiciously located in the reactor.

#### Development of Niobium-Base Alloys

J. A. De Mastry, F. R. Shober, and R. F. Dickerson

Utilization of a niobium-base alloy as an alternate cladding material in future core designs for the EBR requires evaluation of the fabricability and of selected mechanical properties of these alloys. The properties of the niobium-base alloys being developed are to be compared with the properties of a vanadium-10 w/o titanium-1 w/o niobium alloy which has demonstrated properties acceptable for the EBR application. The alloys which are being investigated include unalloyed niobium, niobium-1.84 w/o chromium, niobium-3.21 w/o chromium, niobium-4.33 w/o zirconium, niobium-9.95 w/o tantalum-3.31 w/o chromium, niobium-39.8 w/o titanium-10.6 w/o aluminum, niobium-20.5 w/o titanium-4.28 w/o chromium, and vanadium-11.7 w/o titanium-3.07 w/o niobium.

All alloys being investigated were reduced from 70 to 80 per cent by forging at 2500 F in evacuated molybdenum cans. After reduction at 2500 F rolling was attempted at 75 F. The niobium-1.84 w/o chromium, niobium-4.33 w/o zirconium, niobium-20.5 w/o titanium-4.28 w/o chromium, and vanadium-11.7 w/o titanium-3.07 w/o niobium alloys were reduced approximately 80 per cent at 75 F, but developed severe edge cracks and surface defects. The tensile strengths at 1470 F of specimens cut from the cold worked niobium-base alloys were superior to that of the vanadium-base alloy.

TABLE F-1. CAPSULES PREPARED FOR THE TYPE 347 STAINLESS STEEL IRRADIATION SURVEILLANCE PROGRAM

Capsule	Type of Specimens in Capsules	Proposed Irradiation Temperature, F	Approximate Removal Date <sup>(a)</sup>	Approximate Exposure at Time of Removal <sup>(b)</sup> , nvt	Total Exposure as of November 30, 1959, nvt			Location	Remarks
					Top	Bottom			
BMI-24-1	Tensile and fatigue	600	January, 1959	$1.55 \times 10^{20}$	--	--	BMI	Examined at BMI Hot-Cell Facility for melting	
BMI-24-2	Tensile and fatigue	120	January, 1962	$1.31 \times 10^{22}$	$3.258 \times 10^{21}$	$4.078 \times 10^{21}$	ETR K-8-NE	Being irradiated	
BMI-24-3	Tensile and fatigue	600	--	--	--	--	BMI	To be irradiated	
BMI-24-4	Tensile and fatigue	120	January, 1963	$1.78 \times 10^{22}$	$2.327 \times 10^{21}$	$3.625 \times 10^{21}$	ETR K-8-SE	Being irradiated	
BMI-24-5	Tensile and fatigue	600	--	--	--	--	BMI	To be irradiated	
BMI-24-6	Tensile and fatigue	120	June, 1961	$1.08 \times 10^{22}$	$4.221 \times 10^{21}$	$3.301 \times 10^{21}$	ETR K-8-NE	Being irradiated	F-5
BMI-24-7	Tensile and fatigue	600	--	--	--	--	BMI	To be irradiated	
BMI-24-8	Tensile and fatigue	120	June, 1962	$1.54 \times 10^{22}$	$2.625 \times 10^{21}$	$3.672 \times 10^{21}$	ETR K-8-SE	Being irradiated	
BMI-24-9	Tensile and fatigue	600	--	--	--	--	BMI	To be irradiated	
BMI-24-10	Tensile and fatigue	120	January, 1961	$0.84 \times 10^{22}$	$3.550 \times 10^{21}$	$3.551 \times 10^{21}$	ETR K-8-SE	Being irradiated	
BMI-24-11 <sup>(c)</sup>	Tensile and fatigue	600	--	--	--	--	BMI	Damaged at ETR	
BMI-24-12	Tensile and fatigue	120	June, 1960	$0.61 \times 10^{22}$	$4.583 \times 10^{21}$	$3.994 \times 10^{21}$	ETR L-8-SE	Being irradiated	
BMI-24-13	Impact	600	--	--	--	--	BMI	To be irradiated	
BMI-24-14	Impact	120	June, 1962	$1.54 \times 10^{22}$	$3.963 \times 10^{21}$	$4.038 \times 10^{21}$	ETR K-8-NW	Being irradiated	
BMI-24-15	Impact	600	--	--	--	--	BMI	To be irradiated	

TABLE F-1. (Continued)

Capsule	Type of Specimens in Capsules	Proposed Irradiation Temperature, F	Approximate Removal Date <sup>(a)</sup>	Approximate Exposure at Time of Removal <sup>(b)</sup> , nvt	Total Exposure as of November 30, 1959, nvt			Location	Remarks
					Top	Bottom			
BMI-24-16	Impact	120	June, 1960	$0.61 \times 10^{22}$	$4.011 \times 10^{21}$	$3.607 \times 10^{21}$	ETR K-8-NW	Being irradiated	
BMI-24-17 <sup>(c)</sup>	Tensile and fatigue	600	October, 1958	$3.25 \times 10^{20}$	--	--	BMI	Examined at BMI Hot-Cell Facility after high temperature observed	
BMI-24-18	Tensile and fatigue	120	--	--	$4.96 \times 10^{20}$	$7.98 \times 10^{20}$	ETR	Being irradiated for post-irradiation annealing studies	
BMI-24-19 <sup>(c)</sup>	Tensile and fatigue	600	--	--	--	--	BMI	Fabricated to replace BMI-24-17	
BMI-24-20	Tensile and fatigue	120	--	--	$4.99 \times 10^{20}$	$9.17 \times 10^{20}$	ETR	Being irradiated for post-irradiation annealing studies	H-6
BMI-24-21	Tensile and fatigue	600	--	--	--	--	BMI	Fabricated to replace BMI-24-1	
BMI-24-22	Tensile and fatigue	120	--	--	$6.84 \times 10^{20}$	$1.093 \times 10^{21}$	ETR	Being irradiated for post-irradiation annealing studies	

(a) Based on 6-month lead on loop, plus 2 months for examination.

(b) Based on maximum fast flux at tube of  $1.7 \times 10^{14}$  nv for 6-month periods.

(c) Thermocouple lead capsule.

## F-7

Sections cut from all of the forged slabs (2500 F) were rolled at 800 F in air to 0.150-in. sheet. All alloys rolled satisfactorily except for the niobium-39.8 w/o titanium-10.6 w/o aluminum alloy and the niobium-9.95 w/o tantalum-3.31 w/o chromium alloy, both of which fractured during rolling. After this warm-rolling operation, the rolled sheet was sectioned, and a rolling study was conducted at 75 F. Sections which were belt sanded to remove defects and annealed at 2550 F for 1 hr were cold rolled to 0.030-in. sheet. The fabricated sheet had smooth edges and defect-free surfaces. Alloys rolled at 75 F without belt sanding or annealing had rough surfaces and edges.

Pieces of the above-mentioned cold-rolled sheet prepared from stock that was belt sanded and annealed were then further reduced to 0.010-in. sheet for welding studies. Two methods are being utilized for evaluation of the weldability of the niobium-base alloys. The ductility of the welds is being tested by welding two sheets of 0.010-in. material longitudinally and bending the welded sheet parallel with the direction of the weld in a bench vise. The strength of the welds will be determined by spot welding two 0.010-in.-thick sheets of material together and then pulling the welds apart in a tensile machine. Specimens for both of the above-mentioned tests are being prepared.

Duplicate ingots of unalloyed niobium, niobium-1 w/o chromium, niobium-3 w/o zirconium, niobium-10 w/o titanium-3 w/o chromium, and niobium-4.5 w/o molybdenum alloys have been prepared by double consumable-electrode arc melting. The ingots prepared will be sectioned into 3/4-in. wafers. Forging of these wafers will be attempted at 800 F. If fabrication at 800 F is not successful, higher temperatures will be employed until a satisfactory fabrication temperature is determined. It is hoped that fabrication temperatures near 800 F can be used, so that protection from oxidation will not be required. After sufficient working of the metal has been accomplished, the forged slabs will be rolled to sheet.

After obtaining fabricated material, the tensile strengths of the alloys will be determined at 1470 F, and additional weldability studies will be performed.

#### Development of Corrosion-Resistant Niobium Alloys

D. J. Maykuth, W. D. Klopp, E. F. Adkins,  
R. I. Jaffee, W. E. Berry, and F. W. Fink

The selection and fabrication of niobium-base alloys for possible service in pressurized-water reactors have been completed. Prior work indicated that binary additions of 7 to 12 a/o vanadium offer optimum combinations of low neutron cross section, high-temperature strength, and corrosion resistance. The objective of the most recent work is to determine whether lower alloying levels, which result in improved fabricability, can be used without seriously affecting the alloy's corrosion behavior.

Fabrication of the four double consumable-electrode arc-melted alloy ingots listed below was carried out using pack-rolling techniques. Each ingot was cut into

two slabs which were weld-sealed in evacuated stainless steel cans and flat rolled at 1800 F. All of the ingots rolled to excellent-quality sheet. After surface cleaning by grinding, each was vacuum annealed 1 hr at 1200 C and cut into samples for corrosion testing.

<u>Alloy</u>	<u>Nominal Alloy Content (Balance Niobium), a/o</u>	<u>Annealed Hardness, VHN</u>
NL-11	7.5 V	176
NL-12	7.5 V-0.19 N <sup>(a)</sup>	207
NL-13	7.5 V-2.5 Ti	193
NL-14	7.5 V-2.5 Mo	205

(a) Equivalent to 0.03 w/o nitrogen.

The results of corrosion tests in 600 and 680 F water and 750 F 1500-psi steam continue to indicate that:

- (1) Unalloyed niobium is not sufficiently corrosion resistant for use as a cladding material in pressurized-water reactors.
- (2) Additions of titanium, vanadium, and zirconium singly or in combination markedly improve the corrosion resistance of niobium.
- (3) The most corrosion-resistant alloys are binaries or ternaries containing more than 45 a/o zirconium or a ternary containing 28 a/o titanium-6 a/o chromium.
- (4) A 12.6 a/o vanadium alloy possesses the optimum combination of high-temperature strength, low cross section, and adequate corrosion resistance.
- (5) Ternary additions on the order of 2.5 a/o of aluminum, chromium, iron, molybdenum, nickel, titanium, or zirconium to niobium-2.5 a/o vanadium alloys do not result in increased corrosion resistance.

Corrosion results obtained to date for exposure times ranging up to 280 days are summarized in Table F-2.

The corrosion tests with unalloyed niobium, which are being performed in co-operation with the Bettis and Knolls Laboratories, have been suspended after 120 days of total exposure. The average weight change for groups of six specimens was +64.1 mg per dm<sup>2</sup> for exposure to 680 F water and -1675 mg per dm<sup>2</sup> for exposure to 750 F steam. Specimens in 680 F water slowly lost weight after a peak weight gain of 121 mg per dm<sup>2</sup> at 42 days of exposure. Those exposed to 750 F steam lost weight at an erratic rate after 28 days of exposure.

TABLE F-2. SUMMARY OF CORROSION RESULTS OBTAINED ON NIOBIUM ALLOYS EXPOSED TO HIGH-TEMPERATURE WATER AND STEAM

Alloy Addition (Balance Niobium), a/o	600 F Water		680 F Water		750 F Steam	
	Exposure Time, days	Total Weight Change, mg per cm <sup>2</sup>	Exposure Time, days	Total Weight Change, mg per cm <sup>2</sup>	Exposure Time, days	Total Weight Change, mg per cm <sup>2</sup>
<u>Commercial Niobium, Rocking-Hearth Melts</u>						
Unalloyed Nb	280	-39.9	42 <sup>(a)</sup>	Disintegrated	28 <sup>(a)</sup>	Disintegrated
10.5 Zr	--	--	196 <sup>(a)</sup>	0.67	168	-27.9
26.1 Zr	--	--	196 <sup>(a)</sup>	0.07	--	--
35.7 Zr	--	--	196 <sup>(a)</sup>	0.66	--	--
45.7 Zr	--	--	196 <sup>(a)</sup>	0.55	--	--
1.08 W	--	--	196 <sup>(a)</sup>	-2.60	168	-31.4
4.67 W	--	--	196 <sup>(a)</sup>	-29.3	--	--
9.56 W	--	--	7 <sup>(a)</sup>	Cracked	--	--
2.45 Mo	--	--	196 <sup>(a)</sup>	-7.10	98	Disintegrated in 98 days
5.20 Mo	--	--	196 <sup>(a)</sup>	-1.30	168	-126.4
7.40 Mo	--	--	196 <sup>(a)</sup>	0.62	--	--
4.42 V	--	--	196 <sup>(a)</sup>	0.42	168	-10.0
6.59 V	--	--	196 <sup>(a)</sup>	0.73	168	1.22
8.93 V	--	--	196 <sup>(a)</sup>	0.59	168	1.06
10.7 V	--	--	196 <sup>(a)</sup>	0.78	--	--
13.7 V	--	--	196 <sup>(a)</sup>	0.50	--	--
24.2 V	--	--	196 <sup>(a)</sup>	0	--	--
4.90 Fe	--	--	196 <sup>(a)</sup>	0.10	98	Disintegrated in 98 days
9.41 Ti	--	--	196 <sup>(a)</sup>	0.65	168	1.27
18.8 Ti	--	--	196 <sup>(a)</sup>	0.48	--	--
24.3 Ti	--	--	196 <sup>(a)</sup>	0.52	--	--
30.5 Ti	--	--	196 <sup>(a)</sup>	0.40	--	--
33.8 Ti	--	--	196 <sup>(a)</sup>	0.33	--	--
12.0 Ti-0.5 Cr	--	--	196 <sup>(a)</sup>	0.66	--	--
20.2 Ti-2.1 Cr	--	--	196 <sup>(a)</sup>	0.39	--	--
28.2 Ti-6.1 Cr	--	--	196 <sup>(a)</sup>	0.20	--	--
12.0 Ti-4.2 Mo	--	--	196 <sup>(a)</sup>	0.64	--	--
17.4 Ti-6.2 Mo	--	--	196 <sup>(a)</sup>	0.54	--	--
23.1 Ti-7.8 Mo	--	--	196 <sup>(a)</sup>	0.45	--	--
10.4 Ti-5.0 V	--	--	196 <sup>(a)</sup>	0.56	--	--
16.1 Ti-8.4 V	--	--	196 <sup>(a)</sup>	0.40	--	--
22.6 Ti-11.0 V	--	--	196 <sup>(a)</sup>	0.48	--	--

TABLE F-2. (Continued)

Alloy Addition (Balance Niobium), a/o	600 F Water		680 F Water		750 F Steam	
	Exposure Time, days	Total Weight Change, mg per cm <sup>2</sup>	Exposure Time, days	Total Weight Change, mg per cm <sup>2</sup>	Exposure Time, days	Total Weight Change, mg per cm <sup>2</sup>
<u>High-Purity Niobium, Consumable-Electrode Melts</u>						
Unalloyed Nb	280	0.76	256	-1.90	224 <sup>(a)</sup>	-54.0
7.18 Mo	280	0.73	256 <sup>(a)</sup>	Cracked	70 <sup>(a)</sup>	Cracked
12.5 V	280	0.40	256	0.64	252	0.84
46.8 Zr-5.06 Ti	224	0.30	224	1.04	224	2.58
11.2 Ti-3.2 Mo	224	0.46	224	0.66	224	0.46
18.8 Ti-8.7 Mo	224	0.26	224	0.59	224	0.57
9.9 Zr-9.4 V	140	0.13	140	0.37	140	-3.95
5.7 Zr-11.4 V	140	0.11	140	0.39	140	-1.19
9.1 Ti-6.3 Cr	140	0.09	140	0.40	140	-3.30
<u>High-Purity Niobium, Rocking-Hearth Melts</u>						
Unalloyed Nb	--	--	168	0.65 <sup>(b)</sup>	--	--
Unalloyed Nb	--	--	84 <sup>(a)</sup>	Disintegrated in 84 days	--	--
Unalloyed Nb	--	--	112	0.58 <sup>(b)</sup>	--	--
1.1 Zr	--	--	168 <sup>(a)</sup>	Disintegrated	--	--
2.2 Zr	--	--	84	-14.8	--	--
5 Zr	--	--	140	-8.07	--	--
10.2 Zr	--	--	140	0.05 <sup>(b)</sup>	--	--
40 Zr	--	--	140	0.60	--	--
65 Zr	--	--	140	0.70	--	--
75 Zr	--	--	140	0.84	--	--
90 Zr	--	--	140	1.20	--	--
3.2 Ti	--	--	168	-4.98	--	--
10.5 Ti	--	--	168	0.64	--	--
25.0 Ti	--	--	168	0.47	--	--
<0.02 Cr	--	--	168	0.78 <sup>(b)</sup>	--	--
0.5 Cr	--	--	168	0.17 <sup>(b)</sup>	--	--
0.5 Cr	--	--	140	-2.66	--	--
<0.08 Fe	--	--	140	-0.87	--	--
0.3 Fe	--	--	84	-10.4	--	--
10 Fe	--	--	28 <sup>(a)</sup>	Cracked	--	--

## F-11

TABLE F-2. (Continued)

Alloy Addition (Balance Niobium), a/o	600 F Water		680 F Water		750 F Steam	
	Exposure Time, days	Total Weight Change, mg per cm <sup>2</sup>	Exposure Time, days	Total Weight Change, mg per cm <sup>2</sup>	Exposure Time, days	Total Weight Change, mg per cm <sup>2</sup>
10.9 Zr-5.1 Ti	--	--	140	0.59	--	--
25 Zr-5 Ti	--	--	140	0.01(b)	--	--
25 Zr-15 Ti	--	--	140	0.60	--	--
25 Zr-25 Ti	--	--	140	0.51	--	--
35 Zr-5 Ti	--	--	140	0.58	--	--
35 Zr-15 Ti	--	--	140	0.51	--	--
45 Zr-5 Ti	--	--	140	0.72	--	--
10 Zr-5 Mo	--	--	140	0.32	--	--
35 Zr-5 Mo	--	--	140	0.53	--	--
45 Zr-5 Mo	--	--	140	0.63	--	--
35 Zr-5 Al	--	--	140	0.46	--	--
45 Zr-5 Al	--	--	140	0.60	--	--
10 Zr-5 Cr	--	--	140	0.54	--	--
45 Zr-5 Cr	--	--	140	0.46	--	--
10 Zr-5 Fe	--	--	140	0.29	--	--
2.5 V	--	--	168	0.64	--	--
2.0 V-2.5 Ti	--	--	140	0.79	--	--
2.0 V-2.3 Mo	--	--	140	0.89	--	--
2.2 V-0.54 Fe	--	--	140	0.70	--	--
1.8 V-<0.02 Cr	--	--	140	0.49	--	--
1.8 V-0.14 Al	--	--	140	0.88	--	--
2.5 V-2.5 Zr	--	--	56	-1.70	--	--
2.2 V-0.87 Ni	--	--	28(a)	-1.00	--	--
4.0 V-2.3 Zr	--	--	140	0.60	--	--
5 V-25 Zr	--	--	140	-0.72	--	--
5 V-35 Zr	--	--	140	-1.38	--	--
5 V-45 Zr	--	--	140	0.52	--	--
1 Ce	--	--	14	0.75	--	--
1 Y	--	--	14	-2.19	--	--
5 Y	--	--	14	-5.75	--	--
1 Pd	--	--	14	16.2	--	--
5 V-2.5 Ti	--	--	14	0.19	--	--
5 V-2.5 Cr	--	--	14	0.20	--	--
5 V-2.5 Al	--	--	14	0.16	--	--
10 Zr	--	--	--	--	42	-0.77
10 Ti	--	--	--	--	42	0.40

(a) Off test.

(b) Losing weight.

Corrosion tests have been started on the alloys described below. No results are available to date.

Exposure Conditions	Composition (Balance Niobium), a/o
Consumable-electrode melts exposed to 600 and 680 F water and 750 F steam	7.5 vanadium 7.5 vanadium-0.19 nitrogen 7.5 vanadium-2.5 titanium 7.5 vanadium-2.5 molybdenum
Rocking-hearth melts (50-g ingots) exposed to 680 F water	1, 2.5, and 5 nickel 5 vanadium 5 vanadium-2.5 iron, -nickel, or -molybdenum 0.5 carbon-2.5 and -5 vanadium 0.5 carbon-0.5 titanium-2.5 and -5 vanadium 0.5 carbon-0.5 zirconium-2.5 and -5 vanadium 0.5 oxygen-0.25 titanium-2.5 and -5 vanadium 0.5 oxygen-0.25 zirconium-2.5 and -5 vanadium

A topical report, summarizing all of the results of the research which have been obtained to date, is being prepared.

Investigation of the Creep Properties of Zircaloy-2  
During Irradiation at Elevated Temperatures

F. R. Shober, P. B. Shumaker, A. P. Young,  
M. F. Amateau, and R. F. Dickerson

The effect of irradiation on the creep properties of Zircaloy-2 at elevated temperatures is to be studied by comparing total elongation obtained from creep tests in reactor under a fast neutron flux with those obtained from an identical out-of-reactor test. The initial temperature to be investigated will be 650 F. A study of strain aging in Zircaloy-2 is planned if tests for its detection show positive results. Electron microscopy on thin-films and internal-friction tests are being employed to aid in the strain-aging studies.

The design of capsules for the creep testing of Zircaloy-2 at 650 F during irradiation is partially complete. Specimens are to be exposed to a fast-neutron ( $>1$  Mev) flux of  $1 \times 10^{14}$  nv for approximately 500 hr. Creep characteristics under stresses ranging from 15,000 to 23,000 psi are to be investigated. Principal features of the design include several thermocouples located between a stressed sheet-type specimen and an identical unstressed specimen parallel with it, electric heaters cast into aluminum blocks designed for uniform heat dissipation, a stainless steel bellows which, when compressed by helium pressure inside the capsule, will apply a tensile stress to the specimen, and a magnesium oxide powder annulus as a heat-transfer barrier.

A total of at least four capsules will be built: two for in-reactor tests and two for out-of-reactor control tests. Detail drawings of components are being prepared; fabrication of parts will start during January. Delivery of the stainless steel bellows and of the electric heaters is expected in February.

## F-13

Internal-friction studies have been continued in an effort to detect strain aging in Zircaloy-2 at elevated temperatures. A series of experiments was performed to determine if any internal-friction effects resulting from aging after small strains could be detected. Specimens were strained about 1 per cent in torsion in the internal-friction apparatus at a likely strain-aging temperature. The internal-friction was then measured as a function of time after straining. The temperatures investigated were 350, 377, and 400 C. Experiments employing this technique will generally show the internal friction decreasing with time. This is called the Koster effect and is apparently associated with a redistribution of dislocations. The Koster effect is relatively insensitive to small temperature changes. Any effects of strain aging should be strongly temperature sensitive and should be superimposed on the curves showing the Koster effect. The curves obtained at the above test temperatures did show the decrease of internal friction with time associated with the Koster effect, but nothing related to strain aging. Similar tests will be performed at lower temperatures. A new lot of material will be used to repeat some of the internal-friction experiments.

A new lot of Zircaloy-2 has been received and will be fabricated. It is planned to use this material for all creep experiments and for all strain-aging experiments.

Determination of Oxygen in Sodium at Concentrations Below 10 PPM

D. Ensminger, D. R. Grieser, E. H. Hall, J. W. Kissel,  
J. McCallum, and W. H. Goldthwaite

Feasibility studies are in progress to evaluate new methods for the detection of oxygen in sodium. The objective is to develop a detection technique with the capability of rapidly determining the oxygen concentration of a large sodium system to a sensitivity of  $\pm 1$  ppm at levels below 10 ppm. Present-day techniques are either too slow or lack the necessary sensitivity.

Because of the difficulties inherent in handling extremely pure sodium without contamination, the first round of studies are being conducted with oxygen concentrations in the 20 to 100-ppm range. Techniques which show promise in resolving oxygen level differences in this range will receive further study with sodium containing lower oxygen concentrations. Although the first round of studies are in progress, no definitive answers have been obtained as yet. Difficulties in production, transferring techniques, and needed equipment modifications have delayed the first studies; however, it is anticipated that most of them will have been completed during the next report period.

Ellipsometry

Preliminary polarizing-spectrometer runs have been held up in part by the unsatisfactory optical quality of the cell windows. New cells are being prepared in which the flat window will be replaced by a prism. This will eliminate the need for optical coupling between the sampling cell and an auxiliary prism as required by the previous design. The prism will be supported mechanically and sealed with a high-temperature epoxy resin. The study will resume when the new cells have been completed and loaded with sodium samples.

Electrical Resistivity

The electrical-resistivity device is in the fabrication stage. Because the resistivity of sodium is quite low and only very small changes in resistance are anticipated for small changes in oxygen content of the sodium, a very small, thin tubing is being used to gain sufficient sensitivity. The present design uses a 4-ft length of 28 gage stainless steel hypodermic-needle tubing which has a 0.014-in. OD and a 0.006-in. ID. Considerable difficulty has been experienced in fabricating this tubing into a small, evenly heated unit which can be inserted into the sodium-purification loop. It is expected that this device will be completed and tested during the next report period.

Polarographic Studies

During December a capillary system was checked out with NaK. Observed results were predictable within about 3 per cent experimental error. The NaK tests showed that a redesign of the pressure system was necessary to minimize oxygen contamination. All the necessary apparatus and chemicals to complete this feasibility study are now on hand. A delay in receiving suitable sodium samples has necessitated a 1-month extension of experimental time.

During January it is expected that the feasibility of measuring oxygen content in sodium by two methods will be evaluated:

- (1) Simple measurement of drop-time as a function of temperature
- (2) Polarographic reduction or oxidation.

Mass Spectrographic Study

The incorporation of an electron multiplier in the mass spectrometer is in progress. Simultaneously, a system for metering known sodium samples into the spectrometer is being designed. The preliminary results of this study should be completed within the next report period.

Plugging-Indicator Studies and  
Purification-Loop Operation

The sodium-purification loop, employing a wire-mesh-filled cold trap, is operating and has provided a number of sodium samples containing a moderate level of oxygen. Considerable difficulty has been experienced, however, in maintaining adequate flow rates throughout the loop. Modifications in construction and in operating procedure are being made to improve the system behavior.

Following a period of cold-trapping at 450 F (which corresponds to an oxygen saturation level of 42 ppm), single sodium samples were obtained for the ellipsometry and polarographic studies and a vacuum-distillation calibration run. The vacuum-distillation sampling was accomplished without difficulty, but the spectrographic

F-15

analysis of the residue is not yet available. In addition to these runs, several plugging-indicator analyses were made. The results of the latter indicate oxygen content between about 45 and 64 ppm, however, fully satisfactory runs were not made because of flow difficulties. It is expected that elimination of helium gas pockets from the lines will result in more reliable plugging-indicator runs. A specially designed amplification system is also being constructed to facilitate the recording of plugging-indicator flow velocity. The data are being recorded on standard graph paper through the use of a Mcsely "X-Y" plotter; the two inputs are the temperature of the orifice plate and the flow rate through it.

### STUDIES OF ALLOY FUELS

R. F. Dickerson

Niobium-base binary alloys containing from 10 to 60 w/o uranium are being studied to determine the applicability of these alloys as high-temperature reactor fuels. Data obtained to date indicate that oxygen in amounts up to 0.07 w/o and zirconium in amounts up to 0.74 w/o do not affect corrosion behavior in air, water, steam, CO<sub>2</sub>, and NaK. Corrosion in 600 F water is still in process. Attempts have been made to roll alloys containing 30, 40, 50, and 60 w/o uranium alloys in molten glass at 2500 F. Although this technique has been successful with chromium it was unsuccessful with these niobium alloys. Material is now ready for initial breakdown at 3000 F. Stress-rupture tests have been run at 1600 F on alloys containing 20 w/o uranium and 10 w/o uranium. The 20 w/o uranium alloy ruptured after 197 hr under a stress of 63,000 psi while the 10 w/o uranium alloy has not ruptured after 264 hr under a stress of 40,000 psi.

Corrosion testing of various thorium-uranium-base alloys in 200 C water has been completed. The corrosion resistance of the best alloys is about three times better than that of unalloyed thorium. Hot-hardness measurements reconfirm the fact that carbon is an effective strengthener at low temperatures; however, this effect due to carbon is lost at about 600 C. Yttrium provides solid-solution hardening and, therefore, improves the strength of the thorium-uranium alloys at temperatures above 600 C. Tensile and creep tests at 600 and 700 C are in progress, and heat-treatment studies are in progress. Thorium-10 and -20 w/o uranium alloys have been arc-melted under a dynamic atmosphere of nitrogen maintained at a pressure of 2-1/2 atm. The resulting product was very near the stoichiometric composition of ThN. However, metallographic examination showed a two-phase structure, indicating inhomogeneity.

### Development of Niobium-Uranium Alloys

J. A. DeMastry, S. G. Epstein, A. A. Bauer, and R. F. Dickerson

The fabrication characteristics, mechanical and physical properties, and corrosion behavior in various environments of niobium-uranium alloys are being studied to determine the applicability of these alloys as reactor fuels.

Alloys which contain from 10 to 60 w/o uranium were prepared using niobium containing from 0.03 to 0.07 w/o oxygen and from 0.02 to 0.74 w/o zirconium. The corrosion behavior in air, water, steam,  $\text{CO}_2$ , and NaK and the tensile properties and fabrication behavior of the above materials have been determined. No effects on the above-mentioned properties have been observed due to the variations in oxygen and zirconium contents of the alloys, although there are not sufficient data to conclude that corrosion behavior is unaffected.

Corrosion-test results on niobium-uranium alloys in 600 F water for 182 days are shown in Table F-3. The specimens all have an adherent, dull black oxide on the surface.

TABLE F-3. CORROSION DATA FOR NIOBIUM-URANIUM ALLOYS<sup>(a)</sup> IN 600 F WATER

Nominal Alloy Content (Balance Niobium), w/o	Impurity Content		Specimen Condition	Total Weight Change in 182 Days, mg per $\text{cm}^2$
	Oxygen <sup>(b)</sup> , ppm	Zirconium <sup>(c)</sup> , w/o		
10 U	680	0.74	Fabricated	0.71
	1190	0.17	Fabricated	-0.56
	3170	0.02	Fabricated	-1.43
20 U	458	0.74	Fabricated	1.22
	523	0.17	Fabricated	1.85
	198	0.02	Fabricated	0.84
30 U	586	0.74	As cast	0.58
	669	0.17	Fabricated	-1.38
	165	0.02	As cast	0.55
40 U	661	0.74	As cast	0.63
	579	0.17	As cast	0.42
	261	0.02	As cast	0.76
50 U	375	0.74	As cast	0.71
	334	0.17	As cast	0.68
	271	0.02	As cast	0.11
60 U	471	0.74	As cast	-3.60
	273	0.17	As cast	-3.10
	192	0.02	As cast	-0.80

(a) Average of duplicate specimens.

(b) Analyzed value.

(c) Nominal composition.

Fabrication of alloys containing 30 w/o or more uranium has been unsuccessful to date. Ingots of niobium-30, -40, and -50 w/o uranium alloys have been prepared for fabrication at 3000 F. This past month an attempt was made to roll alloys of 30, 40, 50, and 60 w/o uranium composition in a protective envelope of molten glass at 2500 F. However, the glass adhered only to the 30 w/o uranium-alloy surface; apparently the oxide on the remaining alloys was incompatible with the molten glass and wetting did not

F-17

occur. While the 30 w/o uranium alloy underwent slight reductions before cracking, none of the alloys was fabricable under these conditions.

Specimens of each alloy composition are also being tested for compatibility with liquid sodium at 1500 F. The specimens have been encapsulated with sodium in stainless steel tubes and will be examined after a 500-hr exposure.

Stress-rupture testing of a niobium-20 w/o uranium alloy at 1600 F has been completed. The test was run in a vacuum under a stress of 63,000 psi. Rupture occurred after 197 hr. A specimen of niobium-10 w/o uranium has not ruptured after 264 hr on test at 1600 F under a stress of 40,000 psi. Additional specimens of the niobium-10 and -20 w/o uranium alloys will be tested at 2200 F.

The homogenization of alloy wire bars for an investigation of the effects of oxygen on the composition limits of the gamma loop in the niobium-uranium system is nearly completed. Specimens for equilibrium heat treatments are being sealed in evacuated quartz capsules. Each specimen is wrapped in tantalum foil, and zirconium chips are being included in the capsules to act as gettering agents. Sets of the specimens thus prepared will be heat treated at various temperatures selected on the basis of composition and then metallographically examined.

#### Development of Thorium-Uranium Alloys

M. S. Farkas, A. A. Bauer, and R. F. Dickerson

Thorium-uranium and thorium-uranium-base alloys are being investigated with the aim of improving their irradiation stability and corrosion resistance. The effect of thorium purity, casting methods, and fabrication on the size and distribution of the uranium-rich particles is being investigated. Thorium-5 to 25 w/o uranium-base ternary alloys that have been and are now being studied contain either 5 to 25 w/o zirconium or small amounts of niobium or molybdenum; quaternary alloys containing zirconium and niobium additions are also being investigated.

Corrosion tests in 200 C water have been completed. Thorium alloys heat treated at 1000 C and either furnace cooled or water quenched were tested for 504 hr. Of the group that was furnace cooled, thorium-15 w/o uranium-25 w/o zirconium and thorium-20 w/o uranium-20 w/o zirconium alloys performed well with corrosion rates under 0.9 mg/(cm<sup>2</sup>)(hr). Of the alloys water quenched from 1000 C, the thorium-10 w/o uranium-25 w/o zirconium and thorium-15 w/o uranium-25 w/o zirconium alloys corroded at rates of about 0.5 mg/(cm<sup>2</sup>)(hr), while a thorium-10 w/o uranium-25 w/o zirconium alloy corroded at a rate of about 0.65 mg/(cm<sup>2</sup>)(hr). The corrosion resistance of the best alloys is about three times better than that of thorium, which is reported to corrode at a rate of 1.5 mg/(cm<sup>2</sup>)(hr) in 200 C water.

Hot-hardness measurements were performed on thorium-10 w/o uranium-base alloys with additions of 0.2 w/o carbon, 1.5 w/o molybdenum-0.2 w/o carbon, 2 w/o niobium-0.2 w/o carbon, and 10 w/o yttrium. It was found that carbon is an effective strengthener at low temperatures. However, at about 600 C the strengthening effect

due to carbon is lost. The addition of 10 w/o yttrium to thorium-10 w/o uranium resulted in solid-solution hardening of the thorium matrix. Improvement in hot strength, above that of the base alloy, was obtained above 600 C with yttrium. The softening temperature of all these alloys is about 600 C.

Tensile and creep tests at 600 and 700 C are being performed on thorium-5, -10, and -20 w/o uranium alloys and on thorium-10 w/o uranium-1.5 w/o molybdenum, -2 w/o niobium, -10 w/o zirconium, and -10 w/o zirconium-2 w/o niobium alloys. These tests are being performed to obtain quantitative strength data which will permit an evaluation of the resistance of these alloys to radiation swelling. The ternary and quaternary alloys of this group were chosen because of their excellent hot hardness.

Further investigations to be conducted on thorium-uranium-base alloys include studies of the effect of heat treatment on microstructure and recrystallization behavior.

Thorium-10 w/o and -20 w/o uranium alloys have been arc melted under a dynamic atmosphere of nitrogen maintained at a pressure of 2-1/2 atm absolute. Chemical analyses of the resultant buttons show that 5.4 w/o nitrogen was present in the thorium-10 w/o uranium alloy and 5.7 w/o nitrogen was present in the thorium-20 w/o uranium alloy. Since stoichiometric ThN contains 5.7 w/o nitrogen the (Th, U)N prepared is very near the stoichiometric proportions. Metallographic examination of these nitrides, however, shows a two-phase structure that indicates inhomogeneity.

#### FISSION-GAS RELEASE FROM REFRACTORY FUELS

J. B. Melehan, D. A. Vaughan, R. H. Barnes,  
H. Sheets, S. D. Beck, and F. A. Rough

The objective of this program is to develop an understanding of the important causes of fission-gas release in  $\text{UO}_2$ . Apparatus for the postirradiation determination of diffusion coefficients on single crystals of uranium has been operated successfully. A series of tests on single crystals is to follow. A supporting experiment on the effects of irradiation on single-crystal and sintered  $\text{UO}_2$  surfaces is also under way. Apparatus for in-pile study of fission-gas release is nearing the point where in-pile experiments can be initiated.

#### Characterization of Sintered $\text{UO}_2$ and Model of Gas Release

To aid in understanding fission-gas release from  $\text{UO}_2$  bodies during irradiation and postirradiation heat treatments, the surface structure of various preparations is being examined before and after irradiation. Metallographic specimens were characterized by light- and electron-microscopy techniques and irradiated in the BRR for 1 hr in a flux of  $3.53$  to  $3.59 \times 10^{12}$  nv. The specimens were sealed in an aluminum capsule filled with helium.

F-19

During the past month the irradiated specimens were examined by light and electron microscopy. Identical areas were compared with the preirradiation micrographs. Although the irradiation was low ( $5.5 \times 10^{-6}$  a/o burnup), a number of structural changes occurred. More changes were apparent in the gross structure of the low-density (91 per cent of theoretical) body than could be observed in the 95 per cent dense body or in large single crystals. These gross changes may be described as (1) the growth of large pores and the annihilation of small pores and/or etch pits and (2) the enlargement of some grain boundaries and annihilation of others. In the case of the low-density body, a new grain boundary appeared which encompassed a group of grains whose original grain boundaries became less distinct. In all specimens, a fine structure was detected at 18,000X magnification. This may be described as a surface roughening of the  $\text{UO}_2$  crystals or grains on a submicron scale which was essentially the same regardless of body density or orientation. It is possible that this fine structure may be related to fission-fragment traces. Further study of the fine structure is planned for the next period. Also, new specimens will be prepared for shorter irradiation times, in order to better isolate the results of individual fission events.

Experiments are also in progress to quantitatively evaluate the pore distribution in sintered  $\text{UO}_2$  having varied histories and to relate the observed distributions to surface-area determinations made by gas adsorption.

#### Diffusion in $\text{UO}_2$

Measurements of fission-gas diffusion from single-crystal uranium dioxide during postirradiation heating were initiated during December. An initial run in which a 0.75-g flat plate of irradiated single-crystal uranium dioxide was heat treated for about 1 hr at 1245 C has been completed. The major purpose of this run was to check the apparatus and scintillation counting system for continuous measurement of fission-gas release. Sufficient fission gas was released from the specimen, which had been irradiated for 6 hr in an estimated unperturbed thermal-neutron flux of about  $4 \times 10^{13}$  nv, to permit a continuous measurement of the release rate.

At present, a few minor changes are being made in the apparatus. Measurements of the release rates of fission gases from additional plates of single-crystal uranium dioxide at temperatures of 1200 and 1400 C are scheduled to follow. In these tests, it is planned to emphasize the effects of various surface conditions upon the diffusion results. Initially, diffusion tests will be made upon specimens as polished, hydrogen reduced at 600 C, and vacuum treated at about 1800 C. In order to further establish the surface characteristics of these crystals, surface-area measurements by gas adsorption are being made upon both plates and spheres. So far, interpretation of the results is questionable, but additional tests are to be made.

Experimental studies on the fusion of  $\text{UO}_2$  powder in a plasma-jet flame have shown that vacuum degassing the  $\text{UO}_2$  feed and fusing it in a well-purged apparently leaktight system does not prevent the formation of higher oxides of uranium. Oxygen contamination evidently arises from strongly adsorbed oxygen-containing gases on the  $\text{UO}_2$  feed, preoxidation of the feed before it is charged to the fusion apparatus, and/or degassing of the equipment during operation.

The amount of higher oxides was decreased by almost 50 per cent when the fusions were performed in a plasma containing 15 per cent of hydrogen. Future efforts will be directed toward increasing the powder-retention time in the reducing plasma. After some equipment modifications, it may be possible to operate the plasma generator with hydrogen gas as the only working fluid. It is believed that this process modification will essentially eliminate oxidation of the uranium dioxide. However, experiments are being temporarily suspended.

#### Preparation for In-Pile Study

The in-pile apparatus for study of fission-gas release is undergoing final details of checking and calibration preparatory to insertion of the induction-heating unit into an 8-in. beam tube of the BRR. The apparatus consists of the beam-tube heating unit, a gas-purification system, a fission-gas-collection train, and accessory equipment.

In the study of sintered  $\text{UO}_2$  for in-pile study of gas release, a series of 24 specimens, designated Group 58, was prepared. The specimens were fabricated by ball milling Davison  $\text{UO}_2$  for 15 hr in methanol, pressing in a steel die at 40,000 psi, and sintering in hydrogen for 1 hr at 3000 F. The sintered specimens had a bulk density of 9.42 g per  $\text{cm}^3$  (85.9 per cent of theoretical), 0.1 per cent of open porosity, and an oxygen-to-uranium ratio of about 2.08. Since the specimens were sintered in hydrogen, the high oxygen-to-uranium ratio was quite unexpected. A second series of specimens, designated Group 65, was fabricated by the same procedure. The new specimens were found to have a bulk density of 9.30 g per  $\text{cm}^3$  (84.7 per cent of theoretical), 7.2 per cent of open porosity, and an oxygen-to-uranium ratio of 2.03. It is concluded that the Group 58 specimens inadvertently were oxidized slightly in the sintering furnace during cooling.

Previously, Davison  $\text{UO}_2$  powder was oxidized at 400, 932, 1200, or 1500 F. The oxidized powders then were pressed and sintered in hydrogen for 1 hr at 3000 F. The sintered density of all these pellets was between 95 and 97 per cent of theoretical. The oxygen-to-uranium ratio of sintered pellets made from all the oxidized powders was between 2.01 and 2.02. Examination of polished surfaces indicated that the structures of the  $\text{UO}_2$  ceramics made from oxidized Davison  $\text{UO}_2$  were considerably more uniform than the structure of those made from powder which had not been oxidized. The structure of specimens made from unoxidized powder have had isolated areas of high porosity. The grain size of the specimens made from the oxidized powders was about  $10 \mu$ , compared with a grain size of about  $20 \mu$  for control specimens made from unoxidized  $\text{UO}_2$ . It is felt that the increased uniformity of the pore structure of these specimens is significant. The apparently high oxygen-to-uranium ratios, if real, can be adjusted by increased sintering time in hydrogen. Specimens of similar density but with a typical nonuniform distribution of pores will be compared with these specimens by gas-adsorption surface-area measurements.

F-21

GENERAL FUEL-ELEMENT DEVELOPMENT

S. J. Paprocki

Fuel materials containing 60 to 90 volume per cent of  $UO_2$  dispersed in stainless steel, chromium, molybdenum, and niobium matrices are being developed. The study has included the development of fabrication techniques, determination of thermal conductivity and thermal expansivity, and evaluation of thermal stability. These materials appear extremely promising for high-temperature applications requiring a relatively high fuel concentration.

Solid-phase bonding techniques have been developed for the self-bonding of niobium. Bonding of molybdenum has also been achieved; however, the bond quality as determined by ductility and grain growth across the original bond interface has not been comparable with bonds achieved with niobium. The solid-phase bonding of these refractory metals is especially applicable for reactor application as the usual brittleness encountered with fusion welding and brazing is minimized or eliminated.

A fundamental study is being conducted to determine the mechanism of solid-phase bonding produced through the use of pressure and temperature. A relationship of time, temperature, pressure, and grain orientation is being established for the initial phase of the bonding cycle involving the attainment of intimate contact between the bonding components and the advance phase involving diffusion and grain growth across the bond interface.

Fabrication of Cermet Fuel Elements

S. J. Paprocki, D. L. Keller, G. W. Cunningham, and D. E. Kizer

Methods of producing cermets of 90 per cent of theoretical density or better containing 60 to 90 volume per cent of ceramic fuel are being investigated. Evaluations of fabricated cermets are being made on the basis of microstructure and physical and mechanical properties.

Linear-thermal-expansion measurements have been made on three  $UO_2$ -containing cermets, and the results are reported in Table F-4. Specimen C contained a nominal composition of 80 volume per cent  $UO_2$ -Type 302B stainless steel, Specimen A contained a nominal composition of 70 volume per cent  $UO_2$ -Type 302B stainless steel, and Specimen B contained a nominal composition of 70 volume per cent  $UO_2$ -molybdenum. All specimens were prepared by mixing the correct proportion of metal- $UO_2$  powders in a V-mixer and cold compacting at 30 tsi before pressure bonding for 3 hr at 10,000 psi at temperatures ranging from 2100 to 2300 F. The densities ranged from 91.7 to 97 per cent of theoretical. Linear-thermal-expansion measurements were made in a vertical quartz-tube recording dilatometer with the specimen protected by a vacuum of approximately  $5 \times 10^{-5}$  mm of mercury. The specimens were given two thermal cycles from room temperature to 950 C and back to room temperature at a maximum heating and cooling rate of 3 C per minute. The error of the linear-thermal-expansion values is estimated to not exceed 2 per cent.

TABLE F-4. MEAN LINEAR-THERMAL-EXPANSION COEFFICIENTS FOR THREE UO<sub>2</sub> CERMETS<sup>(a)</sup>

Temperature Range, C	Mean Linear-Thermal-Expansion Coefficients Over Temperature Ranges Shown, 10 <sup>-6</sup> per C											
	Specimen C				Specimen A <sup>(b)</sup>				Specimen B			
	First Thermal Cycle		Second Thermal Cycle		Second Thermal Cycle		Third Thermal Cycle		First Thermal Cycle		Second Thermal Cycle	
Heating	Cooling	Heating	Cooling	Heating	Cooling	Heating	Cooling	Heating	Cooling	Heating	Cooling	Heating
20-100	10.2	9.0	9.7	8.3	9.6	8.7	10.4	8.8	6.5	6.6	6.6	6.3
20-200	10.2	9.0	9.9	8.7	9.7	8.9	10.5	8.8	6.7	6.7	6.7	6.3
20-300	10.3	9.1	10.0	9.1	10.0	9.3	10.7	8.9	6.9	6.8	6.8	6.4
20-400	10.4	9.3	10.2	9.3	10.3	9.6	10.9	9.2	7.1	6.9	6.9	6.6
20-500	10.6	9.5	10.4	9.5	10.6	9.9	11.1	9.5	7.3	7.1	7.0	6.8
20-600	10.7	9.8	10.6	9.8	10.8	10.2	11.3	9.9	7.5	7.3	7.2	7.0
20-700	10.8	10.1	10.7	10.2	11.0	10.7	11.4	10.4	7.7	7.5	7.4	7.2
20-800	10.9	10.5	10.8	10.5	11.1	11.1	11.5	10.9	7.9	7.8	7.7	7.5
20-900	11.0	10.8	11.0	10.9	11.3	11.4	11.6	11.4	8.2	8.0	7.9	7.8
20-950	11.0	11.0	11.2	11.0	11.3	11.6	11.6	11.7	8.3	8.1	8.0	7.9

(a) Compositions:

Specimen A 70 volume per cent UO<sub>2</sub>-Type 302B stainless steelSpecimen B 70 volume per cent UO<sub>2</sub>-molybdenumSpecimen C 80 volume per cent UO<sub>2</sub>-Type 302B stainless steel.

(b) Due to malfunction in the recording dilatometer, the first thermal cycle was not used.

F-23

Three cermet rods of 80 volume per cent  $\text{UO}_2$  dispersed in stainless steel and chromium have been fabricated. Spherical  $\text{UO}_2$  was used in preparing one  $\text{UO}_2$ -stainless steel cermet and the chromium cermet. The second  $\text{UO}_2$ -stainless steel cermet contained high-fired  $\text{UO}_2$ . After pressure bonding 3 hr at 2300 F under a helium gas pressure of 10,000 psi, measured densities were, respectively, 97.2, 97.1, and 98.4 per cent of theoretical.

The three specimens are currently being prepared for thermal-conductivity measurements. An additional cermet rod containing 80 volume per cent spherical  $\text{UO}_2$  dispersed in molybdenum was pressure bonded for 3 hr at 2400 F under a helium gas pressure of 10,000 psi. During the pressure-bonding run, melting of the stainless steel cladding occurred, resulting in a can failure. An additional specimen is being prepared for possible thermal-conductivity measurements.

#### Gas-Pressure Bonding of Molybdenum- and Niobium-Clad Fuel Elements

S. J. Paprocki, E. S. Hodge, and P. J. Gripshover

Molybdenum and niobium retain their strengths at elevated temperatures and possess favorable nuclear properties. These characteristics make them potential cladding and structural materials for high-temperature-reactor applications. The gas-pressure-bonding process is being investigated as a method of cladding ceramic and cermet-type fuels with molybdenum and niobium.

Evaluation of two niobium-clad compartmentalized flat-plate fuel elements previously fabricated by bonding at 2100 F for 3 hr at 10,000 psi has been completed. One specimen measuring 0.060 by 1.370 by 3.860 in. and containing three cores was clad with 0.010 in. of niobium and the other, similar, specimen was clad with 0.020 in. of niobium. Metallographic examination revealed excellent bonding in most areas of these specimens. During burst testing, however, it was observed that part of the cladding over the cores was brittle while the cladding over the niobium frame was ductile. Chemical analysis of the cladding revealed that the oxygen content had increased 800 ppm in areas over the uranium dioxide-17 w/o alumina cores. This verified that the niobium is reacting with the alumina contained in the core during pressure bonding. The presence of the high oxygen content explains the brittle fracture of the cladding over the core areas. An additional compartmented specimen is being bonded which contains only uranium dioxide cores. This specimen will be burst tested to determine bond integrity between compartments and deflection properties of the cladding after pressure bonding.

Molybdenum-clad specimens have to be bonded at 2300 F to achieve a metallurgical bond. All of the can materials investigated for pressure bonding of molybdenum at this temperature alloyed with the cladding; consequently, edge welding of molybdenum envelopes that do not require an outer can is being investigated. Several molybdenum-clad specimens were fusion edge welded between copper blocks in a helium atmosphere. The edge-welded envelopes were tested for leaks subsequent to pressure bonding at 2300 F at 10,000 psi for 3 hr. Evaluation of these specimens revealed some entrapped helium along the bond interface in the form of small spherical voids. The observed

voids were anticipated; however, the specimens did yield an opportunity to evaluate the ductility of molybdenum-clad specimens bonded at these conditions. The cladding was ductile after bonding; however, it exhibited directional properties.

A series of both molybdenum- and niobium-clad specimens is being prepared by edge welding in an electron-beam welding unit. These specimens are being fusion edge welded in three sides in a helium tank with the fourth side sealed during evacuation by electron-beam welding. This should produce specimens suitable for evaluating an optimum bonding procedure with a minimum introduction of contamination during welding and bonding of the specimens.

#### Factors Affecting Pressure Bonding

G. W. Cunningham and J. W. Spretnak

The mechanism and kinetics of solid-phase bonding of metals under application of heat and pressure is being studied primarily by conducting experiments on self-bonding characteristics of copper. At the present time, data are being obtained so that a relationship may be established between hot hardness and the pressure required to place the metal surfaces in intimate contact at any particular temperature. Also, specimens are being prepared to study the effect of grain orientation on grain growth across the interface.

In a series of specimens run at 1400 F, pressures as low as 4000 psi were found to be sufficient to place the metal surface in intimate contact. Additional specimens run at lower pressures will be required to establish the relationship between the applied pressure and the fraction of the interface which is in intimate contact. Other series are planned to be run at temperatures of 600, 800, and 1200 F.

The method of bonding large-grained specimens to study the effect of grain orientation on grain growth across the interface appears very promising. Grains on the order of 1/8 in. in diameter were obtained when plates previously annealed 2 hr at 1800 F were bonded at 1800 F and 3000 psi for 5 min. Under these conditions, grain growth across the interface was complete and, therefore, could not be related to a particular orientation, but, by varying conditions of pressure and temperature, one should be able to obtain satisfactory specimens for studies of grain-orientation effects. Additional specimens are being prepared.

FF-1

## FF. FUEL-CYCLE PROGRAM STUDIES

GAS-PRESSURE BONDING OF CERAMIC, CERMET,  
AND DISPERSION FUEL ELEMENTS

S. J. Paprocki, S. W. Porembka, D. L. Keller, E. S. Hodge,  
C. B. Boyer, and J. B. Fox

This program is concerned with the development of a fabrication technique which will reduce the manufacturing costs and maintain or improve the quality of ceramic, cermet, and dispersion fuel elements. The gas-pressure-bonding process was selected as a promising method of fabrication for achieving these objectives. The study is being directed toward the refinement and further development of the gas-pressure-bonding process to accomplish simultaneous densification and cladding of ceramic, cermet, and dispersion fuels with stainless steel.

Uranium Dioxide Compaction Studies

Studies to date have been concerned with the development of high-density green  $UC_2$  cores which will achieve a desired range of densities on pressure bonding. Previous studies of  $UO_2$  compaction involved the cold-pressing characteristics and tap densities of seven powder types and several powder mixtures. Present efforts include the investigation of ideal packing size distribution, ultrasonic compaction, and presintering.

A mixture of various particle sizes of fused  $UO_2$  representing an ideal size distribution for rhombohedral packing was investigated. This mixture should permit a density of 86.4 per cent of theoretical under ideal conditions. The size distribution consists of the following:

Mesh Size	Amount, w/o
Minus 42 plus 48	74.5
Minus 110 plus 115	5.3
Minus 200 plus 250	1.7
Minus 250 plus 270	2.9
Minus 270 plus 325	2.0
Minus 325	13.6

The effect of varying compacting pressure on the pressed density is given in Table FF-1. Good densities were attained with the range of pressures studied.

TABLE FF-1. RESULTS OF COMPACTING EXPERIMENTS WITH UO<sub>2</sub> OF IDEAL RHOMBOHEDRAL SIZE DISTRIBUTION

Specimen	Compacting Pressure, tsi	Specimen Size			Green Density	
		Weight, g	Height, in.	Diameter, in.	G per Cm <sup>3</sup>	Per Cent of Theoretical
U-1305	50	14.00	0.399	0.539	9.36	85.5
U-1306	45	14.00	0.400	0.539	9.35	85.3
U-1307	40	13.98	0.402	0.539	9.28	84.7
U-1308	35	13.94	0.406	0.538	9.26	84.5
U-1309	30	13.91	0.408	0.538	9.16	83.6
U-1310	25	13.91	0.411	0.538	9.08	82.8
U-1311	20	13.99	0.416	0.538	9.06	82.6
U-1312	15	13.82	0.421	0.537	8.87	80.9
U-1313	10	13.83	0.427	0.537	8.74	79.9

A preliminary study was undertaken to study the effect of ultrasonics on the compaction of various types and mixtures of UO<sub>2</sub>. The methods investigated included both the ultrasonic vibration of a powder-filled tube and the direct packing by ultrasonically vibrating a tool in contact with the powder. The powder-filled tubes, which were approximately 1/2 in. in ID, were immersed in a Sonogen cleaning tank and ultrasonically vibrated using distilled water as the liquid medium. In the direct method, increments of 3 to 4 ml of powder were loaded into a graduate and, using a Sheffield Cavitron, ultrasonic energy was applied to a tool in contact with the powder. The process was repeated until the tube was filled. Density increases of up to 3 per cent with the filled tubes and up to 9.5 per cent with the direct method were noted. Details of the tests are given in Table FF-2. It is believed that a damping effect in the powder-filled tubes yielded the low-density increases. Additional tests of smaller diameter powder-filled tubes and direct ultrasonic packing of powder having an ideal particle-size distribution are planned.

Presintering was evaluated in order to attain high-strength dewaxed pellets to facilitate tube loading prior to pressure bonding, and to attain a possible higher density to minimize wrinkling of the cladding material. Only in isolated cases was increased density noted. In these instances MCW ceramic grade UO<sub>2</sub> and MCW dense ceramic grade powders were employed. The densities attained by these materials were not sufficient to lessen the possibility of severe cladding wrinkling. In all cases, complete removal of binder was evident; however, these specimens will be inspected metallographically to determine any amounts of impurity contamination. The high-pressed-density compacts revealed lower densities after sintering, apparently due to the evolution of binder. In general, compacts, dewaxed by this process were found easy to handle with little apparent powdering. Results of these tests are listed in Table FF-3. Utilization of such compacts in pressure-bonded fuel rods would minimize bond-line contamination because of less powdering during loading and evaluation.

#### Gas-Pressure Bonding

Gas-pressure-bonding studies to date have included the determination of the densification characteristics of various UO<sub>2</sub> powders and the integrity of stainless-stainless

TABLE FF-2. RESULTS OF EXPERIMENTAL ULTRASONIC COMPACTION OF UO<sub>2</sub>

Material	Compaction Produced by Tap Packing			Ultrasonic Method <sup>(a)</sup>	Compaction Produced by Ultrasonic Vibration		
	Volume, ml	G per Cm <sup>3</sup>	Per Cent of Theoretical		Volume, ml	G per Cm <sup>3</sup>	Per Cent of Theoretical
MCW ceramic grade UO <sub>2</sub>	5.7	2.73	24.9	1	5.8	2.68	24.4
MCW dense ceramic grade UO <sub>2</sub>	6.7	3.54	32.3	1	6.7	3.54	32.3
NUMEC high-fired UO <sub>2</sub>	5.6	5.68	51.8	1	5.6	5.68	51.8
				3	4.4	5.86	53.6
MCW high-fired UO <sub>2</sub>	5.8	6.02	54.9	1	5.8	6.02	54.9
				3	5.3	6.58	60.1
MCW spherical UO <sub>2</sub>	7.4	5.64	51.4	1	7.3	5.72	52.2
				2	7.25	5.77	52.7
				3	7.2	5.81	53.1
MCW special dense UO <sub>2</sub>	6.9	6.75	61.6	1	6.7	6.96	63.6
				2	6.7	6.96	63.6
				3	6.2	7.65	69.8
Spencer fused UO <sub>2</sub>	7.6	6.34	57.8	1	7.3	6.60	60.2
				2	7.2	6.70	61.2
				3	6.9	7.13	65.1
75 w/o MCW special dense UO <sub>2</sub> and 25 w/o MCW ceramic grade UO <sub>2</sub>	6.3	5.57	50.9	1	6.3	5.57	50.9
				2	6.3	5.57	50.9
				3	5.3	6.61	60.4
75 w/o Spencer fused UO <sub>2</sub> and 25 w/o ceramic grade UO <sub>2</sub>	5.2	5.48	50.0	3	4.9	5.82	53.2
75 w/o Spencer fused UO <sub>2</sub> and 25 w/o MCW high-fired UO <sub>2</sub>	7.0	7.32	66.7	1	6.8	7.54	69.0
				2	6.7	7.64	69.7
				3	6.4	8.00	73.0

(a) Ultrasonic compaction methods were as follows:

(1) Powder in graduate was immersed in Sonogen cleaning tank under 100 F water. Power: 75 ma for 4 min at 39 kc.

(2) Powder in graduate was immersed in Sonogen cleaning tank under 100 F water. Power: 90 ma for 5 min at 39 kc.

(3) Direct application of ultrasonic energy from a 1000-w Sheffield Cavitron was made to a tool in contact with the powder. Power: 20 kc, 10 per cent setting, 100 to 150 w, 6-amp bias setting.

TABLE FF-3. RESULTS OF PRESINTERING

U-Number	Type of UO <sub>2</sub>	As-Pressed Compacts			Density	
		Weight, g	Height, in.	Diameter, in.	G per Cm <sup>3</sup>	Per Cent of Theoretical
U-1265	Ceramic grade	13.27	0.657	0.501	6.24	56.9
U-1266	Dense ceramic grade	11.93	0.500	0.541	6.31	57.6
U-1267	NUMEC high fired	13.81	0.453	0.540	8.13	74.2
U-1268	MCW high fired	14.37	0.486	0.539	7.92	72.3
U-1269	MCW spherical	14.56	0.465	0.540	8.32	75.9
U-1270	MCW special dense	16.56	0.509	0.539	8.69	79.3
U-1271	Spencer fused	15.36	0.442	0.539	9.25	84.4
U-1272	75 w/o special dense-25 w/o ceramic	13.90	0.465	0.540	7.94	72.4
U-1273	75 w/o Spencer fused-25 w/o ceramic	13.89	0.451	0.540	8.18	74.6
U-1274	75 w/o Spencer fused-25 w/o MCW high fired	13.91	0.406	0.538	9.23	84.2
U-1285	Ceramic grade	11.89	0.516	0.540	6.12	55.8
U-1286	Dense ceramic grade	11.92	0.494	0.541	5.83	53.2
U-1287	NUMEC high fired	13.70	0.471	0.539	7.77	70.9
U-1288	MCW high fired	13.95	0.459	0.539	8.09	73.8
U-1289	MCW spherical	14.64	0.468	0.540	9.30	84.9
U-1290	MCW special dense	17.50	0.539	0.539	8.66	79.0
U-1291	Spencer fused	15.42	0.445	0.538	9.29	84.8
U-1292	75 w/o special dense-25 w/o ceramic	13.94	0.470	0.540	7.91	72.2
U-1293	75 w/o Spencer fused-25 w/o ceramic	13.94	0.449	0.540	8.27	75.5
U-1294	75 w/o Spencer fused-25 w/o MCW high fired	13.93	0.400	0.538	9.33	85.1
U-1295	Ceramic grade	10.93	0.472	0.540	5.51	50.3
U-1296	Dense ceramic grade	12.63	0.526	0.540	6.38	58.2
U-1297	NUMEC high fired	13.71	0.464	0.539	7.89	72.0
U-1298	MCW high fired	13.91	0.462	0.539	8.07	73.6
U-1299	MCW spherical	14.44	0.451	0.540	8.50	77.6
U-1300	MCW special dense	16.35	0.503	0.539	8.76	79.9
U-1301	Spencer fused	15.80	0.453	0.538	9.37	85.5
U-1302	75 w/o special dense-25 w/o ceramic	13.97	0.464	0.540	8.04	73.3
U-1303	75 w/o Spencer fused-25 w/o ceramic	13.94	0.444	0.540	8.33	76.0
U-1304	75 w/o Spencer fused-25 w/o MCW high fired	13.92	0.404	0.538	9.24	84.3
U-1275	Ceramic grade	10.85	0.468	0.540	6.15	56.1
U-1276	Dense ceramic grade	11.94	0.496	0.541	6.40	58.4
U-1277	NUMEC high fired	13.38	0.453	0.539	7.29	66.5
U-1278	MCW high fired	12.28	0.405	0.539	8.09	73.8
U-1279	MCW spherical	14.39	0.457	0.540	8.41	76.7
U-1280	MCW special dense	16.26	0.501	0.539	8.65	78.9
U-1281	Spencer fused	13.80	0.402	0.539	9.16	83.5
U-1282	75 w/o special dense-25 w/o ceramic	13.91	0.468	0.540	7.91	72.2
U-1283	75 w/o Spencer fused-25 w/o ceramic	13.94	0.444	0.539	8.40	76.6
U-1284	75 w/o Spencer fused-25 w/o MCW high fired	13.93	0.404	0.538	9.25	84.3

UO<sub>2</sub> COMPACTS PRESSED AT 40 TSI

Time, hr	Sintering Conditions		Sintered Compacts			Density		Remarks
	Temperature, F	Dew Point, F	Height, in.	Diameter, in.	G per Cm <sup>3</sup>	Per Cent of Theoretical		
4	2000	-49	0.655	0.495	6.40	58.4	Scaly	
4	2000	-49	0.498	0.536	6.45	58.9	Cracked	
4	2000	-49	0.454	0.540	8.01	73.1	Bad edges	
4	2000	-49	0.487	0.539	7.82	71.4	Good	
4	2000	-49	0.466	0.540	8.28	75.5	Bad edges	
4	2000	-49	0.510	0.539	8.66	79.0	Bad edges	
4	2000	-49	0.442	0.539	9.20	83.9	Extremely bad edges	
4	2000	-49	0.464	0.538	8.02	73.2	Good	
4	2000	-49	0.450	0.538	8.24	75.2	Good	
4	2000	-49	0.406	0.539	9.08	82.8	Good	
4	2100	-26	0.516	0.529	6.38	58.2	Cracked	
4	2100	-26	0.497	0.535	6.52	59.5	Cracked	
4	2100	-26	0.485	0.540	7.43	67.8	Cracked	
4	2100	-26	0.467	0.540	7.93	72.4	Good	
4	2100	-26	0.469	0.541	8.29	75.6	Powdery, edge chipped	
4	2100	-26	0.541	0.540	8.58	78.3	Edge chipped	
4	2100	-26	0.446	0.540	9.16	83.6	Poor strength	
4	2100	-26	0.470	0.538	7.91	72.2	Good	
4	2100	-26	0.448	0.538	8.35	76.2	Good	
4	2100	-32	0.401	0.539	9.22	84.1	Fair	
4	2200	-32	0.471	0.528	6.40	58.4	Cracked	
4	2200	-32	0.526	0.531	6.58	60.0	Cracked	
4	2200	-32	0.466	0.539	7.85	71.6	Good	
4	2200	-32	0.465	0.539	7.98	72.8	Bad edges	
4	2200	-32	0.451	0.540	8.55	78.0	Good	
4	2200	-32	0.506	0.540	8.57	78.2	Powdery	
4	2200	-32	0.454	0.540	9.18	83.8	Powdery, bad edges	
4	2200	-32	0.463	0.537	8.12	74.1	Very good	
4	2200	-32	0.443	0.538	8.42	76.8	Very good	
4	2200	-32	0.409	0.539	9.06	82.6	Poor strength	
4	2300	-47	0.460	0.525	6.63	60.5	Cracked	
4	2300	-47	0.493	0.527	6.74	61.5	Cracked	
4	2300	-47	0.453	0.537	7.95	72.5	Good	
4	2300	-47	0.405	0.539	8.03	73.3	Powdery	
4	2300	-47	0.422	0.540	8.32	75.9	Good	
4	2300	-47	0.502	0.539	8.61	78.6	Edges cracked	
4	2300	-47	0.403	0.539	9.14	83.4	Edges cracked	
4	2300	-47	0.466	0.536	8.04	73.4	Very good	
4	2300	-47	0.442	0.537	8.50	77.6	Good	
4	2300	-47	0.405	0.539	9.11	83.1	Fair	

bond after gas-pressure bonding at 1900 to 2200 F. In view of the warpage and dimensional nonuniformity experienced with low-density  $UO_2$  in earlier work, present efforts are directed to the utilization of high-density  $UO_2$  and element designs other than the cylindrical rod. Present studies also include a more complete evaluation of gas-pressure-bonded  $UO_2$ .

Eight tubes containing  $UO_2$  powders of various types prepared both with and without binders were pressure bonded to establish the effects of bonding conditions upon the stoichiometry of the different types of  $UO_2$ . Those tubes containing binders were heated to 600 F in vacuum. Bonding details and stoichiometry results are reported in Table FF-4. It was noted that the ceramic grade of uranium dioxide tends to return to stoichiometry under the bonding conditions studied. No significant differences were noted between those tubes initially containing binders and those without binders. A possible slight tendency to off-stoichiometry is indicated in the results for tubes containing MCW special dense  $UO_2$ .

Of the various element designs that are being considered to minimize surface roughness, warpage, and dimensional nonuniformity which occur when pressure bonding elements containing tapped powders or cores of a low density, the corrugated rod or tube appears most promising. Additional specimens of this type and also other designs are being prepared.

A preliminary investigation was conducted to demonstrate the feasibility of pressure bonding an edge-welded stainless steel-clad  $UO_2$  compartmentalized flat plate. Type 304 stainless steel components were machined from 10 to 100-mil as-rolled sheet. The  $UO_2$  cores possessed a high initial density. The over-all plate dimensions were 0.120 by 1.875 by 5.500 in. It contained nine cores measuring 0.100 by 0.2495 by 1.500 in. Preliminary examination of the bonded specimen revealed excellent dimensional control and good bonds. Compartmental integrity will be established by burst tests.

Future work will concern a more complete evaluation of the fuel-element designs selected for pressure bonding and permeability and thermal-conductivity tests of pressure-bonded  $UO_2$ .

#### DEVELOPMENT OF URANIUM CARBIDE-TYPE FUEL MATERIALS

F. A. Rough and W. Chubb

In an effort to reduce the cost of electrical power produced from nuclear energy, the AEC has sponsored a series of research programs designed to investigate and develop uranium carbides as reactor fuels. A portion of this work is in progress at Battelle, and involves development of techniques for production of carbide shapes, determination of the physical and mechanical properties of uranium carbides, determination of the chemical behavior of uranium carbides in contact with various solids, liquids, and gases, and investigation of the mechanism by which neutron irradiation and fission produce damage in the carbides.

TABLE FF-4. RESULTS OF STOICHIOMETRY STUDY

Tube	Type of UO <sub>2</sub> Powder	Binder	As-Received Analysis		Bonding Conditions			Postbonding Analysis	
			Uranium, w/o	Oxygen-to-Uranium Ratio	Time, hr	Temperature, F	Pressure, psi	Uranium, w/o	Oxygen-to-Uranium Ratio
PB-20	MCW special dense	Carbowax 6000-MEOH	88.14	2.00	4	2100	10,000	88.07	2.02
PB-21	Spencer fused	Carbowax 6000-MEOH	88.15	2.00	4	2100	10,000	88.15	2.00
PB-22	MCW ceramic	Carbowax 6000-MEOH	87.72	2.08	4	2100	10,000	88.09	2.01
PB-23	MCW ceramic	Carbowax 6000-MEOH	87.72	2.08	3	2200	10,000	88.13	2.00
PB-24	MCW special dense	None	88.14	2.00	4	2100	10,000	88.10	2.01
PB-25	Spencer fused	None	88.15	2.00	4	2100	10,000	88.14	2.00
PB-26	MCW ceramic	None	87.72	2.08	4	2100	10,000	88.10	2.01
PB-27	MCW ceramic	None	87.72	2.08	3	2200	10,000	88.12	2.01

Past work has resulted in scaling up the skull-melting process to produce right-cylindrical shapes having cross-sectional areas of over 6 sq in. Work is continuing in an effort to make the process more versatile and reliable. Other studies have resulted in determination of the electrical resistivities, the densities, the rupture strength, corrosion rates, and interdiffusion rates of the various uranium carbides. Preliminary data have also been obtained with respect to the compatibility of uranium monocarbide with Inconel, steel, stainless steel, aluminum, copper, molybdenum, and tantalum. Much of these data were summarized in a topical report (BMI-1370) covering the first 6 months of research on this program.

Work during recent weeks has resulted in an increase in the reliability of certain data on the physical properties of uranium carbides. The average density of sixteen samples of as-cast uranium-4.8 w/o carbon specimens was 1.35 g per  $\text{cm}^3$ , and average density of sixteen samples of as-cast uranium-7.0 w/o carbon specimens was 12.4 g per  $\text{cm}^3$ . These values are not significantly different from those reported in BMI-1370. The average resistivities of the same specimens were 38 microhm-cm and 50 microhm-cm, respectively. These resistivities are slightly lower than those reported in BMI-1370; this increase in conductivity probably represents an improvement in the internal quality of the castings. It has been observed that the addition of certain metals, such as niobium, to uranium monocarbide results in a marked improvement in the metallic luster of the specimens. If such specimens prove to be cast cermets, the improvement in properties could be of considerable significance.

#### Alternate Fabrication Methods for UC

S. J. Paprocki, D. L. Keller, D. E. Kizer, and J. M. Fackelmann

Various methods of producing dense UC by powder-metallurgy techniques are being investigated. The methods being considered include sintering of UC powder made by different procedures such as the reaction of uranium metal and  $\text{UO}_2$  with carbon or the reaction of uranium metal and methane, as well as studies of hot-pressing techniques which involve simultaneous reaction and densification.

Several compacts of 4.8 w/o carbon (Morite Type A activated charcoal)-95.2 w/o uranium metal powder were hot pressed at temperatures ranging from 1050 to 1150 C. Densities varied from 71.5 to 78.5 per cent of theoretical - the latter value having been obtained after holding at 1150 C for 4 hr. The microstructure of these specimens consisted of UC, uranium,  $\text{UO}_2$ , and two unidentified phases. Since the size of the uranium metal powder used was minus 325 mesh, surface reactions may have contaminated the metal with  $\text{UO}_2$  or other impurities and prevented the complete formation of UC. Similar compacts are being prepared with uranium hydride substituted for uranium in an attempt to provide an active clean metal surface during the hot-pressing operation. In addition, uranium metal shot has been ordered and will be used for additional hot-pressing studies of uranium-carbon mixes.

Compacts of UC that were pressed at 15 tsi were sintered at temperatures of 1900 to 2120 C for time periods of 5 to 30 min. Densities showed no significant variation,

## FF-9

ranging from 68.3 to 71.8 per cent of theoretical, as shown in Table FF-5. The powder used was minus 325-mesh arc-melted UC having the oxygen and carbon contents shown in Table FF-5. Carbon content dropped about 0.2 w/o during the sintering operation as calculated in Table FF-5. Metallographic examination of these compacts is in progress. Microscopic examination of similar specimens often has shown a two- or three-zone sintering effect where a 30-mil rim of a 200-mil-diameter specimen contained free uranium and coarse UC grains, and possessed a high density. In progressing toward the center, the amount of free uranium decreased to an undetectable amount, porosity increased, and particle size and shape were practically unchanged from their original unsintered conditions. The thickness of the dense layer as a function of time at temperature will be measured in order to gain information on the mechanisms involved.

TABLE FF-5. SINTERING AND ANALYTICAL DATA FOR UC POWDER AND COMPACTS

Specimen	Powder Analysis			Time, min	Sintering Data		Total Carbon Content After Sintering, w/o
	Oxygen, ppm	Total	Carbon, w/o Free		Temperature, C	Density, per cent of theoretical	
16	3040	4.79	0.01	10	1900	67.7	--
18	790	4.83	0.03	30	1900	69.9	4.56
19	790	4.83	0.03	30	1900	70.7	--
20	790	4.83	0.03	10	2005	68.4	4.72
21	790	4.83	0.03	10	2005	68.4	--
24	790	4.83	0.03	30	2000	69.1	--
25	790	4.83	0.03	30	2000	68.3	4.67
22	790	4.83	0.03	5	2120	71.8	4.59

A mixture of the stoichiometric composition of UC was prepared from  $\text{UO}_2$  and carbon powders. This powder mixture (uncompacted) was slowly heated to 1500 C in a graphite crucible under vacuum. Considerable outgassing was noted at 1300 C, but a pressure of  $200 \mu$  or lower was maintained throughout the run. The specimen was held at 1500 C until a vacuum of  $1 \mu$  was obtained, and then it was furnace cooled. An X-ray diffraction analysis revealed the presence of  $\text{UO}_2$ , UC, and unknowns. Additional specimens will be compacted and run at a lower pressure in an attempt to remove the remaining  $\text{UO}_2$ .

The above studies are continuing, and, in addition, UC powder produced by various processes is being classified as to size and shape, gaseous contaminants, and carbon content.

Melting and Casting Techniques for Uranium-Carbon Alloys

B. L. Boesser, W. M. Phillips, E. L. Foster, and  
R. F. Dickerson

Reliable techniques for the production of high-quality cast shapes of uranium carbide are being developed. During the past month, the preparation of cast shapes of uranium carbide by skull-type arc-melting procedures was continued. These efforts have as a specific objective the establishment of techniques for the control of composition and the preparation of cast shapes containing about 5.0 w/o carbon. To this end, a small carbide skull contained in a graphite crucible liner was removed, and liner and skull were replaced by a solid carbide skull prepared in the following manner:

- (1) The bottom portion of the skull was melted in place using prealloyed UC containing approximately 5 w/o carbon.
- (2) The balance of the skull was melted in place from charges of metallic uranium and 4 w/o carbon.

Only two castings have been melted and poured from this skull. The resulting castings, while they were exceptionally homogeneous (end-to-end variations along the 7-in. length were less than 0.1 w/o carbon) and sound, contained about 6 w/o carbon. The graphite electrode losses do not account for this gain in carbon over that of the charge composition. Unreacted chunks of graphite found in the top of the skull indicate that in melting that portion of the skull made from uranium and carbon (4 w/o), the melted uranium metal segregated by settling before complete alloying with the carbon was accomplished. This effect would result in enrichment of the material near the top of the skull in carbon.

Immediate plans will involve an adjustment of the composition of the skull liner by addition of uranium and preparation of cast shapes containing 5.0 w/o carbon. Demonstration of compositional control will be established by preparing a series of castings 3/4 in. in diameter and 8 in. long. The design and preparation of molds and a mold-heating device that can be used to produce a number of cylindrical cast shapes with one pouring are also in progress.

Metallurgical and Engineering Properties of  
Uranium Monocarbide

W. M. Phillips, E. L. Foster, and R. F. Dickerson

A study of the properties of uranium carbides is in progress to determine and enhance the properties of these materials. Properties of interest are density, resistivity, thermal conductivity, strength, and corrosion resistance. The effects of such variables as impurity content, carbon content, alloy content, and heat treatment are being evaluated in terms of the above properties.

FF-11

Work on the effect of carbon content, of annealing temperature, and of as-cast diameter has been in progress during the past month. The data obtained up to the present time indicate little effect of annealing temperatures up to 1800 C, on the resistivity and density of the material. Sixteen specimens containing 4.8 w/o carbon had an average density of 13.5 g per cm<sup>3</sup> and an average resistivity of 38 microhm-cm. A similar number of 7.0 w/o carbon alloys had an average density of 12.4 g per cm<sup>3</sup> and an average resistivity of 50 microhm-cm.

In an attempt to improve the corrosion resistance of UC, additions of 0.5 and 10.0 w/o chromium, iron, molybdenum, nickel, niobium, tantalum, tungsten, or zirconium have been made to uranium monocarbide. The alloys containing 10 w/o iron, molybdenum, niobium, or tantalum have a more silvery metallic appearance, indicating possible improved properties. Testing of these specimens is presently in progress.

Additional work on the compatibility of uranium monocarbide with Inconel, mild steel, niobium, stainless steel, and zirconium is planned to determine the lowest temperature at which reaction between UC and these materials can be observed after an exposure of 100 hr. Future work will also include a study of the kinetics of formation of U<sub>2</sub>C<sub>3</sub> and additional work on the effects of binary additions to uranium carbide.

#### Uranium Monocarbide Diffusion Studies

W. Chubb, R. W. Getz, and F. A. Rough

Uranium monocarbide is being considered as a fuel for nuclear reactors operating at high temperatures. Certain characteristics of this material, such as creep strength and resistance to radiation damage, are closely related to the rate of interdiffusion of uranium and carbon and to the rates of self-diffusion of uranium and carbon in uranium monocarbide. The rates of interdiffusion of uranium and carbon at various temperatures were determined and reported earlier; the self-diffusion of uranium in uranium monocarbide is presently being investigated. Diffusion couples have been bonded successfully, and the techniques necessary for determining the extent of self-diffusion of uranium in uranium carbide have been developed. Currently, a preliminary diffusion couple is being sampled in preparation for neutron activation and analysis.

The diffusion couples are made by placing a 0.001-in.-thick foil of enriched uranium (93 per cent uranium-235) between two 0.25-in.-lengths of depleted uranium (0.04 per cent uranium-235) monocarbide rod. The couple is then wrapped in a 0.002-in.-thick tantalum foil, placed in a graphite jig, and bonded in vacuum for 4 hr at 1400 C. Two bonded couples have been diffusion annealed, one for 1.5 hr at 1800 C and one for 7 hr at 1600 C. Metallographic inspection of the bonds indicated that the former was satisfactorily bonded and annealed and that the latter was unsatisfactory.

The couple diffusion annealed at 1800 C is being prepared for neutron activation in the BRR. An aluminum dish is being used in taking samples at 0.001-in. intervals along the couple. These samples are obtained by grinding the couple on 600-grit silicon carbide powder in the presence of a small amount of 0.1 N nitric acid solution. The gamma activity of the neutron-activated samples will be used to determine the amounts

FF-12

of uranium-235 and uranium-238 present in the samples. From the resultant data it will be possible to calculate the rate of self-diffusion of uranium in uranium monocarbide.

Future work will include the preparation of additional diffusion couples and the neutron activation of samples from these diffusion couples in the BRR.

#### Irradiation Effects in UC

A. E. Austin and C. M. Schwartz

The changes in structure of UC with irradiation and fission are being studied. Electron-microscope examination has been made of specimens with estimated burnups of 0.05 and 0.2 a/o uranium. The specimen with lower burnup was irradiated at a calculated temperature of 600 F, while the specimen with 0.2 a/o burnup was irradiated at about 1300 F. The specimens were replicated as described in a previous progress report.

The electron micrographs show a fine pit structure tending to concentrate in long traces which may indicate incipient cracks. The specimen with 0.2 a/o burnup consisted of the normal UC grain structure containing the straight UC<sub>2</sub> needle precipitate, apparently unchanged. The specimen with 0.05 a/o burnup contained deformed warped UC<sub>2</sub> needles with cracks along their sides. This difference in the microstructure of these specimens may be due to the differences in temperature of irradiation. At the higher temperature, 1300 F, self-annealing of the strains resulting from fission may occur. Further work is in progress on comparing the fine pit structure with unirradiated material.

The deformation of UC<sub>2</sub> needles or plates in carbides having UC as a matrix described above and apparent disappearance of the UC<sub>2</sub> phase in the center portion of specimens irradiated for Atomics International indicate a need for study of the effects of irradiation upon strain in this material. Equipment has been modified and techniques developed to prepare suitable samples for studies of lattice strain by X-ray diffraction methods on irradiated samples. A series of specimens having burnups from 0.01 a/o uranium or less up to 0.5 a/o uranium is to be studied. Delivery of enriched uranium for preparation of the specimens is expected momentarily.

## GG-1 and GG-2

## GG. VOID-DISTRIBUTION AND HEAT-TRANSFER STUDIES

D. V. Grillot, R. Wooten, H. M. Epstein, and J. W. Chastain

During the month, a stable void-detection system was attained by adding a voltage regulator to the circuit. Magnetic shielding and forced-convection cooling also were installed to aid detector stability. Despite these modifications, the detector is still temperature sensitive and will have to be calibrated for temperature rise.

Continued problems have been encountered in maintaining a satisfactory test section. Electrical short circuits or pressure leaks occur around the pressure taps. The last test section lasted for several weeks while a number of calibration runs were made. Welding personnel are optimistic about making test sections which will have longer life.

A test section without pressure taps is being used to investigate two-phase flow instabilities. Two-phase flow instability was not anticipated in the present experiment. A previous experiment performed at Battelle using an almost identical system resulted in no flow instabilities. The lack of instability in this previous experiment has been attributed to higher operating pressures.

Originally, instability in the present experiment was such that the system was incapable of reaching the subcooled-boiling region. This violent flow instability was attributed to insufficient cooling of the steam-liquid mixture emerging from the test section. With additional cooling the loop has performed more satisfactorily. Sub-cooled conditions have been attained, but oscillation in the flow have caused variations in the position of the subcooled-boiling region in the test section. These fluctuations have prevented measuring void fraction.

It is believed that collapsing steam bubbles in the condenser cause fluctuations in pressures which, in turn, cause changes in flow rate, water temperature, and in void distribution within the test section.

A possible solution is to throttle the system at the inlet to the test section. The driving force, viz., the pressure preceding the test section, will then be large enough to overcome pressure changes which exist in the condenser. Possibly a more feasible solution is to install a steam separator at the test-section exit. A steam separator would eliminate two-phase flow from a major portion of the loop, and it would also function as a surge tank in that part of the loop which is experiencing the greatest pressure and flow fluctuations.

This latter solution is being tried presently. Solution of flow instability should eliminate the last major difficulty and permit meaningful data to be obtained.



## H-1

## H. PHYSICAL RESEARCH

F. A. Rough

Studies of physical research on niobium-gas reactions and on growth of UO<sub>2</sub> single crystals are under way for the AEC Division of Research.

In the study of niobium-gas reactions, consistent kinetic experiments have been obtained at 200 to 600 C by first vacuum heating at 1100 C to establish uniform surface conditions. Equations describing the reaction rates are given.

In the preparation of UO<sub>2</sub> single crystals from the vapor phase, procedures involving both direct vaporization of UO<sub>2</sub> and reaction of UF<sub>4</sub> and H<sub>2</sub>O are being studied. Fusion methods for growth of single crystals are also being studied, including floating-zone and other methods.

Niobium-Gas Reactions

W. M. Albrecht and W. D. Goode

A fundamental study of the reactions of nitrogen with niobium is being made. The study consists of determinations of reaction kinetics and mechanisms and includes determination of diffusion coefficients and solubility of nitrogen in niobium.

Reaction rates, diffusion coefficients, and solubility of nitrogen in niobium in the range 675 to 1600 C were presented in BMI-1360.

Kinetic experiments have been made at 200 to 600 C. The samples used in these experiments were vacuum annealed at 1100 C for 45 min. The reaction rates were found to follow the logarithmic law\*

$$w (\mu \text{ g per cm}^2) = k \log (a t + 1),$$

where w is the weight gain and t is time. The values for the constants k and a are shown in Table H-1. It is seen that the value of a remains practically constant over the entire temperature range, the average value being  $4.1 \times 10^{-3} \text{ sec}^{-1}$ . The value of k was found to vary with temperature, T, according to the equation

$$k (\mu \text{ g per cm}^2) = 2.17 \exp [-(5,160 \pm 98)/RT].$$

X-ray diffraction examination of the surface of samples reacted at 300 and 500 C showed the presence of Nb<sub>2</sub>N and NbN.

A paper describing all the work in the niobium-nitrogen system is being prepared.

\*Kubaschewski, O., and Hopkins, B. E., Oxidation of Metals and Alloys, Academic Press Inc., New York (1953), p 38.

TABLE H-1. SUMMARY OF LOGARITHMIC RATE CONSTANTS FOR THE REACTION OF NITROGEN WITH NIOBIUM

Temperature, C	Constants in the Logarithmic Rate Equation	
	k, $\mu\text{g per cm}^2$	a, $10^{-3} \text{ sec}^{-1}$
200	0.85	4.2
250	1.61	4.2
300	2.46	4.2
400	4.43	4.2
450	5.44	3.9
500	8.22	4.2
550	9.40	4.1
600	10.9	3.4

Growth of  $\text{UO}_2$  Crystals From the Vapor Phase

C. A. Alexander and R. B. Filbert, Jr.

During the past month, experiments were continued in producing  $\text{UO}_2$  crystals from the vapor phase. Attention was directed toward two additional processes besides the decomposition of gaseous  $\text{UO}_3$  which was begun in November. The additional processes are direct vaporization of  $\text{UO}_2$  and production of  $\text{UO}_2(\text{g})$  through the reaction of  $\text{UF}_4(\text{g})$  and  $\text{H}_2\text{O}(\text{g})$ .

In the direct-vaporization experiments, approximately 5 g of  $\text{UO}_2$  was placed in a V-shaped tantalum-foil boat which was clamped to 1/4-in.-diameter molybdenum electrodes. A low-voltage high-current transformer was employed as a power source. The tantalum-foil furnace was heated to approximately 2300 C in vacuum. Exact temperature measurements could not be made because the foil furnace was completely enclosed in a double radiation shield. In a 1/2-hr run, crystals of about 0.1 mm were grown. Microscopic analysis indicated a bluish cast to the crystals rather than the red usually observed in  $\text{UO}_2$ . It was concluded that the impurity level of the crystal was quite high.

Thermodynamic computations indicate that  $\text{UO}_2(\text{g})$  can be produced from the reaction of  $\text{UF}_4(\text{g})$  with  $\text{H}_2\text{O}(\text{g})$  which yields  $\text{UO}_2$  and HF. The first attempt at producing crystalline  $\text{UO}_2$  by this reaction was carried out at 750 C in a system operating at a total pressure of 50 mm of mercury. Of this pressure, 40 mm was due to water vapor, and the rest was predominantly HF. The vapor pressure of  $\text{UF}_4$  was considerably less than 1 mm of mercury. The reaction proceeded quite rapidly at this water vapor pressure and converted the 40-g charge of solid  $\text{UF}_4$  to brown  $\text{UO}_2$  in about 30 min. No evidence of crystalline  $\text{UO}_2$  was found in the small amount of condensed vapor or in the solid charge that was converted to  $\text{UO}_2$ .

In an effort to control the reaction kinetics, another reduced-pressure run was made. This time the pressure was 11 mm of mercury, with 10 mm of mercury accounted for by the vapor pressure of  $\text{UF}_4$ . Run temperature was 1050 C, and the large

## H-3

UF<sub>4</sub> pressure was employed in an effort to insure that the reaction in the vapor phase would remove the water vapor before the latter could reach the area containing the molten UF<sub>4</sub>. Microscopic examination of the condensed vapor at the end of the run indicated that nearly all of the crystals produced were UF<sub>4</sub>. A few crystals of about 50- $\mu$  size of UO<sub>2</sub> were found. The reaction had progressed only to the extent of about 10 per cent completion when it was terminated. The reason for the slowness of the reaction was that UF<sub>4</sub> condensed on the tube bringing the water vapor into the furnace and effectively stopped the flow of water vapor into the reaction zone. Examination of the UF<sub>4</sub> charge showed a few small crystals of UO<sub>2</sub> in it. It is not known whether these grew in the fluoride or whether they dropped from the condenser into the melt when the cooldown began. The possibility of growing UO<sub>2</sub> crystals from a molten fluoride solution will be checked in future months.

For the coming month, it is planned to make additional runs using the UF<sub>4</sub>-water vapor reaction. The use of a carrier gas for the two reactants will be tried since this is more controllable than the vacuum that has been employed in previous runs. The fluoride reaction has advantages over the congruent vaporization of UO<sub>2</sub> in that the temperatures for the fluoride reaction can easily be reached in conventional resistance furnaces. This does not introduce the possibility of a cation impurity that is so prevalent in the high-temperature runs. The advantage of the fluoride reaction over the decomposition of gaseous UO<sub>3</sub> is that the fluoride reaction can give a stoichiometric UO<sub>2</sub>, while this is not possible in the UO<sub>3</sub> reaction.

For these reasons an effort will be made to establish conditions that will produce crystalline UO<sub>2</sub> from UF<sub>4</sub>.

#### Fusion Methods to Prepare Single Crystals of UO<sub>2</sub>

W. P. Allred and B. Paris

During December research was continued to develop a process by which large single crystals of UO<sub>2</sub> can be grown. The major emphasis was placed upon the floating-zone technique for growing the crystals. The problem of a high-resistance contact to the UO<sub>2</sub> has been alleviated to some extent by use of silver paint. However, some arcing occurred between the molybdenum holders and the UO<sub>2</sub> rod, producing erratic heating and hence fracture of the rod due to fast and uneven heating or cooling. A more satisfactory contact will ultimately be required. Therefore, it is planned to use elemental uranium by mixing it in the portions of the UO<sub>2</sub> rod which are in contact with the molybdenum chucks. It is expected that this procedure will increase the conductivity of the end portion of the rods and thus decrease the arcing.

Use of a current-limiting device has helped to provide more even resistance heating of the UO<sub>2</sub> samples. Samples have also been shaped to help provide even heating.

Lower frequency is being used in attempts to reduce or eliminate arcing between the rf coils and the UO<sub>2</sub> samples.

Additional methods of melting the UO<sub>2</sub> in a fashion suitable for crystal growth has been considered. It is felt that arc or plasma melting could be used to successfully melt

## H-4

the  $\text{UO}_2$  and still produce desirable conditions for crystal growth. Furthermore, in this process the  $\text{UO}_2$  could be used as the crucible, thus eliminating contamination from the crucible. Cabane\* has used a high-intensity arc to zone refine silicon, thorium, titanium, and zirconium. A water-cooled copper boat was used to contain these materials. This method might also be used to purify the  $\text{UO}_2$  as well as to grow large single crystals.

Experimental equipment is now being constructed to study the possibility of using arc and plasma melting to grow single crystals of  $\text{UO}_2$ . The arc will be studied for use in growing the crystals by pulling from the melt and by growing in a horizontal boat.

Experiments on floating-zone melting will be continued also.

---

\*Cabane, G. J., Nuclear Energy, 6, 269 (1958).

I-1

## I. SOLID HOMOGENEOUS FUELED REACTORS

W. S. Diethorn and W. H. Goldthwaite

Battelle is investigating the properties, irradiation damage, and fission-gas retention of fueled-graphite spheres in support of the Pebble-Bed Reactor program.

### LABORATORY EVALUATIONS OF FUELED-GRAPHITE SPHERES

J. F. Lynch, M. C. Brockway, S. Rubin, and W. H. Duckworth

Fueled-graphite spheres supplied by commercial vendors are being investigated in impact and compression tests. Self-welding experiments with coated spheres were not scheduled this month. No spheres were examined in the phase of the program concerned with the permeability of sphere coatings at high, internal gas pressures.

In the high-temperature study of the permeability of SiC-coated spheres, mass spectrometric analysis of the argon purge gas in runs at 1400 and 1850 F reveals some evidence for the release of gas, absorbed on the graphite matrix and released from the coating. In this study argon gas is passed over a heated specimen and analyzed for the presence of nitrogen, oxygen, carbon monoxide, and carbon dioxide. A sphere with a defected coating will be studied to supply information for the interpretation of the 1400 and 1850 F runs.

### FABRICATION DEVELOPMENT OF $\text{Al}_2\text{O}_3$ -CLAD $\text{UO}_2$ FUEL PARTICLES

A. K. Smalley and A. F. Gerds

The oxidation-resistance testing and metallographic examination of  $\text{Al}_2\text{O}_3$ -clad  $\text{UO}_2$ , prepared from two different starting materials, were continued this month.

Three separate batches, made with  $\text{UO}_3$  seed, were heated in air at 1200 F for 5 hr. Weight gains correspond to oxidation of 1, 2, and 4 w/o of the fuel. Batches made from  $\text{UO}_2$ -10 w/o Du Pont F powder seed showed large weight gains after this treatment.

Metallographic examination of these batches revealed the following:

- (1) Fuel particles made from seed  $\text{UO}_3$  contained gross porosity and were surrounded by prominent annular voids.
- (2) The  $\text{UO}_2$ -Du Pont F powder fuel particles contained little gross porosity, and appeared to be about 75 to 80 per cent of theoretical density. There were no annular voids between fuel particles and cladding.

Work now under way will evaluate the effect of  $\text{UO}_2$ - $\text{UO}_3$  seed mixtures on the sintering shrinkage of the fuel core. The objective of this work is to reduce the core-cladding void by adjusting the shrinkage.

The 1000-hr 2500 F heat treatment of  $\text{Al}_2\text{O}_3$ -clad  $\text{UO}_2$ , dispersed in two different carbon matrices, has been completed. Metallographic examination is under way.

### FISSION-PRODUCT RELEASE FROM FUELED-GRAFPHITE SPHERES

W. S. Diethorn

Fission-gas retention and the effect of radiation on fueled-graphite spheres are being investigated in neutron-activation experiments and sweep-gas and static irradiation capsules.

#### Neutron-Activation Studies

H. S. Rosenberg

Two SiC-coated spheres were activated this month. Both spheres passed the hot-oil test before neutron activation and after completion of the postirradiation heat treatment. The data are shown in Table I-1.

TABLE I-1. NEUTRON-ACTIVATION RESULTS

Specimen	Postirradiation Heat-Treatment Temperature, F	Time at Temperature, min	Fission-Gas Release <sup>(a)</sup> , per cent of xenon-133
FA-16, No. S-15	1650	100	$1 \times 10^{-3}$
FA-16, No. S-13	1650	100	$5 \times 10^{-4}$
	2100	80	$1.5 \times 10^{-3}$

(a) Number of atoms released divided by number of atoms present at beginning of heat treatment, times 100.

In-Pile Capsule Experiments

D. B. Hamilton, G. E. Raines, R. J. Burian, and W. H. Goldthwaite

SP-3

The postirradiation examination of this capsule was completed in December. No further work on the capsule specimens is planned.

Metallographic examination of the FA-8 specimen, coated with siliconized SiC, showed that the bond between the coating and graphite matrix was good. There were no cracks in the coating.

SP-4

Operation of Capsule SP-4 in the BRR will continue to mid-March. A uranium-235 burnup of 5 to 6 per cent is expected for the fully enriched spheres in this capsule.

SP-5

It is expected that specimens will be available for insertion of this sweep capsule in the BRR during March, 1960.

SPF-1

This low-flux capsule was inserted in the BRR on December 16. The R/B data are listed in Table I-2. Comparison of the results in Table I-2 with those reported for 1500 F last month in BMI-1398 shows that the R/B values at 1000 F are about three to eight times smaller, depending on species, than the R/B values at 1500 F.

TABLE I-2. SUMMARY OF SPF-1 RESULTS AT 1000 F

Gas Sample	Collection Date, 1959	Flux, n/cm <sup>2</sup> /sec	R/B <sup>(a)</sup>				
			Krypton-87	Krypton-88	Krypton-85m	Xenon-135	Xenon-133
10	12-21	$1.6 \times 10^{10}$	$1.9 \times 10^{-3}$	$0.96 \times 10^{-3}$	$3.8 \times 10^{-3}$	$3.2 \times 10^{-3}$	$5.5 \times 10^{-3}$
11	12-22		$2.4 \times 10^{-3}$	$0.70 \times 10^{-3}$	$3.8 \times 10^{-3}$	$3.8 \times 10^{-3}$	$5.6 \times 10^{-3}$
12	12-23		$2.5 \times 10^{-3}$	$1.2 \times 10^{-3}$	$3.8 \times 10^{-3}$	$4.7 \times 10^{-3}$	$5.9 \times 10^{-3}$

(a) R = the number of atoms released per second.

B = the number of atoms produced per second.

Following the runs at 1000 F, the capsule was operated at 1900 F for several days. These latter data are now being analyzed. This completes the SPF-1 experiment.

SPF-2

This second capsule in the SPF series is being loaded with a fueled-graphite specimen, FA-16, No. 15. Neutron activation results for this specimen are reported in Table I-1. Target data for BRR irradiation of this capsule is February 1, 1960.

J-1

## J. PROBLEMS ASSOCIATED WITH THE RECOVERY OF SPENT REACTOR FUEL ELEMENTS

### CORROSION STUDIES OF THE FLUORIDE-VOLATILITY PROCESS

P. D. Miller, C. L. Peterson W. N. Stiegelmeyer, and F. W. Fink

The corrosion of components from the Unit Operations INOR-8 Fluoride-Volatility dissolver at ORNL has been examined as part of a program of assistance to the Chemical Technology Division. The major results have been reported earlier. Recent metallographic examinations of grain size have shown variations from ASTM-3 to ASTM-9, apparently randomly distributed throughout the vessel. The corrosion did not appear to be directly related to grain size. The accelerated corrosion and large grain size in a salt-inlet line was believed to have been caused by excessive temperatures reached at the point where electrodes were attached for autoresistance heating.

### STUDY OF THE EFFECTS OF IRRADIATION ON CLADDING- AND CORE-DISSOLUTION PROCESSES

R. A. Ewing, H. B. Brugger, and D. N. Sunderman

### Sulfex Process

First tests of the Sulfex process are being conducted on 7-in. prototype Consolidated Edison fuel pins which had been irradiated to a low level (300 to 500 MWD/T) at ORNL. Dissolution of the core of the second fuel pin (previously declad) was completed, and the third and fourth pins were declad and dissolved.

#### Test HS-2 (Pin A-117)

This pin had been declad in the previous hot-cell campaign. The 42.2-g residue was returned to the dissolver and digested with 155 ml of 13 M HNO<sub>3</sub> core dissolvent for 5 hr. Upon removal of the core dissolvent it was observed that the core pellets were covered with a white coating, presumably thorium sulfate, and had been attacked only slightly. (The core pellets had been washed after decladding only with the standard 100 ml of water; evidently this was insufficient to satisfactorily eliminate sulfate contamination.) Approximately 50 ml of water was added to the dissolver, and the core pellets were digested for 3 hr, which removed the white coating. After this washing dissolution proceeded smoothly with a second 155-ml charge of fresh core dissolvent, and was complete in 5 hr. There was no end-cap residue from this test; these had been dissolved by the prolonged decladding period necessary because of passivation.

Test HS-3 (Pin A-108)

The surface of this pin appeared to be generally dull, but passivation was absent. The decladding solution was sampled after 3 hr and withdrawn and filtered after 6 hr. The declad core pellets appeared to be entirely whole, and no indications of shattering were apparent.

To prevent a recurrence of sulfate inhibition of core dissolution, as in the previous test, the core pellets were soaked overnight in 100 ml of water. With this additional washing, no difficulties were encountered; dissolution was satisfactorily completed in the standard 8 hr.

Test HS-4 (Pin A-196)

This test was conducted by the same procedure used for Test HS-3, and proceeded routinely to completion.

Future Work

Samples from the first four runs are currently being analyzed and results will be reported next month. This will complete the Sulfex test of the ORNL-irradiated fuel pins. Following similar Darex tests, additional Sulfex tests are planned on MTR-irradiated (~4000 MWD/T) prototype Consolidated Edison pins.

Darex Process

No Darex dissolution tests were conducted during the month. Darex-process tests are scheduled for January on the two remaining ORNL-irradiated fuel pins.

K-1

## K. DEVELOPMENTS FOR SRE

EVALUATION OF URANIUM MONOCARBIDE  
AS A REACTOR FUEL

F. A. Rough

Examination of two capsules of irradiated specimens of arc-cast uranium monocarbide currently in the hot cell is largely completed. Additional data have been obtained for burnup estimates and on the fission gas contained in the capsules. Two additional capsules of specimens are undergoing irradiation, one of them to an estimated 20,000 MWD/T burnup.

Irradiation of Uranium Monocarbide

D. Stahl, J. H. Stang, and W. H. Goldthwaite

Capsule BMI-23-6, containing cylindrical specimens of UC, has been discharged from MTR the A-13-NE position after an irradiation of six MTR cycles, and is being returned to the Battelle Hot-Cell Facility. Specimen center-line temperatures during the final irradiation cycle, Cycle 131, were in the 1300 to 1400 F range. It is estimated that the burnup for the specimens is approximately 5000 MWD/T of uranium.

The irradiation of Capsule BMI-23-4 is continuing in the A-27-SE position of the MTR for a target burnup of 20,000 MWD/T of uranium; this will require that the capsule be under irradiation until early summer, 1960. Specimen center-line temperatures for December were in the 1100 to 1200 F range.

Postirradiation Examination of Irradiated Uranium Monocarbide

S. Alfant and R. F. Dickerson

The primary objectives of this program are to study the effects of irradiation on uranium monocarbide, and to evaluate it as a fuel material for sodium-cooled reactors. Seven capsules were designed and fabricated to conduct radiation tests on uranium monocarbide. To date, three capsules with specimens containing uranium monocarbide have been irradiated and examined.

The examination of specimens from Capsules BMI-23-3 and BMI-23-5 is now in progress. As reported previously, the postirradiation macroexamination and measurements of the density and dimensions of specimens from both capsules have been completed. Only small changes in density and diameter occurred during irradiation. Radial and transverse cracking with some breaking off at the ends was observed in the 4.6 w/o carbon specimens from Capsule BMI-23-5, which experienced burnups

## K-2

(estimates based on reactor-quoted fluxes) of approximately 0.66 a/o uranium (4940 MWD/T of uranium) and 0.70 a/o (5270 MWD/T of uranium) for the top and bottom specimens, respectively. The same type of cracking but in slightly greater amounts was observed on the 5.0 w/o carbon specimens from Capsule BMI-23-3 which experienced burnups of approximately 1.75 a/o uranium (13,000 MWD/T of uranium) and 1.93 a/o uranium (14,300 MWD/T of uranium) for the top and bottom specimens, respectively. Generally, the cracking observed in specimens from both capsules was not severe, when compared with the cracking observed in specimens from the previously irradiated capsules, BMI-23-1 and BMI-23-2. The differences in composition of the specimens and the higher burnups experienced in Capsule BMI-23-3 did not appear to have an appreciable effect on the type of cracking but more cracking did occur at its higher burnup.

During the past month, work was completed on fission-gas analyses, and on burnup calculations based on dosimetry. The fission gas released from the carbide was determined by analyzing gas samples from the capsules for Krypton-85. However, no activity was detected in the vials containing the samples of fission gas released from Capsule BMI-23-3. The results of the fission-gas analyses are given below. Obviously, the samples for Capsule BMI-23-3 were faulty.

<u>Capsule</u>	<u>Krypton-85 Activity, <math>10^5</math> dps</u>	<u>Total Krypton-85, <math>10^{-5}</math> cm<sup>3</sup></u>
Bmi-23-3	No activity detected	--
	No activity detected	--
	No activity detected	--
BMI-23-5	1.06	8.22
	1.01	8.22
	1.10	8.22

Based on estimated burnup data for Capsule BMI-23-5, the total amount of Krypton 85 produced in the carbide was calculated to be  $20.4 \times 10^{-2}$  cm<sup>3</sup>. For recoil losses, it was assumed that the recoil range of Krypton-85 is  $8 \mu$ , and that the release was one-fourth of the gas generated in the surface layer of  $8-\mu$  depth. The calculated volume of Krypton-85 gas released by recoil is  $8.7 \times 10^{-5}$  cm<sup>3</sup>. Upon comparing the measured value of the Krypton and the amount released due to recoil, it can be seen that the two values are practically equal.

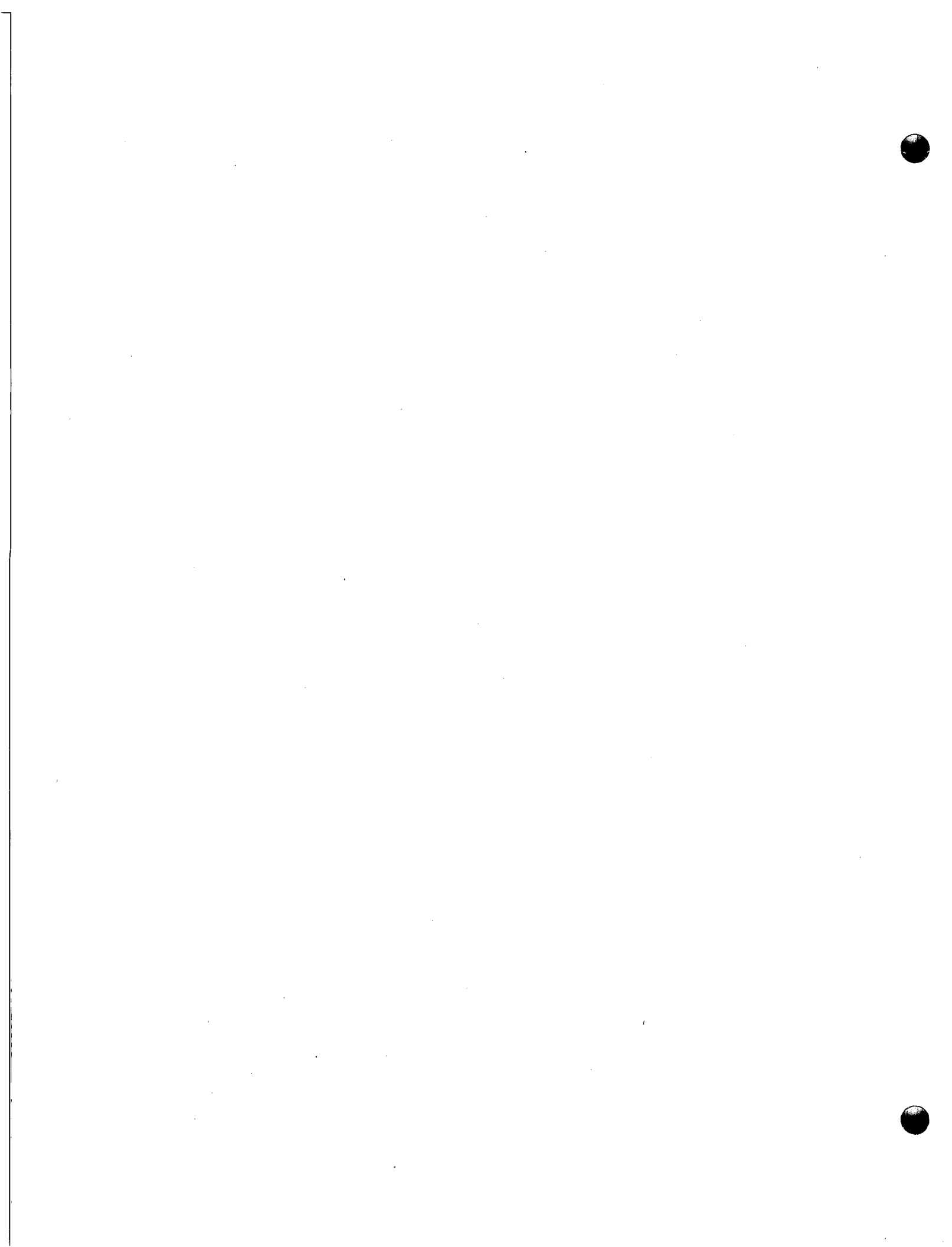
Burnup determinations by analysis of the dosimeters which were wound around the specimens have been completed. The results of these analyses are given in Table K-1.

## K-3 and K-4

TABLE K-1. RESULTS OF NEUTRON DOSIMETRY BASED ON BRAD LEWIS FACTOR AND P-3 FACTOR CALCULATIONS

Capsule Specimen	Maximum Burnup			
	Brad Lewis Factor a/o	MWD/T	P-3 Factor a/o	MWD/T
<b>BMI-23-3</b>				
Top	1.34	10,000	2.00	15,000
Bottom	1.39	10,500	2.07	15,600
<b>BMI-23-5</b>				
Top	0.71	5,300	1.06	7,900
Bottom	0.70	5,250	1.04	7,800

At this time metallographic examination and an isotopic analysis of samples from Capsules BMI-23-3 and BMI-23-5 are being completed.



L-1

## L. TANTALUM AND TANTALUM ALLOYS

J. H. Stang

Studies reported in this section are in conjunction with the LAMPRE program at Los Alamos Scientific Laboratory. During December, melting of binary tantalum alloys resumed (after a recess from October to mid-November), but a problem of electrode erosion necessitated an interruption in the schedule. Several facets of planning were completed for the execution of a new program directed toward identification of phases and determination of solid-solubility limits of impurities in tantalum. Final plans for mechanical-property tests of irradiated tantalum specimens were completed, and initial data were obtained on unirradiated control specimens.

Development of Container Materials for Lampre Applications

D. E. Drennan, M. E. Langston, C. J. Slunder, and J. G. Dunleavy

During most of December it was necessary to discontinue temporarily the arc melting of binary-tantalum-alloy buttons and concentrate effort on solving a difficulty encountered with particularly severe erosion of the tungsten electrode during melting. In several melts made early in December, this erosion was sufficient to produce intolerable contamination with tungsten. To date, attempts to solve the problem have met with some success, and it is expected that a continuing effort can point the way to a complete solution, perhaps by mid-January. It is hoped that, by the end of January, the arc-melting schedule can be resumed.

Effect of Irradiation Damage of Tantalum

C. K. Franklin, F. R. Shober, and R. F. Dickerson

This program involves a study of the effect of irradiation on the mechanical properties (particularly ductility) of tantalum. Two capsules containing sheet specimens of tantalum were irradiated at the MTR, receiving thermal-neutron exposures estimated to be sufficient to produce tantalum-to-tungsten conversions of 1.5 and 3.0 w/o, respectively. These capsules have been opened at the Battelle Hot-Cell Facility, and various specimen property evaluations are scheduled to be made during January. In addition to determination of tensile properties, hardness and bend tests will be made, the latter to obtain a qualitative measure of ductility. In this test, one specimen end will be fixed in a vise and an attempt will be made to bend through a 90-deg arc.

Various property evaluations are being made on unirradiated tantalum and arc-melted tantalum-tungsten alloys to obtain baseline data for the evaluation of irradiation effects. Room-temperature tensile tests completed on four specimens of unirradiated

annealed tantalum indicated an average ultimate tensile strength of approximately 42,000 psi. The total elongation in 1 in. was 40 per cent, and the reduction in area was about 50 per cent.

Precipitate Phase Identification and Interstitial-Type  
Solid Solubility In Tantalum

D. A. Vaughan and C. M. Schwartz

The composition and distribution of the initial precipitate phases caused by interstitial (carbon, nitrogen, and oxygen) impurities in tantalum are being investigated to aid in understanding the corrosion of tantalum by plutonium fuel mixtures. The solid-solubility limits of these impurities in tantalum will be determined at 500, 1000, and 1500 C. Preliminary studies have shown that one source of pedigreed tantalum stock should be employed in this investigation in order to avoid metallic impurities which might modify the solubility study.

During the past month, a supply of Temescal tantalum from LASL stock (K556-5) was obtained. This material is being degassed prior to introduction of known amounts of nitrogen or oxygen by gas-solid reaction. It is planned to study the tantalum-oxygen series first, with additions of 1, 3, and 5 a/o interstitial. These specimens will be examined microscopically and by X-ray diffraction after quench annealing from 1500 C and after heat treating at 1000 C and at 500 C.

Also during the last period, the published literature was reviewed to aid in the selection of compositions for the initial solubility studies, and to consider the compositions of the first compounds to form in the various systems. Although a number of compounds are reported for both oxides and nitrides of tantalum, there are no data on their thermal stabilities or mode of precipitation. This information will be obtained in the present program.

During the next period, the first oxygen alloys should be available for examination.

M-1

## M. DEVELOPMENTAL STUDIES FOR THE PWR

R. W. Dayton

A 33-in.-long fuel element containing  $UO_2$  platelets has been examined. The element was corrosion resistant and did not exhibit intercompartmental leakage. However, metallographic examination showed evidence of contamination. A 40-in. fuel element, made from a machined-receptacle plate, warped during bonding.

Fabrication of Large-Scale PWR-Type Fuel Plates

S. J. Paprocki, E. S. Hodge, and C. C. Simons

The preparation of Zircaloy-2-clad compartmented uranium dioxide fuel elements for PWR Core 2 on a production basis is being considered by Bettis. The feasibility of fabricating this type of fuel element by gas-pressure bonding was established for small-size fuel plates approximately 15 in. long containing 15 core compartments across the width of the fuel plate. In the first scale-up, the length of the fuel element will be increased from 15 in. to 33 or 40 in. The width will remain constant.

The corrosion testing and metallographic examination of a Zircaloy-clad compartmented uranium dioxide fuel plate 33 in. long that was bonded 4 hr at 1550 F at 10,000 psi have been completed. The results of the corrosion testing revealed that, after a 3-day exposure to 680 F water, there was no growth of the defected compartments. The compartments were tested at 700 psi for intercompartmental leakage after the 680 F corrosion test, and no intercompartmental failure was observed. The Zircaloy-2 cladding possessed the characteristic shiny black film of good quality Zircaloy-2. The results of the metallographic examination revealed that the bonds were generally good, with some evidence of spotty contamination at the bond interface. It was noted that in several instances grain growth had occurred around spots of contamination located at the original bond interface. It was necessary to assemble this specimen twice. During the initial assembly, an attempt was made to employ oversize ribs produced by a production machining process. The ribs did not permit a proper assembly of the element; consequently, the element was reassembled with ribs produced by another machining process. Contamination of the surfaces during the first assembly that was not completely removed during washing prior to the second assembly may have produced the contamination at the bond interface.

Four large-scale PWR Core 2-type specimens measuring 0.150 by 4.218 by 40 in. and containing 330 compartmented core inserts were bonded at 1550 F for evaluation at Bettis and Battelle. Three of these four specimens were assembled using shim stock to fill both the longitudinal and transverse void space in the fuel-element receptacle between the core and ribs, while the fourth specimen was assembled without any attempt to fill void space. All of the specimens were fabricated using a integral cover plate and machined receptacle; consequently, the longitudinal ribs were not free to move during assembly to take up void space between the cores and ribs. A visual

examination of the specimen which was assembled without shims to fill longitudinal or transverse void space in the assembled fuel plate disclosed that the side ribs had moved in toward the cores during bonding and eliminated all the longitudinal void space. This, however, produced warpage of the specimen. The transverse void space was partially filled by the cladding flowing into it, producing cladding depressions. Final evaluation of all of the fuel plates will be based on burst tests, leak tests, corrosion tests, and metallographic examinations.

N-1

## N. DEVELOPMENTS FOR THE MGCR

W. C. Riley

Research on core materials in support of the MGCR program is in progress at Battelle. The major effort is on the development and evaluation of  $UO_2$  dispersions in  $BeO$  or  $Al_2O_3$  and dispersions of UC and  $UC_2$  in graphite. Currently, the evaluation consists mainly of static-capsule irradiation in the MTR and BRR.

A study of carbon-transport corrosion studies has been completed, and a topical report is being prepared.

FABRICATION AND CHARACTERIZATION OF FUEL MATERIALS

A. B. Tripler, Jr.

Work on fabrication and characterization of fuel materials was recessed during December.

HIGH-BURNUP IRRADIATION EFFECTS IN FUEL MATERIALS

W. E. Murr, N. E. Miller, J. E. Gates, and R. F. Dickerson

Ceramic-type fuels composed of about 20 volume per cent uranium dioxide in beryllium oxide, 20 volume per cent uranium dioxide in aluminum oxide, 20 volume per cent uranium monocarbide in graphite, and 20 volume per cent uranium dicarbide in graphite are being considered as potential fuels for the MGCR. A program to study the stability of these materials after various radiation exposures at specimen-surface temperatures of about 1500 F is in progress. The evaluation of beryllium oxide- and graphite-matrix specimens includes the irradiation and examination of 24 specimens in 4 instrumented capsules. Each of the four capsules contains six specimens, two of each fuel composition. Each specimen is composed of four fuel pellets, approximately 0.222 in. in diameter by 0.250 in. long, sealed in Type 316 stainless steel tubing under a protective helium atmosphere.

The first capsule of this series was irradiated in the Battelle Research Reactor to a specimen burnup of about 1.1 to 1.7 a/o of the contained uranium at surface temperatures ranging from 1300 to 1550 F. The specimens were in good physical condition after irradiation. The results of the hot-cell examination are reported in BMI-1366 and BMI-1377.

The remaining three capsules, BMI-31-1, BMI-31-2, and BMI-31-3, have been in the MTR since the beginning of cycle 125 and are operating satisfactorily in their

eighth reactor cycle. During the first six cycles of operation, the specimens in Capsule BMI-31-1 experienced an uranium burnup of approximately 9 a/o, those in Capsule BMI-31-2 from 3.1 to 4.2 a/o burnup, and those in Capsule BMI-31-3 from 2.0 to 2.2 a/o. The above values are estimates based on fission power generation calculated from fuel temperatures and the heat-transfer characteristics of each capsule.

A summary of the temperature and heater-power requirements of each capsule during MTR Cycle 131 is shown in Table N-1. Since issuance of BMI-1398, Thermocouple 2 from Capsule BMI-31-1 has failed, leaving three of the six thermocouples still in operation in this capsule. Four thermocouples are still in operation in each of the other two capsules. All three heaters are operating in each capsule, although the electrical power necessary to maintain the temperature near 1500 F has increased for Capsules BMI-31-2 and BMI-31-3.

TABLE N-1. TEMPERATURE AND ELECTRICAL-HEATER POWER CONSUMPTION FOR CAPSULES BMI-31-1, BMI-31-2, AND BMI-31-3, DURING MTR CYCLE 131

Capsule	Electrical-Heater Power Consumption, W	Thermocouple Reading <sup>(a)</sup>					
		No. 1	No. 2	No. 3	No. 4	No. 5	No. 6
BMI-31-1	810	--	--	1480 <sup>(b)</sup>	1465	1255	--
BMI-31-2	2340	1395	--	1440 <sup>(b)</sup>	--	1480	1455
BMI-31-3	2720	1430	1495 <sup>(b)</sup>	--	1450	--	1440

(a) Specimen-surfaces temperatures are calculated to be 25 to 30 F higher.

(b) Designates controlling thermocouple.

A decision has been made to hold Capsule BMI-31-1 in the reactor and allow it to accumulate approximately 20 a/o uranium burnup, rather than remove it from the reactor at the 12 a/o burnup level originally planned.

Exposure of a single capsule in the BRR containing  $\text{UO}_2\text{-Al}_2\text{O}_3$  samples has been completed. Specimens will be sent to the cooperating laboratory for hot-cell examination.

#### DIFFUSION OF FISSION PRODUCTS IN CLADDING MATERIALS

S. G. Epstein, A. A. Bauer, and R. E. Dickerson

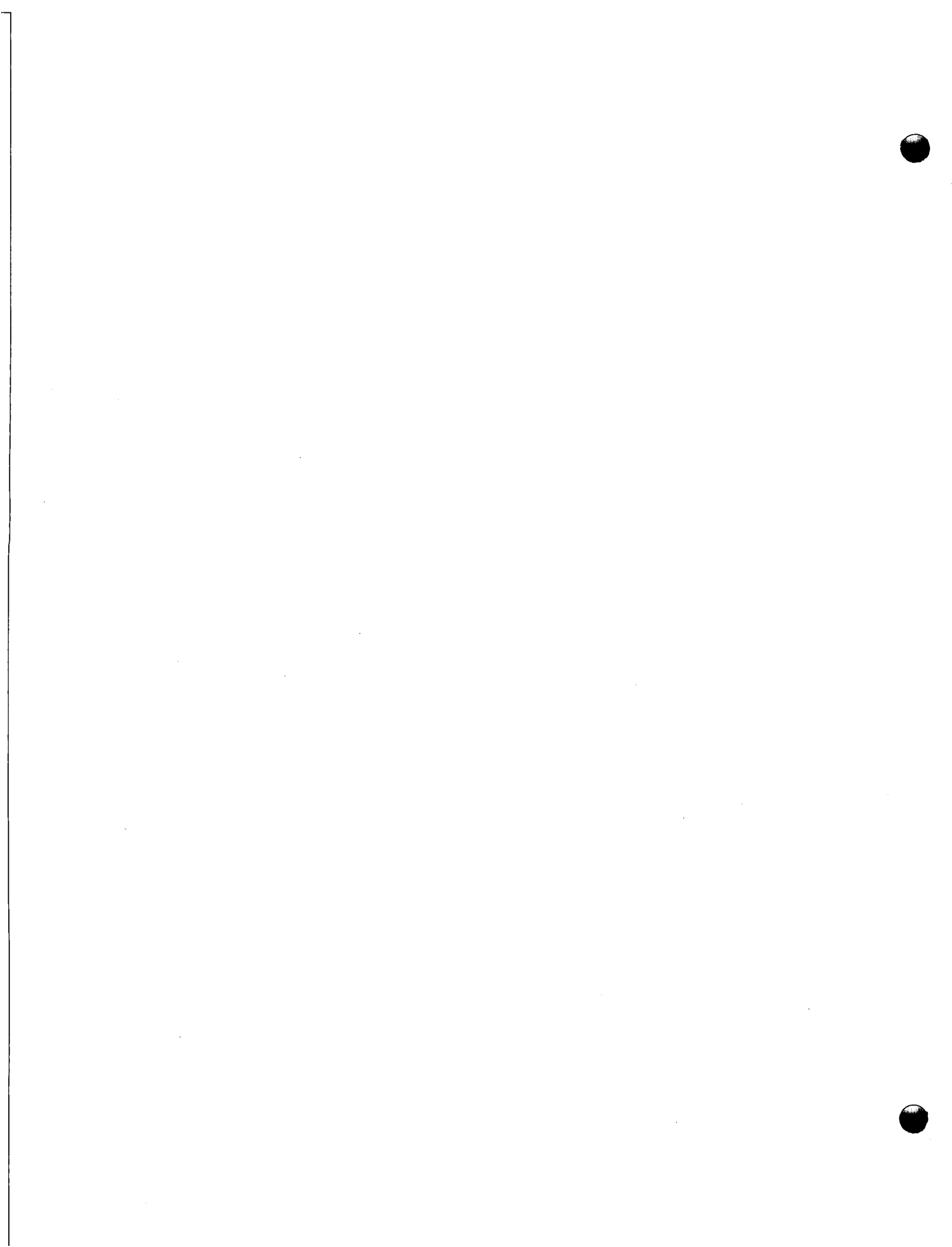
Work on this program has been recessed.

N-3 and N-4

CARBON-TRANSPORT CORROSION STUDIES

N. E. Miller, D. J. Hamman, J. E. Gates, and W. S. Diethorn

Selected metal and graphite specimens have been exposed to radiation in helium-filled quartz tori designed to promote convective flow of the helium and gaseous impurities past the specimens. All experimental work has been completed and a topical report is being prepared.



P-1

## P. DEVELOPMENTAL STUDIES FOR THE SM-2

S. J. Paprocki

Studies are being conducted in assistance to Alco Products to develop fuel, absorber, and suppressor materials for the SM-2.

Fabrication variables have been explored and techniques are being developed for the fabrication of a reference fuel plate consisting of spherical  $UO_2$  fuel and  $ZrB_2$  burnable poison dispersed in stainless steel. Use of high-purity  $ZrB_2$  and control of the sintering and fabrication process has reduced boron losses to an average value of about 5 per cent. The effect of coatings of niobium and tungsten on  $ZrB_2$  in reducing reaction rates and further decreasing boron loss is being investigated.

Reference and alternate fuel specimens are being irradiated in the MTR and ETR. It is planned to continue the tests to about mid-February, when the average calculated fission burnup will vary from about 30 to 65 per cent of the contained uranium-235.

Materials Development

S. J. Paprocki, D. L. Keller, G. W. Cunningham,  
A. K. Foulds, and D. E. Lozier

Fabrication techniques are being evaluated for use in preparing fuel plates, suppressor components, and absorber plates for the SM-2 reactor. Reference materials have been selected, and specifications will be established on the basis of fabrication studies.

Fuel Materials

The reference fuel element contains a core of approximately 26 w/o  $UO_2$  and 1.2 w/o  $ZrB_2$  dispersed in Type 347 prealloyed stainless steel plus a short (1/2 in.) end section of suppressor material containing approximately 17 w/o  $Eu_2O_3$  dispersed in an elemental 18-9 stainless matrix. This 0.030-in.-thick core is clad with 0.005-in.-thick Type 347 stainless steel. Forty fuel plates containing natural or depleted  $UO_2$  are being fabricated for welding studies. Ten of these plates have been completed, and 15 plates are in various stages of completion. These plates are not being prepared by a standard procedure, but include minor variations which will provide useful information for establishing fabrication specifications. Small-scale specimens are also being used to evaluate fabrication techniques.

The fabrication of 28 fuel plates containing fully enriched  $UO_2$  has been previously reported. Twenty of these plates were sent to Alco for critical-assembly tests, and eight of the plates were retained at Battelle for evaluation studies. Three of these

plates were sectioned for boron and uranium analyses, with five 1-in.-sq sections being obtained from each plate for boron analyses and five similar specimens being obtained for uranium analyses. The boron analyses and estimated boron losses are listed in Table P-1. The uranium analyses and metallographic examination have not been completed. It should be noted that, in general, the boron loss is considerably less than the 10 per cent excess boron added; thus, based on these values, boron content could be readily maintained within  $\pm 5$  per cent of the total boron. It should also be pointed out that, with no boron loss, large deviations ( $\pm 10$  per cent) are possible from specimen to specimen even though dimensional variations are maintained within tolerance.

As previously reported, boron losses can be prevented or maintained at a very low level during sintering, but boron losses during roll cladding have not been completely eliminated. A series of specimens roll clad to various stages of completion has been prepared, and boron analyses and metallographic specimens are being obtained. Another series of specimens which will be annealed for various lengths of time after roll cladding, and a specimen pickled after each hot pass will be prepared and boron analyses obtained. These data will be used to correlate with diffusion data in an attempt to propose the mechanism for boron loss.

Other than close control of fabrication procedures, it may be also possible to control boron loss by the use of metal-coated  $ZrB_2$  particles. Three batches of  $ZrB_2$  with coatings of 2 to 3, 4 to 5, and 7 to 8- $\mu$ -thick niobium have been prepared by the fluidized-bed process, and fuel specimens containing these powders have been prepared for roll cladding. The coated powders are being tested by X-ray diffraction, metallography, and chemical and vacuum-fusion analyses. The first batch showed that no reaction occurred between the niobium and the  $ZrB_2$ , and little or no oxygen or other impurities were picked up during the process. Powder with tungsten coatings is now being prepared.

Other studies in progress include the evaluation and specification of stainless steel powder. Specimens containing several special powders produced by a commercial vendor have been prepared but have not been evaluated.

#### Development of Control and Suppressor Materials

A dispersion of Type 347 stainless steel and  $Eu_2O_3$  is presently being considered as a control and suppressor material for the SM-2. An evaluation study is being conducted to determine the optimum method of preparing the  $Eu_2O_3$  particle sizes and the optimum fabrication techniques for the dispersion. The specimens prepared are being evaluated by corrosion testing and metallographic examination. A corrosion specimen, containing 33 w/o  $Eu_2O_3$  prepared by the KAPL method of sizing particles and dispersed in a 71-18-11 matrix, was corrosion tested at Alco Products, Inc., and failed within a 24-hr test period. A duplicate set of specimens containing  $Eu_2O_3$  sized by the same process was fabricated. These specimens were defected by a 0.040-in. hole through the cladding and were corrosion tested in 600 F static degassed water at Battelle. This set of specimens also failed within a 24-hr test period, verifying the previous results. The  $Eu_2O_3$  incorporated in these specimens contained 0.01 w/o silicon, and the dispersion was encased with a low-silicon, stainless steel barrier foil to

## P-3

TABLE P-1. BORON ANALYSES ON ENRICHED SM-2 FUEL PLATES

Plate	Section(a)	Calculated Boron per Section, mg	Boron Analyses		Boron Change, per cent
			After Fabrication w/o	Mg	
EAR-2	A	8.62	0.158	8.69	+0.81
	B	8.50	0.153	8.18	-3.77
	C	8.84	0.161	8.95	+1.25
	D	8.68	0.157	8.58	-1.15
	E	8.44	0.149	8.07	-4.39
	Average	8.62	--	8.49	-1.51
EAR-21	A	8.68	0.143	7.98	-8.06
	B	8.68	0.148	8.01	-7.74
	C	8.50	0.157	8.29	-2.48
	D	8.53	0.152	8.15	-4.45
	E	8.68	0.148	8.01	-7.74
	Average	8.61	--	8.09	-6.04
EAR-22	A	8.90	0.169	9.34	+4.95
	B	8.82	0.149	8.12	-7.95
	C	8.76	0.144	7.74	-11.40
	D	8.76	0.147	7.98	-8.90
	E	8.81	0.170	9.46	+7.39
	Average	8.81	--	8.54	-3.06

(a) 1 by 1-in. sections cut on a diagonal traverse across the core area.

prevent possible reaction with the wrought Type 347 stainless steel cladding. Corrosion specimens were also fabricated containing Eu<sub>2</sub>O<sub>3</sub> contaminated with approximately 10 w/o silicon. These specimens failed at approximately the same rate as did the low-silicon specimens. Additional specimens fabricated by the same techniques but containing commercially available minus 100-mesh air-fired Eu<sub>2</sub>O<sub>3</sub> have shown no weight gain or dimensional changes after a 24-hr corrosion test. Similar specimens are being prepared for corrosion testing at Alco. These tests will be more elaborate than the preliminary screening tests run at Battelle. All specimens to date have contained an 18-11 chromium-nickel-iron matrix and were sintered in a hydrogen-atmosphere furnace. Additional specimens are presently being prepared to evaluate the use of a prealloyed Type 347 stainless steel matrix material and a vacuum sinter.

#### Encapsulation Studies

J. F. Lagedrost, W. E. Murr, and J. H. Stang

Reference subsize SM-2 fuel specimens and alternate fuel materials contained in nickel capsules are being irradiated in the MTR and ETR test facilities. Three non-instrumented capsules are currently being irradiated in core positions of the MTR. One of an anticipated total of seven instrumented capsules is being irradiated in the O-6 position in the ETR beryllium reflector.

The three noninstrumented capsules, designated BMI-32-1, BMI-32-2, and BMI-32-3, were inserted in core positions of the MTR for Cycles 126, 127, and 128, respectively. As of the end of Cycle 131 (December 14), BMI-32-1 had accumulated a total of 2905 MWD and an estimated average specimen fission burnup of 35 per cent, BMI-32-2 had accumulated 2524 MWD and an estimated average specimen fission burnup of 33 per cent, and BMI-32-3 had accumulated 1614 MWD and an estimated average specimen fission burnup of 20 per cent. These burnups are based on reactor-quoted fluxes. It is planned to continue irradiation of these capsules until about mid-February. This will then allow sufficient time to fully evaluate the specimens during the current fiscal year and to draft material specifications.

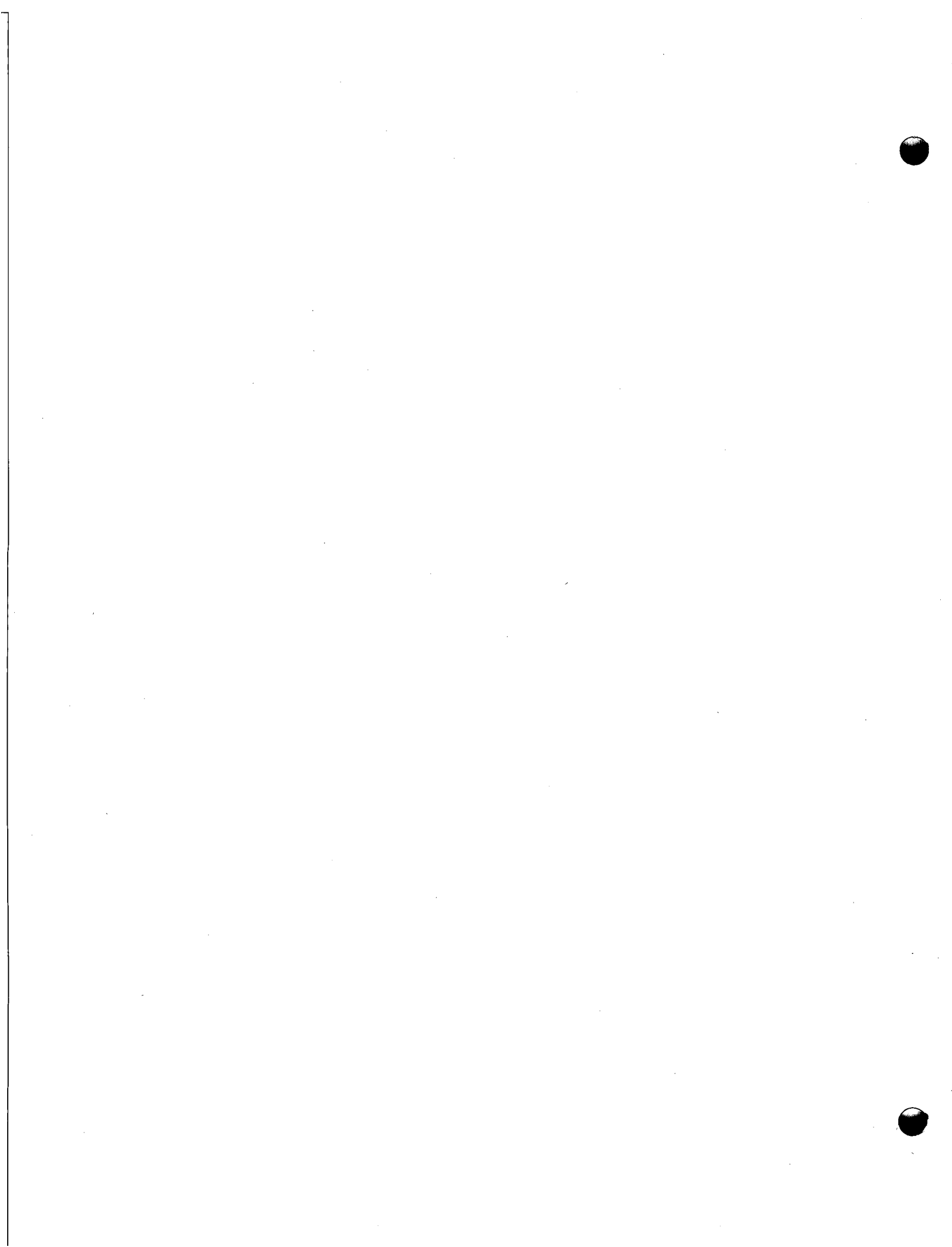
The first instrumented capsule, BMI-32-4, was inserted in an ETR beryllium-reflector position for Cycle 20, which started on September 12. Although the auxiliary electric heaters have failed, specimen temperatures at full reactor power have remained close to 600 to 650 F (calculated, based on thermocouple temperatures of 400 F). One of the original four thermocouples is still operative. During December, the ETR did not operate until the latter part of the month. Cycle 24 accumulated 975 MWD and Cycle 25, which started about December 24, is scheduled to continue until January 10, 1960. At the end of Cycle 24, Capsule BMI-32-4 had accumulated 5842 MWD and an estimated average specimen fission burnup of 17 per cent, based on quoted fluxes.

The second instrumented capsule, BMI-32-5, is nearly assembled and ready for preshipment checkout of the heaters and thermocouples. It is similar to BMI-32-4 in all respects except that a revised heater element-to-lead out wire connector is used. It is believed that this connector eliminates some of the possible causes of heater failure in BMI-32-4.

## P-5 and P-6

Results of the nuclear-mock-up capsules which were run in the MTR and the ETR to determine flux-perturbation factors are being evaluated. Correlation of dosimeter analyses and reactor power-time information is expected to supply the necessary flux data.

A theoretical analysis of heat transfer and temperature distribution in the BMI-32 capsule design is also in progress. The computational work involved is being carried out at the IBM-704 data-processing installation at New York University. The purpose here is to check the original design calculations, which were based primarily on electrical-analog simulation.



Q-1

## Q. GAS-COOLED REACTOR PROGRAM

D. L. Keller

Studies for Aerojet-General Nucleonics (AGN) directed toward the development of compact gas-cooled reactors are reported in this section. The activities on the various tasks are reported under "Materials Development Program" and "In-Pile-Loop Program".

MATERIALS DEVELOPMENT PROGRAM

D. L. Keller

Fuel pellets of Be-UO<sub>2</sub> containing 25 volume per cent UO<sub>2</sub> have been successfully fabricated for capsule-irradiation tests. The fuel pellets made from LOH grade BeO sintered to a density of approximately 98 per cent of theoretical in 2 hr at 2800 F. These pellets will be canned in Hastelloy X and are scheduled for insertion in the BRR for the January 12 startup.

Examination and evaluation of the UO<sub>2</sub> specimens clad with Inconel in Capsules BMI-29-1 and BMI-29-2 are essentially completed. As a result of extensive spectrographic and chemical analyses of the Inconel cladding in the region adjacent to, and including, the melted regions, the cause for melting at low recorded temperatures has been attributed primarily to excessive sulfur contamination of the cladding.

Fabrication of BeO-UO<sub>2</sub> Fuel Pellets

H. D. Sheets and A. K. Smalley

The objective of this program is to prepare UO<sub>2</sub>-containing BeO pellets for both loop and capsule exposures.

During December, 24 pellets about 1/16 in. in diameter and 3/32 in. high were prepared for capsule irradiation in the BRR. The specimens were prepared by mixing 25 volume per cent of MCW ceramic grade minus 325-mesh fully enriched UO<sub>2</sub> with 75 volume per cent of LOH grade BeO and suitable binders, cold pressing pellets in a steel die, and sintering for 2 hr at 2800 F in a hydrogen atmosphere. The bulk density of the sintered pellets ranged from 5.06 to 5.11 g per cm<sup>3</sup> (about 98 per cent of theoretical density). Chemical analyses and micrographic examinations of representative pellets are not yet complete.

Fabrication of about 2500 pellets for a loop-irradiation experiment will be started as soon as the necessary materials are received.

Encapsulation Studies

J. H. Stang, J. F. Lagedrost, G. E. Raines and D. W. Nicholson

Irradiation of Clad Pin-Type Specimens  
Containing Dense UO<sub>2</sub>

At present, limited heat-transfer analyses are continuing to devise reasons for the damage experienced by the clad pin-type specimens in Capsules BMI-27-1 and BMI-27-2. As discussed in BMI-1398, it was found that high local cladding temperatures (above 2000 F in some cases) could have been sustained if fission-heating rates at the ends of the fueled regions had been unusually high owing to minimum self-shielding effects. In pursuing this situation further, UO<sub>2</sub> pellets removed from undamaged specimens irradiated in Capsule BMI-27-2 were forwarded to NRTS for burnup analyses by mass spectrometry. A total of four pellets was submitted. Burnup results recently received indicate that:

- (1) The burnup of a pellet at the end of a stack (six pellets were stacked in each pin) was only about 10 per cent higher than that of a central pellet.
- (2) Burnups calculated on the basis of change of uranium-235 content were lower by a factor of about 2 than those calculated on the basis of irradiation-history data (capsule temperatures, reactor-quoted fluxes, etc.)
- (3) Burnups calculated on the basis of increase in uranium-236 content compare well with those calculated from irradiation history.

At present, the data involved are being studied to appraise various uncertainties associated with them. It seems, however, that end pellet-central pellet burnup ratios are not appreciably different, regardless of method of calculation. This would indicate that the fission-heat-generation rates along the specimen axes were not variable enough during irradiation to cause substantial thermal gradients on the cladding surfaces.

Irradiation of Specimens Containing MCW Spherical  
UO<sub>2</sub> Dispersed in Stainless Steel

This program involves the irradiation of stainless steel-clad specimens of MCW spherical and ORNL hydrothermal UO<sub>2</sub> (30 w/o, highly enriched) dispersed in stainless steel. Two specimens of each type are contained in Capsules BMI-33-1 and BMI-33-2.

Capsule BMI-33-1 was inserted in the MTR A-40-SW position for Cycle 131, which started on November 25. Thermocouple temperatures of approximately 1200 F maximum adjacent to the specimen surfaces during this first cycle indicated that the core center-line temperatures were approximately 300 F below the design value of 1650 F. This is in part attributed to the fact that the flux is somewhat lower than the design level. In order to provide data most useful for the comparative evaluation of

## Q-3

spherical and hydrothermal  $\text{UO}_2$ , the scheduled irradiation of this capsule has been extended from three to six MTR cycles. In the longer exposure, a specimen fission burnup of 15 per cent instead of the previously specified 9 per cent should be reached. With this revised schedule, the capsule will be discharged from the reactor about March 28, 1960.

Capsule BMI-33-2 has been requested for insertion in an MTR position having a thermal-neutron flux about 25 per cent higher than that of the BMI-33-1 position. This should result in specimen-core temperatures near the 1650 F level. The desired 9 per cent fission burnup of the specimens in this capsule will require three MTR cycles. Present information indicates that insertion will take place during Cycle 133 or 134 shutdown (January 4 or 25).

Irradiation of  $\text{UO}_2$ -Graphite Specimens With an Integral Corrosion-Gas-Flow System

As pointed out in previous reports of this series, this program originally involved a high-temperature capsule-irradiation experiment to be conducted at the Battelle Research Reactor. During October, the actual experiment was postponed until further notice, but a partial effort continued to complete certain laboratory heat-transfer experiments and to complete the capsule design. These phases of the program have now been completed and have confirmed the feasibility of the design. Until authorization is given to initiate the assembly of a system for irradiation, further work is not planned.

Irradiation of Specimens Containing  $\text{UO}_2$  Dispersed in  $\text{BeO}$

This project is concerned with an investigation of the irradiation stability at 1725 F of Hastelloy X-clad  $\text{UO}_2$  specimens dispersed in  $\text{BeO}$ . Six specimens are to be contained in an instrumented (heaters and thermocouples) double-wall capsule. Each specimen contains a 1-in. -long fueled section consisting of six 0.16-in. -diameter fueled pellets. Each end pellet is 1/8 in. long and contains 17 volume per cent  $\text{UO}_2$  (highly enriched); the four central pellets are each 3/16 in. long and contain 25 volume per cent  $\text{UO}_2$  (highly enriched).

During December, the hazards analysis and the design and fabrication of capsule components were completed. The present schedule calls for capsule assembly during the first week of January, and insertion in BRR Position 12 for the January 12 startup. The irradiation will require four 2-week reactor cycles.

Effects of Irradiation

J. H. Saling, W. E. Murr, J. E. Gates,  
and R. F. Dickerson

A study of the radiation stability of fuel-element materials for compact gas-cooled reactors includes (1) the evaluation of encapsulated solid and annularly loaded  $\text{UO}_2$

specimens clad with Inconel, and (2) the evaluation of encapsulated specimens of  $UO_2$  dispersed in graphite and clad with Inconel 702, Hastelloy X, or Carpenter 20 Cb, and (3) the evaluation of in-pile-loop subassemblies containing PWR-type fuel pins of solid  $UO_2$  clad with Inconel.

#### Capsule Program

Analyses of the cladding material of specimens from Capsule BMI-27-1 by emission spectrographic techniques have been completed, and preliminary results of analyses of the cladding material by wet-chemistry techniques have been obtained. The analyses indicate that the cladding material is principally Inconel, with some contaminants present in relatively large quantities. The emission spectrographic analyses indicate that 3 to 7 w/o boron was present in the cladding from each of the annularly loaded fuel pins, and that approximately 2 w/o boron was present in the cladding of Specimen GE-Solid 8, which was the top specimen in Capsule BMI-27-1. The cladding of the other specimens from this capsule contained from 0.1 to 0.5 w/o boron. Trace quantities of the following elements were also found in the cladding material: aluminum, calcium, chromium, cobalt, copper, iron, magnesium, manganese, molybdenum, nickel, silicon, sodium, titanium, uranium, and zirconium. Some of these elements such as aluminum, copper, and titanium were present in quantities larger than would be normally expected. The preliminary results of wet-chemistry analyses for sulfur indicate that sulfur was also present in the cladding material. In some cases it appears that the quantity of sulfur present was greater than 10 w/o. This amount of sulfur in the Inconel would account for the melting of the cladding material at the measured irradiation temperatures.

Results of the isotopic analyses of the fuel material from specimens irradiated in Capsule BMI-27-2 have been received, and burnups are presently being calculated from these data. Fission-gas-release data will be revised when these calculations are completed.

The examination of specimens irradiated in Capsule BMI-29-1 is continuing. This fully instrumented (three heaters and six thermocouples) capsule contained six specimens of 8 w/o  $UO_2$  dispersed in a graphite matrix, each approximately 1.0 in. long by 0.260 in. in diameter. In groups of two, the specimens were clad either with 0.025-in.-thick Hastelloy X, Carpenter 20 Cb, or Inconel 702 tubing. The capsule was irradiated in the MTR to an estimated specimen burnup of about 8 a/o of the uranium at specimen surface temperatures between 1600 and 1775 F. Density and dimensional measurements obtained on the six specimens were reported last month in BMI-1398. In general, the specimens showed no change in appearance or physical dimensions.

Samples of gas obtained from inside Capsule BMI-29-1 were analyzed with a gamma-ray spectrometer to determine whether a cladding failure had occurred in any of the specimens during irradiation. No radioactivity was detected in any of the gas samples, indicating that the cladding of all specimens was intact. Quantities as small as  $1.9 \times 10^{-2}$  microcurie of krypton-85 could have been detected with the spectrometer.

A postirradiation metallographic examination was performed on two specimens, 5X and 6X, from Capsule BMI-29-1, both clad with Hastelloy X. These specimens were sectioned for longitudinal and transverse examination of both the core and cladding,

## Q-5

and were examined metallographically both in the polished and etched conditions. The objective of the examination was mainly to determine the condition of the silicon-silicon carbide coating on the graphite fuel specimens and the condition of the Hastelloy X cladding. It was observed that a considerable reaction zone was present at the silicon carbide-Hastelloy X interface. Presumably, the Hastelloy X lost nickel by preferential diffusion into the silicon coating, resulting in the formation of numerous small voids in the Hastelloy cladding. As the nickel content increased in the silicon-rich coating to about 50 w/o, a nickel-silicon eutectic was formed, permitting melting to occur at about 1760 F. Similar conditions were observed in an unirradiated control specimen that was heated for 10 weeks at 1800 F.

Additional examinations planned for specimens irradiated in Capsule BMI-29-1 include sampling the gas collected inside the Carpenter 20 Cb cladding on one specimen, macroscopic examination of longitudinal sections of all four remaining specimens, and a microscopic examination of one specimen clad with Inconel 702 and one clad with Carpenter 20 Cb.

An analysis of the dosimeter wires removed from Capsule BMI-29-1 is in progress. It is not planned to determine the burnup of these specimens by radiochemical analysis.

#### In-Pile-Loop Subassemblies

The metallographic examination of sections from Subassembly 1B-1 $\gamma$ T and chemical analysis of the spacer from Pin 16 are being continued. The results of these examinations will be reported as soon as they become available.

#### GCRE Critical-Assembly Experiments

R. A. Egen, D. A. Dingee, W. S. Hogan, and J. W. Chastain

The critical assembly is being modified to conduct experiments with a mock-up of the ML-1-1B reactor. When completed the active core will approximate a right cylinder 22 in. in diameter and height. Sixty-one fuel-element positions will be surrounded by a 4-in.-thick lead reflector. The spacing between adjacent fuel elements in the core will be nonuniform to produce a radially flattened power distribution.

Uranium dioxide dispersed in alumina and jacketed with Inconel X will be used to fuel the reactor. Nineteen pins will make up each fuel element. The inner 7 pins will simulate 35 volume per cent dispersion of UO<sub>2</sub> in BeO; the outer 12 pins will simulate a 70 volume per cent dispersion.

During the past month many of the core components were fabricated. These include the fuel-element-positioning grid plates, scissor-acting control blades, and lead reflector. It is expected that the remaining items will be completed next month to allow the core framework to be assembled. The fuel is expected to arrive from AGN early in March.

IN-PILE-LOOP PROGRAM

G. A. Francis

An in-pile recirculating-gas-loop program is being conducted to perform the irradiation of fuel subassemblies for Aerojet General Nucleonics. The program began about 3-1/2 years ago with design of a loop for use in the Battelle Research Reactor. Subsequently, the design of a loop for installation in the Engineering Test Reactor was started.

The loop at the BRR is between experiments, with irradiation of the sixth subassembly scheduled to begin by mid-February. The ETR loop blowers have been reinstalled, and the system is now being operated in a final checkout before a specimen is inserted. The progress on the different phases of the loop program is reported under the following headings.

BRR Loop Program

S. J. Basham and W. H. Goldthwaite

Plans call for a flux run with an AGN specimen designated 1B-2 $\phi$ T during the first reactor shutdown in February and the start of a 4-month irradiation of a specimen designated 1B-2T-1 by mid-February. This schedule is based on the receipt of experiment hazards information in early January and the receipt of the specimens by the middle of the first week in February.

Preparation for the irradiations continued during this report period. As a result of corrosion which was discussed in a previous report, the decision had been made to replace aluminum tubing in both the primary coolant and instrument air systems. The change from aluminum to stainless steel tubing was completed during the regular reactor shutdown on December 28, 1959.

Near the middle of December, the loop was operated in-pile for a 24-hr period without a fuel specimen to check for the presence of fuel particles in the loop test section. Gas samples which were taken periodically during the run were analyzed by gamma-ray spectrometry. The results showed that argon-41 was the only isotope present in quantities measurable by the experimental method being utilized. From this test, it was concluded that the loop contamination, if any, is too low to be a source of fission-gas-activity problems during future specimen irradiations.

The continuous loop-gas-monitoring system was received late in December. The installation and calibration of the system should be completed during the next report period.

Q-7

ETR Loop Program

E. O. Fromm, S. L. Cosgrove, J. V. Baum,  
D. E. Roop, and G. A. Francis

Blower Modification and Tests

Subsequent to the installation of the loop and blowers at the reactor, the three blowers in the loop system and the spare blower had been returned to Battelle for modification to improve their reliability.

As described in BMI-1398, one blower was modified and operated at Battelle for approximately 800 hr. Two other blowers have been modified and a new impeller has been machined for the fourth blower. Blowers designated B and C have been returned to the site. During January it is expected that Blower A will also be returned to the site and that Blower D will be put on an extended life test at Battelle.

On November 27, Blower B was stopped after operating for 305 hr. This operating period was obtained with the use of Andok "C" grease. At the start of the run, Andok "C" grease was forced into the bearings with the manual greasers on the blower. The blower was started on November 14, stopped briefly for an examination of the belt on November 19, and then operated until November 27. Inlet-gas temperatures ranged from 189 to 197 F. Inlet pressure was 177 to 189 psig. This blower was partially inspected on November 27, but the impeller shaft and bearings were not removed from the housing. The belt was found to have stretched slightly during the first 100 hr of operation. After readjustment on November 19, no further stretch was noted.

On November 27 Blower C was placed on the test stand and operated. This blower was operated under the same conditions as Blower B except that the bearings of Blower C were packed with GE Special, an experimental grease supplied by Shell Oil Company. Blower C was started and stopped more than 30 times at the start of the test. Each cycle included a power-on interval of approximately 3 sec followed by a coast-down interval. The belt stretched only a very small amount. The belt was readjusted and checked with a mechanical belt-tension indicator, and then the unit was pressurized and operated. Operating temperatures included inlet-gas temperatures from 191 to 208 F, inlet pressures of 184 to 191 psig, and outlet-gas temperatures from 220 to 234 F. This unit operated without incident until December 1. From 4:05 pm until 8:30 pm some erratic bearing temperatures were experienced. At 2:00 pm the highest temperature recorded for Bearing 1 was 173 F. Between 4:00 and 8:30 pm the temperature of Bearing 1 was up to 190 F. Bearings 3 and 4 did not show any appreciable change in temperature during this period. The blower was not stopped, and, after 8:30 pm, the temperature dropped back to 176 F for Bearing 1. No change in other operating conditions could be determined during the time of the bearing-temperature changes. Inlet temperature, pressure, and coolant flow remained steady. Blower C was operated until December 10 at 8:00 am for a total time of 302 hr.

Blowers B and C were then dismantled and examined. The details of the grease analysis are summarized in a subsequent section of this report. Blowers B and C were then regreased with Shell GE Special grease, and each was operated approximately 24 hr. These units were then crated. On December 20 they were shipped to the ETR.

On December 17, Blower A was lubricated with GE Special grease and assembled for operation. This blower operated without incident until December 23. It was stopped after a total running time of 151 hr.

During the operating periods for Blowers A, B, and C, the operating characteristics of gas-flow rate versus blower pressure rise were obtained. The results showed that Blower A, before modification of the impeller and housing, had a pressure rise of approximately 23.7 psi compared with a pressure rise of 21 psi for the modified unit at a flow rate of 0.9 lb per sec and approximately 100 F inlet-gas temperature. The impeller and housing modifications have resulted in a decrease of approximately 11.4 per cent for the blower-pressure generation. Similar changes in characteristics were exhibited by Blowers B and C.

The impeller and housing modifications for all three blowers included 15 holes through the impeller to balance the operating pressures on the impeller faces, and increased operating clearance for both faces of the impeller. The impeller clearances obtained were as follows:

		<u>Clearance, in.</u>
Blower A		
Front		0.021
Rear		0.021
Blower B		
Front		0.025
Rear		0.022
Blower C		
Front		0.021
Rear		0.017

Other modifications were the same as previously reported for Blower B.

Blower D is being prepared for operation at Battelle during January. It is planned that this unit will be operated for at least 1000 hr to determine the life of a single packing of the GE Special grease.

#### Analysis of Blower Bearing Grease

When Blowers B and C were dismantled and examined, the GE special grease appeared to be nearer its unused condition than the Andok "C". In order to substantiate this observation, four grease samples were subjected to laboratory examination. The samples were designated as:

Sample	Description
1	Andok "C" (Standard Oil of N. J.), unused
2	Andok "C" after 300 hr in blower bearing
3	GE Special (Shell Oil Sample 1185, ILC Sample X9-1169), unused
4	GE Special after 300 hr in blower bearing.

## Q-9 and Q-10

Analytical data are summarized in the following tabulation:

Sample	Residue <sup>(a)</sup>		Oil Content, per cent	Soap Content, per cent	Loss During Analysis <sup>(b)</sup> , w/o
	Amount, w/o	Description			
1	0.043	Black nonmagnetic powder	64.0	34.7	1.3
2	0.272	Black, fibrous material, partially magnetic	63.5	36.1	0.1
3	0.171	Brown gum	87.3	9.5	3.0
4	0.342	Gray powder, partially magnetic	87.4	11.4	0.9

(a) That material insoluble in both hexane and aqueous isopropanol.

(b) Soap is the most likely component to be lost during analysis.

The insoluble residue in unused Andok "C" grease (Sample 1) was probably contamination resulting from the use of contaminated components or dirty processing equipment. The brown, gummy residue from unused GE Special grease (Sample 3) was probably an additive component (this grease is suspected to contain an antibleeding additive).

The following conclusions may be drawn from these data:

- (1) Both greases permitted a small, approximately equal amount of wear during bearing operation.
- (2) Neither grease showed significant bleeding under the conditions of use.

In view of these conclusions, the GE Special grease, because of its much higher oil content, was selected for use in this bearing application.

#### Loop Checkout and Testing at the Reactor

The prefilter and dryer to treat plant air for use as emergency in-pile-tube coolant has been installed and used. Late in the report period, Blowers B and C were received at the reactor site, installed in the loop, and put into operation.

The change of the loop control of a variable-flow basis was completed. The testing of the new control system cannot be completed until the electrical preheater is operational. At present the erratic heater control is being studied by the supplier, the manufacturer, the reactor operator, and the experimenter. The insertion of the first experiment in the loop during January could be delayed if the heater is not available for both flow-control tests and the experiment itself.

RWD:CR T/all